Two-dimensional melting

Katherine J. Strandburg*

Physics Department, Carnegie-Mellon University, Pittsburgh, Pennsylvania 15213

For a decade now the subject of the nature of the two-dimensional melting transition has remained controversial. An elegant theory based on the unbinding of pairs of crystal defects suggested that two-dimensional solids might melt by a transition sequence involving two continuous transitions separated by a novel, nearest-neighbor-bond-orientationally ordered fluid—the hexatic phase. Competing theories predict that the transition is of the usual first-order type observed in three-dimensional systems. This paper is a critical review of the current status of research into the problem of two-dimensional melting, with an emphasis on computer simulations. An attempt is made to point out unresolved issues pertaining to this fascinating and still open question.

CONTENTS

The nature of the melting transition in two-dimensional systems has been a matter of hot controversy in the past several years. Kosterlitz, Thouless, Halperin, Nelson, and Young (KTHNY) have suggested that the transition may be fundamentally different from that observed in ordinary three-dimensional systems (Kosterlitz and Thouless, 1973, 1978; Halperin and Nelson, 1978; Nelson and Halperin, 1979; Young, 1979). Competing theories propose that the transition is of the usual first-order type observed in three-dimensional systems (Ramakrishnan, 1982; Chui, 1982, 1983; Kleinert, 1983; Joos and Duesbery, 1985). A large body of experimental and simulation research into two-dimensional melting followed the announcement of the KTHNY theory. In spite of all this effort, the question as to the nature of two-dimensional melting remains unresolved. Recent experimental work supporting the existence of continuous melting transitions in some two-dimensional systems indicates the need for further theoretical and computation-

*Present address: Materials Science Division, Argonne National Laboratory, Argonne, IL 60439.

al work to lead to an understanding of the experimental results.

In this paper I intend to summarize and perhaps clarify the current situation with regard to research in two-dimensional melting with an emphasis on computer simulations. In particular, I will point out important gaps in our current understanding. Where appropriate, I will highlight directions which I believe will be fruitful for future research.

The paper begins with an introduction to the ideas important in the study of two-dimensional phase transitions. An overview of the current status of theoretical, simulational, and experimental research in this subject follows. Conclusions and suggestions for further research are summarized in the final section.

I. THEORETICAL SUMMARY

A. The Kosterlitz-Thouless transition

Phase transitions in two-dimensional systems with continuous symmetry are of great interest due to the absence, in these systems, of conventional long-range order at low temperatures (Mermin and Wagner, 1966). The two-dimensional XY model provides a simple example of such a system, since the spins may point in any direction in the continuous range $[0,2\pi]$. We begin by discussing theoretical ideas for the XY model, since it is a simpler case than melting. In a rough way the origin of the lack of long-range order is illustrated in Fig. 1. Figure 1 illustrates a long-wavelength spin wave in an XY spin system. Assuming a harmonic interaction for small differences in angle between neighboring spins, the energy of such a spin wave is proportional in one dimension to $L(2\pi/L)^2$, in two dimensions to $L^2(2\pi/L)^2$, and in three dimensions to $L^3(2\pi/L)^2$, where L is the linear dimension of the system. In three dimensions, therefore, these distortions are forbidden in the thermodynamic limit, leading to the presence of long-range order at low temperatures. In one dimension these distortions are favored, leading to the nonexistence of an ordered phase, while two dimensions is a borderline case.

FIG. 1. Spin wave in an XY spin system.

More careful study of the two-dimensional case confirms that long-range order cannot occur (Mermin and Wagner, 1966). However, the two-dimensional XY model is characterized at low temperatures by what has come to be known as quasi-long-range order. In a ferromagnetic phase, for example, the spin-spin correlation function decays at long distances to a nonzero constant, indicating long-range ordering of the spins. In a paramagnetic phase the behavior of this correlation function is described asymptotically by exponential decay to zero characterized by a correlation length. At the critical point, however, the spin-spin correlations exhibit a slow, algebraic decay with decay exponent η. Critical-point-like algebraic decay of the correlation function over a region of the phase diagram is the signature of quasi-long-range order. A phase in which the correlation function exhibits algebraic decay is known as a "critical phase" and is characterized in renormalization-group language as a line of fixed points. The exponent η will be temperature dependent in such a phase.

Such critical phases are not characteristic of all two-dimensional systems. The critical behavior depends also on the order-parameter dimension n. The XY model has $n=2$. The Ising model has $n=1$ and, since a long-wavelength spin wave cannot occur in this model, long-range order does persist at low temperatures and the classic two-dimensional Ising transition results. For $n=3$, fluctuations are strong enough to destroy the quasi-long-range order and to suppress the transition temperature to zero. Examples of two-dimensional systems with $n=2$ are superfluid films, thin superconductors, XY models, and two-dimensional solids.

Kosterlitz and Thouless advanced a theory that describes the transitions in two-dimensional (2D) superfluids, superconductors, and XY models based on the physical idea of topological defects called vortices as the mechanism driving the transitions in these systems (Kosterlitz and Thouless, 1973, 1978). Figure 2 illustrates spin vortices of positive and negative vorticity in an XY system. Such vortices disrupt the spin alignments even at large distances. Mathematically, such vortices correspond to singularities of the order-parameter field.

The essential physics of the Kosterlitz-Thouless (KT) theory is revealed by a simple calculation. Creating an

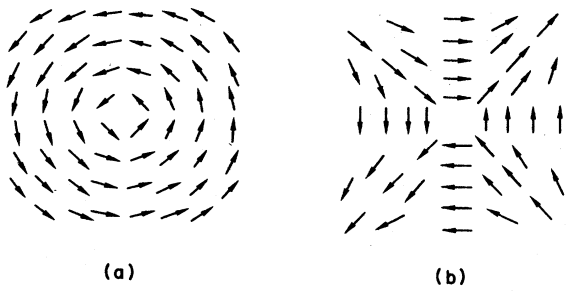

FIG. 2. Spin vortices: (a) negative vorticity; (b) positive vorticity.

isolated vortex requires an infinite amount of energy: Consider an XY model characterized by a nearest-neighbor interaction of strength J. The energy cost due to the spins a distance r from the center of the vortex is, in the harmonic approximation, $J/2(2\pi/2\pi r)^2(2\pi r)$, and therefore the total contribution from a vortex in a system of size L is given by

$$E_v = \frac{J}{2}\int_a^L \left[\frac{2\pi}{r}\right] dr = J\pi \ln\left[\frac{L}{a}\right], \tag{1}$$

where a is the lattice spacing. The entropic contribution of such a vortex due to the freedom to place it at any lattice site is also logarithmic in L, however, leading to a free energy

$$F_v = J\pi \ln\left[\frac{L}{a}\right] - k_B T \ln\left[\frac{L}{a}\right]^2. \tag{2}$$

This simple calculation predicts a transition at a temperature $k_B T_c = \pi J/2$, from a phase in which vortices are forbidden to a disordered phase in which they abound.

This simple picture is not really adequate, however, since a bound pair of oppositely "charged" vortices has a finite energy and does not disrupt the spin ordering at long distances. Such pairs will be thermally excited even at low temperatures. The reduced Hamiltonian for a system of vortices is

$$H_v = -\pi K \sum_{|\mathbf{r}-\mathbf{r}'|>a} s(\mathbf{r})s(\mathbf{r}')\ln\left[\frac{|\mathbf{r}-\mathbf{r}'|}{a}\right] + E_c \sum_{\mathbf{r}} s^2(\mathbf{r}) . \tag{3}$$

Here $s(r)$ is the vorticity for the vortex at site r, defined as -1 and $+1$ for the vortices in Figs. 2(a) and 2(b), respectively. The harmonic approximation used in deriving the logarithmic interaction energy is inadequate at small r, and therefore a core energy E_c is introduced to describe the contribution of the region within a core diameter a. The factor $1/k_B T$ is assumed to have been absorbed into the definition of the coupling K and core energy E_c. Note that the Hamiltonian is just that of a two-dimensional two-component Coulomb gas with a chemical potential E_c.

The mechanism for the KT transition is the unbinding of a dilute gas of vortex pairs. The calculation of the behavior of the vortex system requires that the screening of the vortex interaction by thermally excited vortex pairs be considered. The bound pairs of defects act analogously to a dielectric by screening the interaction between opposite "charges." The vortex unbinding occurs at a temperature when the "dielectric constant" characterizing the system diverges (or, equivalently, the coupling constant K goes to zero).

The KT theory is a renormalization-group treatment of the screening effects. The theory predicts a continuous transition from the low-temperature phase (characterized by quasi-long-range order) to the high-temperature, disordered phase. The transition will be characterized by only essential singularities in the energy and specific heat. The coupling constant K, however, will renormalize to a universal limiting value (at the transition temperature) and then jump discontinuously to zero. (This jump manifests itself in the 2D superfluid transition, for example, as a discontinuous jump in the superfluid density.) The spin-spin correlation length is expected to diverge exponentially as the transition temperature is approached from the disordered phase.

It should be mentioned that the transition temperature predicted by the KT renormalization-group theory is the same as that predicted by the simple discussion above, with the coupling constant replaced by its renormalized value. In a sense, this is to be expected since the renormalized coupling constant gives the interaction energy (including screening) for a pair of infinite separation. The KT predictions for the 2D superfluid, superconductor, and XY model are confirmed by experiment and computer simulation (see, for example, Saito and Muller-Krumbhaar, 1984; Fernandez and Ferreira, 1986; Strandburg, 1987 and references therein).

B. KTHNY theory of two-dimensional melting

The two-dimensional melting transition poses additional complications for a defect-unbinding theory. Two-dimensional particle systems are characterized by two different order parameters and, correspondingly, by two types of topological defects. In addition, experimental 2D particle systems are often subject to a substrate potential. In order to deal with these complications, the basic ideas of Kosterlitz and Thouless were elaborated upon by Halperin and Nelson and, independently, by Young (Halperin and Nelson, 1978; Nelson and Halperin, 1979; Young, 1979). The Halperin-Nelson-Young (HNY) theory has been reviewed in detail several times (Nelson, 1980). Here we provide only a brief description of the basic ideas and results of the calculation.

1. The melting transition

The 2D solid is characterized by quasi-long-range positional order, as evidenced by the algebraic decay of the density-density correlation function. This positional order may be destroyed by free dislocations (see Fig. 3) in a dislocation-unbinding transition. A dislocation may be viewed as an extra row of atoms stuck partway into the crystal. The theory of this transition differs somewhat from that of the vortex-unbinding transition described above due to the fact that dislocations are described not by a scalar "charge" but by a Burgers vector. The Burgers vector for the dislocation in Fig. 3 is shown. It is defined as the amount by which a path around the dislocation (e.g., four steps to the left, four down, four right, four up) fails to close.

A simple argument from elastic theory analogous to that for the vortex shows that the energy of a single dislocation also diverges logarithmically with system size. The dislocation Hamiltonian contains an additional term due to the vector character of these defects:

$$H_{\text{disloc}}=\frac{-K}{8\pi}\sum_{\mathbf{r}\neq\mathbf{r}}\left[\mathbf{b}(\mathbf{r})\cdot\mathbf{b}(\mathbf{r}')\ln\left(\frac{|\mathbf{r}-\mathbf{r}'|}{a}\right)-\frac{\mathbf{b}(\mathbf{r})\cdot(\mathbf{r}-\mathbf{r}')\mathbf{b}(\mathbf{r}')\cdot(\mathbf{r}-\mathbf{r}')}{|\mathbf{r}-\mathbf{r}'|^2}\right]+E_c\sum_{\mathbf{r}}|\mathbf{b}(\mathbf{r})|^2 . \tag{4}$$

K is related to the Lamé elastic constants by

$$K=\frac{4\mu(\mu+\lambda)}{2\mu+\lambda} . \tag{5}$$

The elastic Hamiltonian for the 2D triangular solid is given by

$$H_E=\tfrac{1}{2}\int d^2r(2\mu u_{ij}^2+\lambda u_{kk}^2) ,$$

where (6)

$$u_{ij}(\mathbf{r})=\frac{1}{2}\left[\frac{\partial u_i(\mathbf{r})}{\partial r_j}+\frac{\partial u_j(\mathbf{r})}{\partial r_i}\right]$$

and $u(r)$ is the atomic displacement field. Note that the definitions of μ and λ used here contain a factor of $1/k_BT$. The HNY renormalization-group analysis of the dislocation-unbinding transition leads to the following predictions.

(1) The density-density correlation function defined as

$$g_{\mathbf{G}}(|\mathbf{r}-\mathbf{r}'|)=\langle e^{i\mathbf{G}\cdot[\mathbf{u}(\mathbf{r})-\mathbf{u}(\mathbf{r}')]}\rangle \tag{7}$$

(where $\mathbf{G}$ is a reciprocal-lattice vector), will decay in the solid phase as

$$g_{\mathbf{G}}(r)\sim r^{-\eta}\quad\text{where } \tfrac{1}{4}\leq\eta(T_m)\leq\tfrac{1}{3} \tag{8}$$

for the first Bragg point. This divergence leads to power-law singularities in x-ray diffraction patterns, rather than δ-function Bragg peaks.

(2) The combination of elastic constants

$$K=\frac{4\mu(\mu+\lambda)}{2\mu+\lambda}\sim 16\pi/(1-c|t|^{\nu})\quad\text{as } T\to T_m \text{ from above} , \tag{9}$$

where

$$t=(T-T_m)/T_m \text{ and } \nu=0.396\ldots .$$

(3) In the liquid just above freezing the positional correlation length

$$\xi\sim\exp(c/|t|^{\nu}) . \tag{10}$$

(4) A "bump" in the specific heat due to the gradual dissociation of dislocation pairs should occur above the melting temperature T_m. There is no specific-heat divergence associated with the transition. This point should not be stressed too heavily, however, since the actual peak height, width, and location relative to the melting temperature are highly model-dependent parameters. For example, Monte Carlo simulations of the XY model yield a specific-heat peak sharper and nearer to the transition than is found in calculations for the corresponding Villain model. In addition, if there exists a bicritical core energy below which the transition is first order, one may expect to see rather sharp specific-heat peaks near the multicritical point. In a finite computer simulation or resolution-limited experiment the distinction between a true divergence or first-order δ function and a sharp but still finite peak may be very difficult to draw.

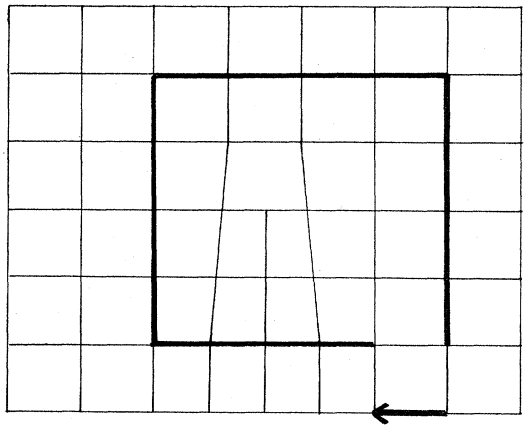

FIG. 3. Dislocation on a square lattice. The Burgers vector of this dislocation is shown. Note that a dislocation does not destroy the bond-orientational order of the lattice.

2. The hexatic phase and the hexatic-isotropic transition

The above predictions are very similar to those made by Kosterlitz and Thouless for the vortex-unbinding transition. Halperin and Nelson found, however, that

the liquid above this dislocation-unbinding transition is not isotropic. Solids are characterized by two types of ordering. Besides the quasi-long-range positional ordering already described, there is long-range order in the orientation of nearest-neighbor bonds. Halperin and Nelson found that the dissociation of dislocation pairs, which destroyed the quasi-long-range positional order, left a fluid characterized by quasi-long-range order in the nearest-neighbor-bond orientations.

The nearest-neighbor-bond-angular order is measured by the bond-angular correlation function

$$g_6(|\mathbf{r}-\mathbf{r}'|)=\langle e^{i6[\theta(\mathbf{r})-\theta(\mathbf{r}')]}\rangle , \tag{11}$$

where θ is the angle made by a bond between a particle at $\mathbf{r}$ and its nearest neighbor with respect to an arbitrary fixed axis. In the anisotropic fluid just above melting, which Halperin and Nelson titled the "hexatic phase," the orientational correlation function

$$g_6(r)\sim r^{-\eta_6(T)} , \tag{12}$$

where

$$\eta_6=\frac{18k_BT}{\pi K_A} .$$

Because the bond-orientational order is only quasi-long-ranged, the x-ray diffraction pattern from an infinite hexatic sample would consist of an isotropic ring. However, finite-size effects will modify this pattern, so that the sixfold modulation expected in the thermodynamic limit for long-range bond-orientational order will be observed in real experiments and simulations even in the quasi-long-range hexatic phase.

A second type of crystalline defect, the disclination, disrupts the bond-angular order (see Fig. 4). A disclination is characterized by a mismatch in orientation as one circumnavigates it (see the arrows in Fig. 4). Alternatively, a disclination can be viewed as an atom having the "wrong" number of nearest neighbors as measured by a Voronoi polygon construction. The Voronoi polygon construction is a generalization of the Wigner-Seitz cell and is useful for disordered systems.

As is depicted in Fig. 5, a dislocation may be viewed as a tightly bound pair of disclinations. In the solid, dislocations are bound very strongly with a potential that increases as the square of the separation. In the hexatic phase, however, this interaction is screened by the presence of free dislocations and the potential grows only logarithmically with separation.

Disclinations interact in the hexatic phase with the screened Hamiltonian

$$H_{\rm disc}=-\frac{\pi K_A}{36}\sum_{\mathbf{r}\neq\mathbf{r}'} s(\mathbf{r})s(\mathbf{r}')\ln\left[\frac{|\mathbf{r}-\mathbf{r}'|}{a}\right] + E_{cd}\sum_{\mathbf{r}} s^2(\mathbf{r}) , \tag{13}$$

where K_A is the coupling constant related to distortions of the bond-angle field and is called the Frank constant (in analogy to that of liquid crystals). K_A is infinite in the solid and zero in the isotropic liquid. The $s(r)$ are in this case the disclination "charges" corresponding in a triangular lattice, for example, to $+1$ for an atom with seven nearest neighbors and -1 for an atom with five. The disclination core energy E_{cd} is not simply related to the original dislocation core energy E_c.

The disclination Hamiltonian is now of the form (3) and the results of the KT theory for the XY model may be carried over to predict a continuous disclination-unbinding transition at a temperature $T_i > T_m$ into an isotropic fluid. At this transition, the following predictions are made.

(1) The Frank constant $K_A(T_i)\rightarrow 72/\pi$ and then

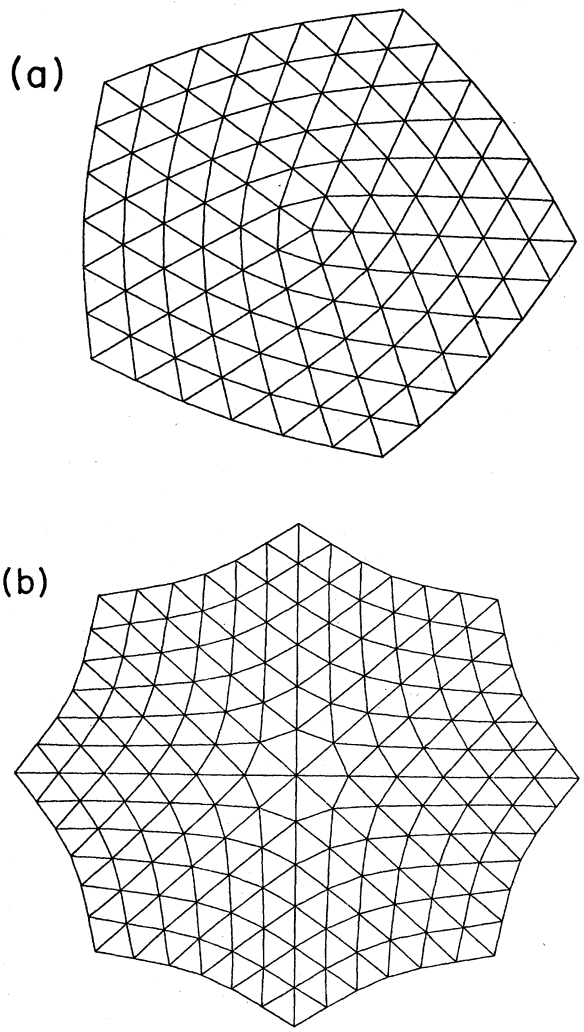

FIG. 4. Positive and negative disclinations in a triangular lattice. Note the rotation of the triangular cells by 60° (a) clockwise, and (b) counterclockwise, as a clockwise path around the disclination is traveled. Note that these disclinations may also be described as particles having (a) five, and (b) seven neighbors, respectively, rather than six.

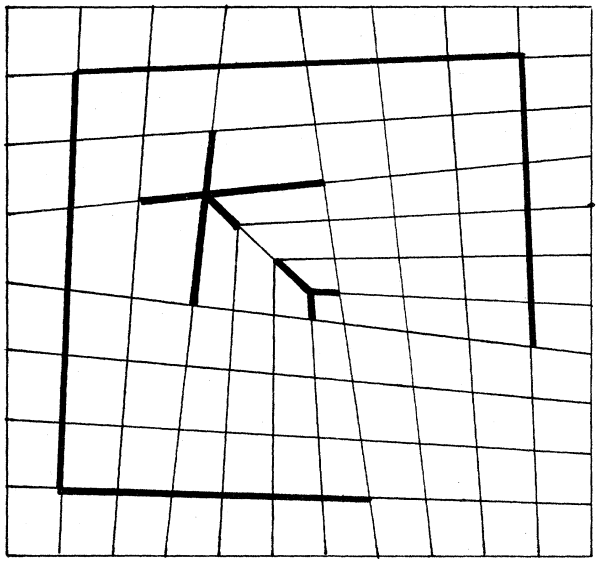

FIG. 5. Dislocation that may be viewed as a bound disclination pair. A path around the dislocation fails to close, as shown. The two disclinations, one having five nearest neighbors and one having three, are also shown.

jumps discontinuously to zero as $T \to T_i$ from below. As $T \to T_m$ from above, K_A diverges proportionally to the square of the positional correlation length.

(2) The bond-angle correlation function exponent $\eta_6(T_i) = \frac{1}{4}$.

(3) The orientational correlation length goes as $\xi_6 \sim \exp(b/|T - T_i|^{1/2})$ as $T \to T_i$ from above. Calculations of the expected width of the critical region in which this form is valid indicate that the correlation length may be very large (10^4–10^9 A) before this form is observed, and that even experimental systems may not be large enough to observe this behavior (Cardy, 1982; Greif *et al.*, 1982; Dahm, 1984). The correlation length was calculated using the HN recursion relations and assuming a value for the core energy. However, the critical width is sensitive to core energy. Since, as will be discussed below, little is known about core energies for specific experimental or simulated systems, estimates for the width of the critical region for particular systems have not been made.

(4) The energy and specific heat display only essential singularities at T_i. The specific heat should, however, show a peak above T_i due to the gradual dissociation of disclination pairs.

The KTHNY picture of the 2D melting transition is summarized in Table I.

3. KTHNY theory in the presence of a substrate

Since many of the experiments discussed below involve atoms adsorbed on graphite, we review here briefly the modifications to this theory which obtain in the presence of a weak incommensurate substrate potential (Nelson and Halperin, 1979; Young, 1979). The melting transition is modified only slightly. An additional term in the elastic Hamiltonian (describing a tendency to align with the substrate axes),

$$H_E = \tfrac{1}{2}\gamma \int d^2r (\partial_y u_x - \partial_x u_y)^2 \tag{14}$$

(where γ is an additional elastic constant describing resistance to twist), leads to a new dislocation Hamiltonian

$$H_{\text{disloc}} = \frac{-K_1}{8\pi} \sum_{\mathbf{r}\neq\mathbf{r}'} \mathbf{b}(\mathbf{r})\cdot\mathbf{b}(\mathbf{r}') \ln\left[\frac{|\mathbf{r}-\mathbf{r}'|}{a}\right] + \frac{K_2}{8\pi} \sum_{\mathbf{r}\neq\mathbf{r}'} \frac{\mathbf{b}(\mathbf{r})\cdot(\mathbf{r}-\mathbf{r}')\mathbf{b}(\mathbf{r}')\cdot(\mathbf{r}-\mathbf{r}')}{|\mathbf{r}-\mathbf{r}'|^2} + E_c \sum_{\mathbf{r}} |\mathbf{b}(\mathbf{r})|^2 , \tag{15}$$

with

$$K_1 = \frac{4\mu(\mu+\lambda)}{2\mu+\lambda} + \frac{4\mu\gamma}{\mu+\gamma} \to 16\pi \text{ at } T_m ,$$

$$K_2 = \frac{4\mu(\mu+\lambda)}{2\mu+\lambda} - \frac{4\mu\gamma}{\mu+\gamma} .$$

Renormalization-group recursion relations were derived for this Hamiltonian by Young (1979) and by Nelson and Halperin (1979).

TABLE I. Summary of some predictions of the KTHNY theory for two-dimensional melting.

	Solid	Hexatic	Liquid
Dislocations	Bound in pairs	Free	Free
Disclinations	Bound in quartets	Bound in pairs	Free
Positional correlations	Quasi-long-range	Short range	Short range
Bond-orientational correlations	Long range	Quasi-long-range	Short range
Elastic constant $K = \frac{4\pi\mu(\mu+\lambda)}{2\mu+\lambda}$	Finite, nonzero	Zero	Zero
Frank constant K_A	Infinite	Finite, nonzero	Zero
	T_m: $K \to 16\pi$ as $T \to T_m$ from below	T_i: $K_A \to 72/\pi$ as $T \to T_i$ from below	

The exponent ν from Eq. (9) is now expected to be given by $0.3696\ldots<\nu<0.4$ and the values of η_G are modified.

Above the melting transition, however, the effect of a substrate potential is more significant. The bond-orientational order is now long ranged. Instead of isotropic rings the diffraction pattern will now consist even in the thermodynamic limit of diffuse spots whose radial and angular half-widths have a temperature-independent ratio near the transition (Aeppli and Bruinsma, 1984). The disclination transition is washed out when the substrate has sixfold symmetry. However, for small enough substrate field a remnant of the hexatic to isotropic transition will still be observable, just as a ferromagnet in a weak magnetic field will still show remnants of critical behavior. For a square substrate Halperin and Nelson predict that the KT-type disclination-unbinding transition will be replaced by an Ising-like transition corresponding to the two equivalent ways of putting a hexagonal adsorbate on a square substrate (Nelson and Halperin, 1979).

Moreover, an "orientational epitaxy" effect has been predicted at low temperature by Novaco and McTague (1977) (McTague and Novaco, 1979). The adsorbate may have a preferred orientation with respect to the substrate. This preferred orientation may not be along one of the substrate symmetry axes. In this case, two equivalent oriented states exist (e.g., rotated $\pm 10°$ from the substrate axes). An Ising-type transition is also expected if the melting transition takes place while the adsorbate is in the rotated state.

The KTHNY theory is, of course, dependent upon various approximations and assumptions. The transition sequence described here can be preempted by a first-order transition resulting from a number of effects. The KTHNY theory involves an expansion in fugacity and thus uses a dilute gas, or large core energy, approximation. A change in behavior could occur as the core energy is decreased. Such a change has been observed when the XY model is modified so as to change the effective vortex core energy (Swendsen, 1982; Domany *et al.*, 1984; Van Himbergen, 1984), as well as in simulations of the dislocation and disclination systems discussed in Sec. III (Saito, 1982a, 1982b; Strandburg, 1986). The core energy will depend on system parameters such as the density and the form of the atomic interactions. Collective dislocation excitations also could be of importance.

C. Grain-boundary-induced melting

The possibility of grain-boundary-induced melting in which the dislocation-unbinding transition is preempted by a first-order transition involving a proliferation of grain boundaries has also been proposed (Fisher *et al.*, 1979; Chui, 1982, 1983). Grain boundaries are collective excitations of dislocations, as shown in Fig. 6. A grain boundary has the effect of rotating one patch of crystal with respect to another. Although a grain boundary may

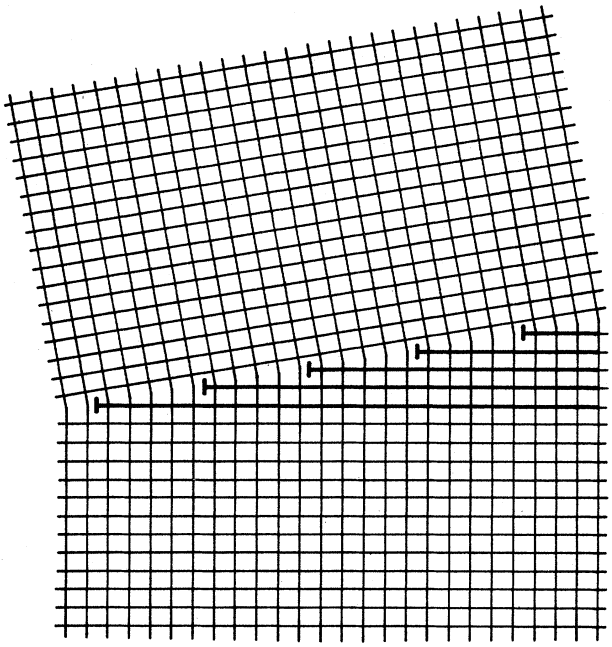

FIG. 6. Small-angle grain boundary. The grain boundary can be seen to be made up of a line of dislocations.

be viewed as a string of dislocations (see Fig. 6), infinite parallel grain boundaries interact with a potential that is not long range, due to cancellations occurring only in that limit. Thus a transition in which grain boundaries appear may be distinct from the KTHNY dislocation-unbinding transition. A calculation by Fisher, Halperin, and Morf (1979) for small-angle grain boundaries, which included the possibility of "vibrations" around a straight grain boundary configuration, concluded that the melting transition due to small-angle grain boundaries was identical to the KTHNY mechanism.

However, Chui (1982, 1983) calculated the free energies of possible low-angle grain boundary configurations in more detail. Using a low-density approximation, he considered the effects on the grain boundary free energy of transverse and longitudinal fluctuations, grain boundary crossing energies, coupling of grain boundaries to dislocation pairs, and coupling of grain boundaries to density changes. The calculations were performed in the limit of low densities of both grain boundaries and dislocation pairs and did not include the effects of renormalizations of the core energy and elastic constants. Chui concluded that the KTHNY melting mechanism would be preempted by a first-order transition irrespective of the value of the core energy. The first-order nature of the transition was due to a negative grain boundary crossing energy, a coupling with the density change, and the interaction with bound dislocation pairs. He predicted a change from weakly first-order to strongly first-order transitions for core energies below a critical value of 2.8. (For a comment on core energy units see Sec. II.B.1.)

Chui's calculation involves the assumption that the distance s between the dislocations making up a grain

boundary is small compared to the distance z between grain boundaries. For E_c less than 2.8 this assumption breaks down, however, and s gets very large. Thus Chui's prediction of a first-order transition for $E_c < 2.8$ is not reliable. Indeed for $z \ll s$, the KTHNY description of a dilute gas of dislocation pairs would appear to be more appropriate.

Simulations of the disclination system (Strandburg, 1986), which are described below, indicate a change from KTHNY melting to first-order melting below a core energy near 2.8. These simulations lend support to Chui's prediction of the crossover core energy, but contradict his assertion that melting remains first order for higher core energies. Possibly, Chui's theory correctly describes the situation for $E_c < 2.8$, but the behavior becomes KTHNY-like for $E_c > 2.8$ as the distance between dislocation pairs becomes large and Chui's approximation breaks down. One of the factors important in Chui's calculations is a coupling of grain boundaries to a density discontinuity. This effect is not included in simulations of defect systems, since they use lattice models.

In addition, it is possible for a first-order transition to lead to a hexatic phase rather than to the isotropic fluid phase. If, for example, the grain boundaries remain bound in pairs above melting, the grain boundary melting can lead to a hexatic phase. An approximate calculation by Chui of the free energy of bound grain boundaries indicates that they will not remain bound above a grain-boundary-induced melting transition.

Fisher, Halperin, and Morf (1979) comment that the dislocation correlations predicted by Nelson and Halperin for the hexatic phase show an angular dependence that may be described as a strong tendency of dislocations to arrange themselves in small-angle grain boundaries. Since dislocations have a tendency to form grain boundaries in the hexatic phase, one must be careful in interpreting the presence of grain boundary loops in defect plots obtained from simulations as evidence against the hexatic phase, and in favor of a transition to an isotropic liquid. An isotropic liquid requires grain boundaries that are not bound in pairs.

D. Possibilities of first-order transition through simultaneous dislocation and disclination unbinding

In the KTHNY theory the dislocation interactions in the solid phase are treated independently of the disclination interaction in the hexatic phase. The free dislocations in the hexatic phase screen the disclination interaction, producing the logarithmic disclination interaction of Eq. (13). The values of the Frank constant K_A and the disclination core energy E_{cd} thus obtained are related in a nontrivial way to the initial values of K and E_c. A Debye approximation gives K_A proportional to E_c and to the square of the positional correlation length. If the screened interactions are sufficiently weak as the dislocations unbind, a simultaneous disclination unbinding may occur precipitating a first-order transition. The KTHNY theory does not deal with the effects of disclinations and dislocations concurrently and therefore leaves this possibility open.

Kleinert (1983) has argued by means of mean-field theory calculations that the scenario described above occurs and that melting is a first-order process. However, as is well known, mean-field theory predictions for phase transitions are often incorrect since they do not treat fluctuations properly. These fluctuations are particularly important in two dimensions.

Kleinert's calculations were performed for a model that is based on the zero-temperature disclination interaction. Since dislocations can be composed of disclinations (see Fig. 5), this model includes the possibility of both the dislocation- and disclination-unbinding transitions. This model had been proposed earlier by Nelson (1982) in a dual form known as the Laplacian roughening model. This model has been the subject of extensive Monte Carlo simulations to be discussed in Sec. III.B (Janke and Kleinert, 1980, 1984; Strandburg *et al.*, 1983; Janke and Toussaint, 1986; Strandburg, 1986).

Kleinert (1983) has also noted that the logarithmic dislocation interaction [Eq. (4)] does not give the correct energy for separated disclination pairs (which may be formed by lining up dislocations at intervals of one lattice constant). He points out that the simple interaction [Eq. (4)] gives an excess energy $E_c R$ to the string of Burgers vectors comprising the disclination pair. This string should actually have zero energy since it may be drawn in various ways to represent the same disclination pair.

This observation is not a problem for the KTHNY theory, however, since KTHNY use Eq. (4) to describe disclination interactions only in the solid phase. Since disclination pairs interact as $r^2 \ln r$ in the solid phase, they are very heavily suppressed at temperatures below melting. The KTHNY theory makes the very reasonable assumption that disclinations occur only in tightly bound pairs (i.e., dislocations).

Disclinations become important only when, in the presence of unbound dislocations, their interaction is screened to logarithmic (as in the hexatic phase). The question of whether this screening is sufficient to precipitate a concurrent unbinding of dislocations and disclinations remains a quantitative question. Evidence from Monte Carlo simulations indicates that the nature of the transition depends on the magnitude of the defect core energy (Saito, 1982a, 1982b; Strandburg, 1986).

E. Vacancies and interstitials

Point defects such as vacancies and interstitials may also play an important role in the melting process. Because of the relatively hard cores of most atomic interactions, vacancies usually have a much lower energy than interstitials. Vacancies are of considerable importance in the equilibration of dislocations. Implications of the importance of vacancies to dislocation motion in interpreta-

tion of simulation results will be discussed in Sec. II.A.

Joos and Duesbery (1985) have recently performed a zero-temperature calculation of defect energies in rare-gas systems, discussed at some length in Sec. II. The low energy calculated for localized vacancies leads them to conclude that the melting transition will be driven by vacancies rather than by dislocation unbinding.

Below a certain density the energy of a vacancy becomes negative in these systems. The rare gases are described fairly well by a Lennard-Jones interaction potential. The competition between attractive and repulsive parts of the potential leads to the existence of a "preferred" lattice spacing. As the lattice is expanded beyond this spacing, eventually it is energetically favorable to break up the system and allow separation into islands of solid at a smaller lattice spacing and lakes of condensed vacancies. Thus vacancies may certainly be said to drive the transition, at low temperatures, from solid to solid-gas coexistence as a function of decreasing density. The Joos and Duesbery calculation of the lattice spacing at which this density-driven transition occurs is in good agreement with experimental rare-gas-on-graphite phase diagrams.

However, vacancies are an unlikely mechanism for the melting transition at higher densities and temperatures or in systems such as the $1/r^n$ potentials that do not have a "preferred" lattice spacing. They also cannot explain the purely temperature-driven melting from solid-gas to fluid-gas coexistence. Since vacancies do have a rather low energy, they exist in a non-negligible equilibrium concentration in the solid. However, since they are localized defects, vacancies do not disrupt the lattice structure at long distances. Only by aggregating into structures on the order of the system size can they affect the long-range order of the system and thus causing melting. Aggregates are favored since their energy is lower than that of an equivalent number of isolated vacancies. Such large aggregates are, however, no longer usefully viewed as vacancies. Indeed, as Joos and Duesbery point out, a string of vacancies that crosses the system is precisely an unbound dislocation pair.

F. Density wave theory

A density wave theory of melting, by Ramakrishnan (1982), leads to a prediction of a first-order transition. The predicted entropy change on melting and height of the first peak of the structure factor are consistent with values obtained in computer simulations. Since such a mean-field theory neglects the fluctuations that lead to the loss of long-range positional order, its ability to predict the order and character of the melting transition is questionable. If the transition is first order and therefore due to local effects, then such a theory should give good results. On the other hand, the agreement of such a theory with finite size and time simulations (which also neglect possibly important long-wavelength fluctuations) is not conclusive for the nature of the transition in the thermodynamic limit.

II. DEFECT ENERGIES AND INTERACTIONS

The dislocation, disclination, and grain boundary theories described above are based on a lattice model of defects interacting with potentials obtained from elasticity theory. Several questions arise regarding the applicability of these models to two-dimensional particle systems. How valid is the elasticity theory description of defect interactions in actual 2D solids? How may the parameters of the lattice model be connected to real systems? The relevant parameters are defect coupling constants K and K_A, defect core diameters, and defect core energies. In both of these areas knowledge is currently rather limited.

A. Validity of the elasticity description

A possible difficulty for the KTHNY Chui and Kleinert calculations would be a breakdown of the elasticity theory, in the context of which these defect-mediated melting theories are derived. Anharmonic effects can be of importance in real systems. In this section the validity of the elastic description for real systems is discussed.

Harmonic behavior of the 2D solid at low temperatures has been verified in several simulated systems through studies of the behavior of the squared displacements of atoms from their lattice sites (Young and Alder, 1974; Gann *et al.*, 1979; Tobochnik and Chester, 1979). However, these results concern the defect-free solid and do not tell us whether the defects themselves interact as predicted by elasticity theory.

For the 2D electron ($1/r$ potential) system Fisher, Halperin, and Morf (1979) have calculated the energies of various defect configurations both by a variational method relying on elasticity theory and by numerical relaxation techniques. They find that the long-distance elastic form of the dislocation interaction is valid down to distances of about three lattice spacings. They also calculate energies for various localized defects. In the electron case [in contrast to the rare gases studied by Joos and Duesbery (1985, 1986)] interstitials have a lower energy than vacancies. This result is due to the necessity of a neutralizing positive background in the electron system, which provides an effective attractive interaction.

Ladd and Hoover (1982) have calculated the energy of pairs of dislocations in a system interacting with piecewise-linear forces. They conclude that the interactions are consistent with continuum elastic theory for dislocation separations greater than a few lattice spacings.

Calculations by Joos and Duesbery (1985, 1986) for the rare gases indicate a much more complicated picture. Joos and Duesbery use realistic potentials to calculate zero-temperature dislocation energies for 2D xenon and krypton with and without a graphite substrate. Numerical static relaxation techniques are used. These calculations should give a good qualitative description of the situation for 2D Lennard-Jones potential systems as well.

The defects studied were pairs of dislocations formed by lines of vacancies or interstitials (see Fig. 7). Their results for the dislocation pair interaction as a function of separation are shown in Fig. 8. They indicate that the long-distance elasticity limit is reached for vacancy lines only for distances on the order of 30 lattice spacings. That the Lennard-Jones potential leads to extended dislocation cores has also been pointed out by Hoover, Hoover, and Moss (1979). Vacancy strings of size less than 30 lattice spacings have significantly lower energy than might be expected on the basis of elasticity theory. The interstitial-type pairs obey the elasticity predictions for considerably shorter pair separations. This difference is due to the asymmetry of the Lennard-Jones potential.

The Joos and Duesbery results have two rather serious implications for Monte Carlo simulations of melting of 2D Lennard-Jones systems. First, the lower energy of vacancies and vacancy aggregates compared to that of interstitials means that simulations with periodic boundary conditions and a fixed number of particles may give seriously flawed results. In such systems vacancies and interstitials are almost always created in pairs, since the creation of a lone vacancy requires large-scale rearrangements of the lattice, which are essentially impossible to achieve in the time available for simulations.

Since the presence of vacancies is required for some dislocation motions, the suppression of vacancy formation will inhibit dislocation equilibration. Broughton *et al.* (1982) and Stillinger and Weber (1981) studied the melting of $1/r^{12}$ potential and Gaussian core model systems, respectively, in the presence of a single vacancy. They found that the presence of the vacancy was significant in obtaining agreement between the fluid to solid and solid to fluid traverses of the transition. Behavior in the perfect solid was typical of a system with an artificially high kinetic barrier to melting. However, they concluded that even in the presence of the vacancy the melting appeared to be first order.

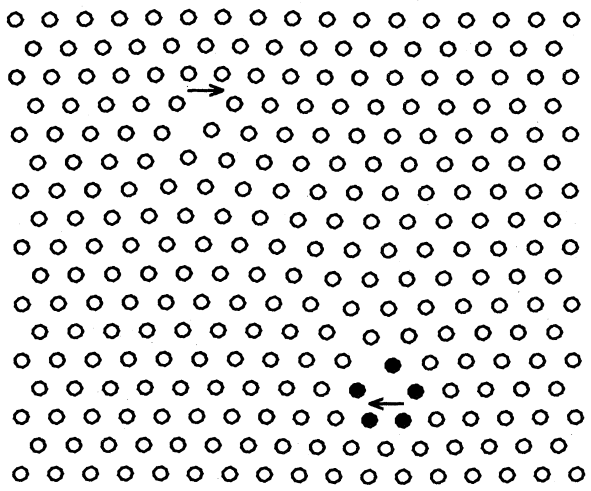

FIG. 7. Vacancy dislocation dipole in a triangular lattice obtained by removal of eleven atoms in a row. The arrows indicate the directions of the Burgers vectors (Joos and Duesbery, 1985).

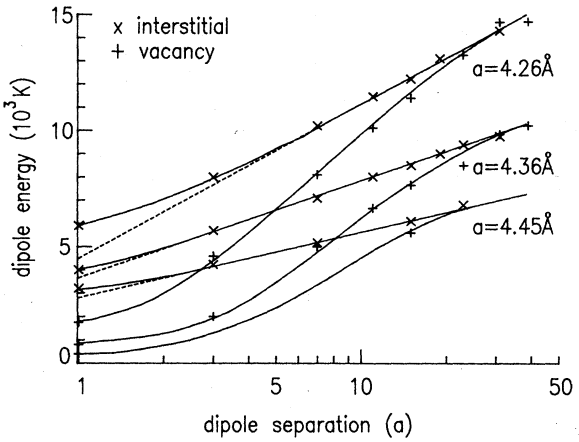

FIG. 8. Dislocation dipole energies for floating Xe monolayers (Joos and Duesbery, 1985).

It is possible that the difficulty of vacancy formation is responsible for the fact that nearly all simulations of 2D systems display first-order transitions, whereas continuous transitions are seen in many experiments (see Sec. IV). Significantly, what appears to be a continuous transition is observed in simulations of a Lennard-Jones system, which allow for motion in the third dimension (Abraham, 1983; see Sec. V.F for a discussion of the order of the transition in this case). Constant chemical potential simulations that allow for density fluctuations and vacancy formation would be extremely helpful. However, these simulations have been plagued by technical difficulties. New efforts in this direction are certainly warranted.

The Joos and Duesbery calculation also has important implications for the validity of the extrapolation from the results of finite-size simulations to the thermodynamic limit. If the elastic regime is not reached until 30 lattice spacings, then system sizes much larger than the typical 1000 particles will be needed in order to ascertain the long-distance behavior of the system. The form of the dislocation interaction shown in Fig. 8 also indicates that one may expect to see an equilibrium concentration of "localized" defects of sizes on the order of ten lattice spacings even in the solid. This fact will make a meaningful interpretation of maps of defect positions (see Sec. V.C.1) extremely difficult indeed.

Large defect aggregates have indeed been observed just prior to melting in simulations of Lennard-Jones systems (Tobochnik and Chester, 1979). The appearance of these clusters has usually been interpreted as evidence of first-order transitions and, in particular, of grain boundary melting. If, however, the elastic limit has not yet been reached, these clusters should perhaps be regarded as part of the dislocation "core."

The implication of the Joos and Duesbery (1985, 1986)

results for simulations is that the study of size dependence is essential to the understanding of the 2D melting transition. Toxvaerd (1981, 1983) has performed studies of size dependence of various quantities in repulsive Lennard-Jones and Lennard-Jones systems. Substantial diffusion was observed in an 8100 particle system at a temperature and density at which none had been observed at smaller sizes. Diffusion may be important for the melting behavior in the thermodynamic limit. Also, the shear modulus μ showed a substantial and roughly logarithmic decrease as a function of system size for sizes up to 1024 particles near the melting transition. Calculations by Hoover *et al.* (1984; see also Toxvaerd, 1984) using a quasiharmonic approximation (low-temperature limit) gives a slight increase in μ as the size is increased. The amount of increase is inversely proportional to the system size. However, the quasiharmonic calculations are valid only at low temperatures, since they do not include the effects of defects. The significant decrease in μ as system size is increased observed by Toxvaerd implies that systems of size 1024 and smaller are not large enough to test predictions for elastic constants near the melting transition.

Significantly, Toxvaerd also found that the density of crystal defects (as measured by a Voronoi polygon construction) increased as the size of the system increased. This increase may be due to the large defect core implied by the results of Joos and Duesbery.

Even if the system size and interaction potential are chosen so that the defect pair interactions may be described properly in elastic theory, there remain qualitative anharmonic phenomena that are simply not included in the elastic description. Large-angle grain boundaries are examples of such phenomena, which may conceivably be important for melting (Fisher *et al.*, 1979). Substrate interactions may also destroy the applicability of the harmonic description. If they are sufficiently strong, they completely dominate the adsorbate behavior, producing commensurate phases describable by lattice theories.

B. Parameters of the defect description. Calculation of the parameters

The parameters of the HN model are the combination of elastic constants K, the Frank constant K_A, the dislocation and disclination core energies, and the defect core radii. It should be emphasized that most of the predictions of the KTHNY theory can be checked without knowing these parameters. However, determination of these parameters for atomic systems would be extremely useful for the following.

(1) Prediction of the melting temperature.

(2) Study of melting behavior as a function of these parameters. It would be of interest, for example, to be able to link density changes in Lennard-Jones systems to changes in defect core energies.

(3) Comparison of the results of atomistic simulations and experiments to results of defect simulations that show a change in melting behavior as a function of core energy.

One of the difficulties in making these connections has been a certain amount of confusion about the definitions of these parameters. All of the theoretical calculations begin with so-called "unrenormalized" values of the melting parameters, i.e., the values obtained when no dislocation pairs are present in the solid. It is often assumed that these "unrenormalized" values are identical to zero-temperature values. However, in real systems, phonons are known to affect these parameters, even when no defects are present (Fisher *et al.*, 1979; Morf, 1979). Since the HN calculations do not take phonons into account, it seems reasonable to include their effects before applying the KTHNY theory.

This problem was pointed out and this conclusion reached by Fisher *et al.* (1979) and by Morf (1979) in calculations for the 2D electron system. Using the results from the defect energy calculation described in this section, they calculated the melting temperature from the HN recursion relations using both zero-temperature and "phonon-renormalized" values. These phonon-renormalized values gave a prediction for the melting temperature in good agreement with that observed in experiments and simulations.

A more subtle difficulty in determining the appropriate "unrenormalized" values of the parameters concerns the identification of the appropriate length scale on which these parameters must be measured. The smallest length in the KTHNY calculation is the defect core radius. Thus, all changes to the theoretical parameters that are due to effects occurring on smaller length scales must be included before the theory may be applied. The discussion of the previous section indicates that it may be necessary to include in the unrenormalized values the effects of defect aggregates localized to distances smaller than the distance at which elastic theory begins to describe the defect interaction. These aggregates may be expected to have substantial effects on the elastic constants as well as on the defect core energies.

The elastic constant K is defined as

$$K=\frac{4\mu(\mu+\lambda)}{2\mu+\lambda},$$

where μ and λ are the Lamé elastic constants in units of k_BT/a_0^2, with a_0 being the lattice spacing of the atomic system. The renormalized value K_R may be computed in simulations either by straining the system and measuring the response or by using the formulas derived by Squire *et al.* (1968; see also Stewart, 1974). Low-temperature values may be used to extrapolate to an "unrenormalized" value appropriate at the melting temperature (Fisher *et al.*, 1979; Morf, 1979). However, the discussion of extended defect cores suggests that these values may not be appropriate for use as input to the KTHNY theory for some systems.

The dislocation core energy and core radius are difficult to obtain by either experiment or computer

simulation. The core energy and core radius are not independent quantities. The core radius is the distance outside of which the dislocation energy obeys the logarithmic form of Eq. (4). The core energy is the energetic contribution of the region within that radius. Two difficulties exist in determination of these parameters for atomistic systems: (1) determination of their absolute values in the system in question and (2) expressing these values in the appropriate units for comparison to defect theories and simulations.

As mentioned in Sec. II.A (Fisher *et al.*, 1979; Hoover *et al.*, 1979; Joos and Duesbery, 1985, 1986), dislocation energies have been determined for a few systems using zero-temperature relaxation calculations. The difficulties in using zero-temperature values have already been mentioned. Another method has been to count, using the Voronoi polygon construction, the number of defects present at low temperatures and to calculate the core energy from an Arrhenius law $[\rho=\exp(-2E_c/k_BT)]$ (Tobochnik and Chester, 1982; Murray and Van Winkle, 1987). Unfortunately, the number of defects present at low temperatures is small and therefore statistics in the simulation are bad. At higher temperatures defect interactions are often important and the Arrhenius law is no longer adequate.

This method assumes that the energy of the smallest defect pairs gives the appropriate "unrenormalized" value. If the elastic limit is not reached until about 10 lattice spacings, as in Lennard-Jones-type systems, this assumption is incorrect and the measured value will be the energy for creation of small localized defects rather than the desired dislocation core energy.

Experimentally, core energies are also very difficult to determine. Arrhenius-type fits to the specific heat may be used (subject to the caveats above) and have been done in the cases of ^{4}He (Ecke and Dash, 1983; Hurlbut and Dash, 1984, 1985; Strandburg *et al.*, 1985) and ethylene (Kim *et al.*, 1986) on graphite. A similar analysis of neutron scattering data has been performed for ^{3}He on graphite (Feile *et al.*, 1982). The dislocation core energies thus obtained are approximately 4, 15, and 5, respectively (in units of the temperature of the specific-heat maximum), in the portions of the phase diagrams investigated. In these cases the low-T form of the specific heat with one excitation energy fits the data up to very near the melting point. Possibly the effects of defect clustering are small in these systems.

In order to be useful for comparison to defect theories these core energies must be expressed in units of the "unrenormalized" elastic constant K. These values of K are in most cases not known. The electron system appears to have a rather small core radius of about three lattice spacings. In this case one may assume that the renormalization due to small defect aggregates is negligible. Making this assumption, and using the phonon-renormalized values, the dimensionless core energy $16\pi E_c/K=4.4$ is obtained. Good agreement with experiments and simulations is obtained when the transition temperature is determined using these values as input to the KTHNY theory (Fisher *et al.*, 1979; Morf, 1979).

Two other important parameters in the KTHNY theory are the unrenormalized Frank constant (disclination coupling constant in the hexatic phase) K_A and the hexatic phase disclination core energy. These quantities have not been determined in any atomistic systems so far. The renormalized value for K_A has been computed for the Laplacian roughening model (Strandburg *et al.*, 1983). The unrenormalized values are not known, even for that system, however. The unrenormalized disclination core energy mentioned here includes the effects of screening by free dislocations and is not simply related to the low-temperature disclination core energy (which is just half the unrenormalized dislocation core energy). Clearly the investigation of the connection of properties of atomistic systems to the parameters of the defect theories remains an important area for future research.

III. SIMULATIONS OF THE DEFECT SYSTEMS

Leaving aside questions of the connection of the elastic description to realistic atomic systems one may investigate the validity of the defect theories within the elastic framework, particularly as the defect core energy is varied. Simulations of the defect model itself have addressed this issue rather successfully.

A. Saito's dislocation simulation

The first of these simulations was performed by Saito (1982a, 1982b) on a dislocation gas system. In this simulation, dislocations of unit length were allowed to point in any of six directions allowed by a triangular lattice. These dislocations were placed on a triangular mesh and interacted with a potential which, while behaving like the logarithmic dislocation Hamiltonian at large separations, was modified to take into account the periodic boundary conditions and the lattice structure of the mesh. This potential was then fit to the logarithmic form [Eq. (4)] to determine an initial core energy for dislocations. The core energy for this simulation was $16\pi E_c/K=4.6$, where this value differs from that quoted by Saito to maintain agreement with HN conventions for the units. Since Saito's model included only dislocations, only one transition was possible. It was, however, possible to analyze the nature of the transition itself, as well as the identity of the phase above the transition.

Saito's results showed that the transition for this natural core energy obeyed the KTHNY predictions. Specifically, he observed the unbinding of dislocation pairs at the transition, and the elastic constant K_R (determined from a dislocation correlation function), passing through 16π at the transition. The dislocation correlations above the transition fit the predicted hexatic phase form very well. The height of the specific-heat peak was size independent for systems containing 418 and 1672 lattice sites, as is expected for the KTHNY melting mechanism. The transition temperature as estimated from the

elastic constant $K_R \rightarrow 16\pi$ was approximately 12% above the temperature of the specific-heat maximum, and the width of the peak was also about 12%. The Frank constant K_A obtained the value $72/\pi$ approximately 20% above the melting temperature. However, the hexatic to isotropic transition cannot occur in this system since dislocations alone are considered, so no conclusions about the width of the hexatic phase may be drawn from this temperature dependence.

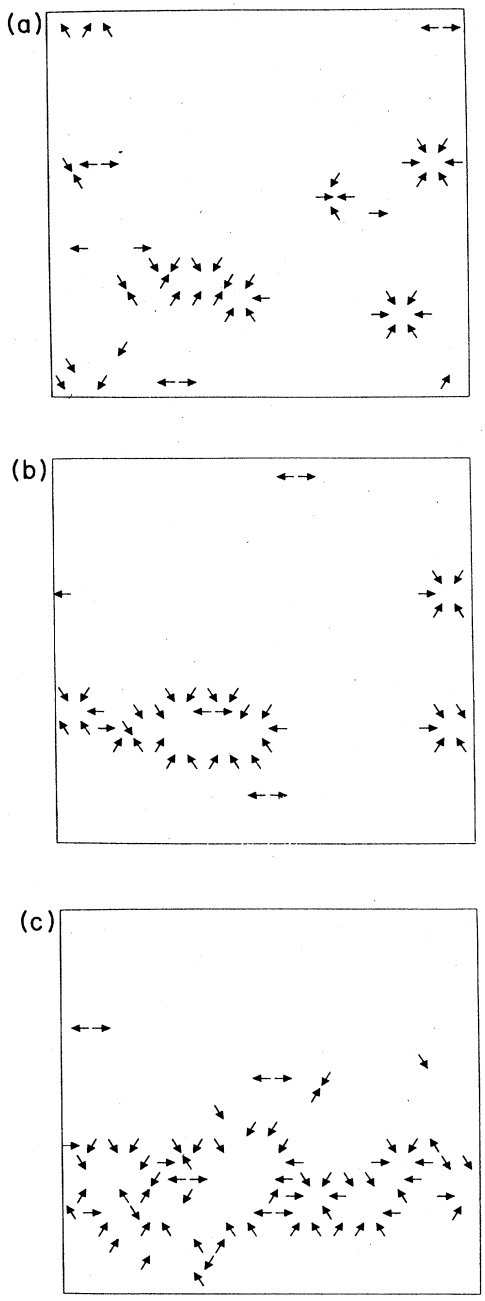

FIG. 9. Dislocation configurations near melting at Saito's lower core energy indicating the presence of grain boundaries and loops. Configurations are shown after (a) 1300, (b) 1400, and (c) 1500 Monte Carlo steps per site at the melting temperature (Saito, 1982).

Saito next lowered the dislocation core energy by subtracting a constant from the finite-sized form of the dislocation interaction. The core energy for this second simulation was $16\pi E_c/K = 3.6$. Here Saito observed a strong discontinuity and hysteresis in the energy dislocation density, elastic constant K_R, and specific heat, which he interpreted as the signature of a first-order transition. However, one hesitates to take hysteresis as a definitive sign of first-order behavior in a computer simulation where serious questions of equilibrium may be raised. A careful study of the size dependence of the specific heat would be desirable in this system. At a first-order transition, the specific heat should show a peak whose height scales proportional to the number of lattice sites.

Calculations of orientational correlations in the high-temperature phase at this lower core energy indicate that it is an isotropic liquid phase, as would be expected as the result of a grain-boundary-driven first-order transition. Configuration snapshots show the formation of grain boundaries at this transition (see Fig. 9). The work of Saito indicates therefore that at least in the system containing dislocations alone, the KTHNY theory describes the transition at high core energies, while a crossover to a first-order transition, probably driven by grain boundaries, occurs at lower core energies.

B. The Laplacian roughening model and the disclination system

An investigation of the disclination system was suggested by Nelson (1982). At low temperatures, where they are strongly bound into dislocations, disclinations interact with a potential of the form

$$H_{\text{disc}}^{\text{bare}} = \frac{K}{16\pi} \sum_{\mathbf{r}\neq\mathbf{r}'} s(\mathbf{r}) s(\mathbf{r}') \mid \mathbf{r}-\mathbf{r}' \mid^2 \ln \left| \frac{\mathbf{r}-\mathbf{r}'}{a} \right| + E_c \sum_{\mathbf{r}} s^2(\mathbf{r}) , \tag{16}$$

where $s(\mathbf{r})$ is the disclination "charge" at site r.

A model containing a system of charges interacting with the potential of Eq. (16) can exhibit, in principle, either the full KTHNY sequence of two continuous transitions separated by a hexatic phase or a grain-boundary-driven first-order melting transition. In principle, point defects such as vacancies may also be composed of disclinations. However, the energetics of these small localized defects are generally dominated by anharmonic effects and therefore will not be accurately represented by the elastic theory interactions.

Nelson proposed the Laplacian roughening model, a model for interface roughening that is dual to the disclination system. Simulations of the roughening model dual to the XY model have proved to be very useful in studying the KT transition in that system (Saito and Muller-Krumbhaar, 1984).

1. The duality relation

Duality transformations are characterized by an inverse relation between the temperature scales of the dual models. They are transformations which, when applied to the partition function of one model, show that it is equivalent to the partition function for another, dual model. Suppose we begin with a Hamiltonian of the form

$$H=\frac{J}{2k_BT}\sum_{\mathbf{r}\neq\mathbf{r}'}h(\mathbf{r})G(\mathbf{r}-\mathbf{r}')h(\mathbf{r}')\ , \tag{17}$$

where the $h(\mathbf{r})$ are integers.

The partition function for this Hamiltonian is

$$Z=\prod_{\mathbf{r}}\sum_{h(\mathbf{r})=-\infty}^{\infty}e^{-H[h(\mathbf{r})]}\ . \tag{18}$$

Using the Poisson sum rule (which amounts to inserting δ functions at integer values of h) the partition function (18) becomes

$$Z=\prod_{\mathbf{r}}\sum_{m(\mathbf{r})=-\infty}^{\infty}\int dh(\mathbf{r})\exp\left[-H[h(\mathbf{r})]+2\pi i\sum_{\mathbf{r}'}m(\mathbf{r}')h(\mathbf{r}')\right]\ , \tag{19}$$

where the $m(\mathbf{r})$ are integers and the $h(\mathbf{r})$ are now continuous variables.

Since the Hamiltonian in Eq. (17) is quadratic, the integrals over the continuous values of h may be performed by completing the square in momentum space to yield

$$Z=Z_0\prod_{\mathbf{r}}\sum_{m(\mathbf{r})=-\infty}^{\infty}\exp\left[\frac{-2\pi^2k_BT}{J}\sum_{\mathbf{q}}G^{-1}(\mathbf{q})m(\mathbf{q})m(-\mathbf{q})\right]\ , \tag{20}$$

where Z_0 is the factor obtained from the integration and the remainder is the part left over from completing the square. Z is thus related to a partition function for variables $m(\mathbf{r})$ interacting with a Hamiltonian

$$H^{\text{dual}}=\frac{2\pi^2k_BT}{J}\sum_{\mathbf{q}}G^{-1}(\mathbf{q})m(-\mathbf{q}) \tag{21}$$

and whose effective temperature is inversely related to that of the original model.

Such transformations allow the possibility of, for example, doing a low-temperature approximation for each model and thereby obtaining low- and high-temperature results for both. Their main virtue in the present case comes from the fact that the long-range interactions characteristic of the disclination model transform into short-range, easily simulable models.

2. Simulations of the Laplacian roughening model

The Laplacian roughening model (LRM) is defined by the Hamiltonian

$$H_{LR}=\frac{J}{2k_BT}\sum_{\mathbf{r}}|\Delta h(\mathbf{r})|^2\ ,$$

where

$$\Delta h(\mathbf{r})\equiv\tfrac{2}{3}\left[\sum_j[h(\mathbf{r}+\hat{\delta}_j)-h(\mathbf{r})]\right]\ . \tag{22}$$

The $\{\hat{\delta}_j\}$ are the nearest-neighbor vectors and the $\{h(\mathbf{r})\}$ are integer height variables.

Just as in the case of Saito's study of dislocation melting, the potential given here is modified to take account of the lattice. It is characterized by a natural core energy, obtained by the Monte Carlo simulation described below (Strandburg *et al.*, 1983), of $16\pi E_c/K=4.1$. A comparison of the Laplacian roughening and melting phase diagrams predicted by the KTHNY theory is shown in Fig. 10.

The behavior of the Laplacian roughening model was investigated by Monte Carlo simulation by Strandburg, Solla, and Chester (1983). Two continuous transitions separated by a phase dual to the hexatic phase were observed in these simulations. The transitions were located by studying correlations in interface height and local interface tilt across the system. The height-height and tilt-tilt correlation functions change from saturated to divergent at long distances at the roughening and unorienting transitions, respectively.

A word about the way in which these correlation functions were used is in order here. The KTHNY theory may be used in these systems to predict not only the asymptotic behavior of these correlation functions, but also their finite-size, periodic forms over the full range available in the simulated system. Fits to these forms

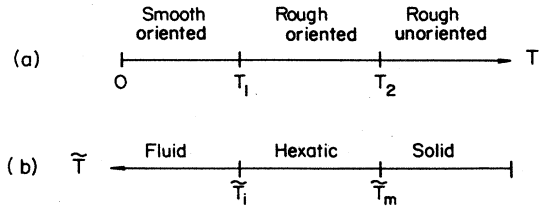

FIG. 10. Correspondence between (a) the phase diagram of the Laplacian roughening model as a function of temperature T, and (b) that of the dual disclination system as a function of temperature $\tilde{T}$, as predicted by the KTHNY theory of melting (Strandburg, Solla, and Chester, 1983).

thus provide a very good test of the KTHNY predictions. This situation is to be contrasted with that of atomistic systems, in which only the long-distance behavior of the correlation functions is predicted. Determination of the asymptotic behavior in these atomic systems is quite difficult, as will be discussed in Sec. V.C.4.

In the smooth, oriented phase the height-height correlations saturate rapidly to a constant. Figure 11 shows the behavior of the height-height correlation function in the intermediate and high-temperature phases along with the fits to the theoretical predictions.

In order to provide a model-independent check of the transition temperatures, an estimate of the change from "saturating" to "diverging" behavior of the correlation functions was made. Here the finite system size does create some difficulty since true divergences can never be seen. In order to quantify the difference between saturation and "divergence" in a finite system, the quantity r_{asym} was defined to be the distance at which the correlation function comes within 1% of its value at the size of the system. This quantity shows a distinct jump (see Fig. 12) that was identified as the transition temperature. This method of estimating the transition temperature gives results in extremely good agreement with the results of the fits mentioned above and gives strong evidence of the existence of a phase in which the height-height correlations have "diverged" while the tilt-tilt correlations remain saturated. Extremely good agreement between the phase diagram as determined by the fits to the KTHNY predictions and by this model-independent method was obtained.

It is important to note that although two transitions

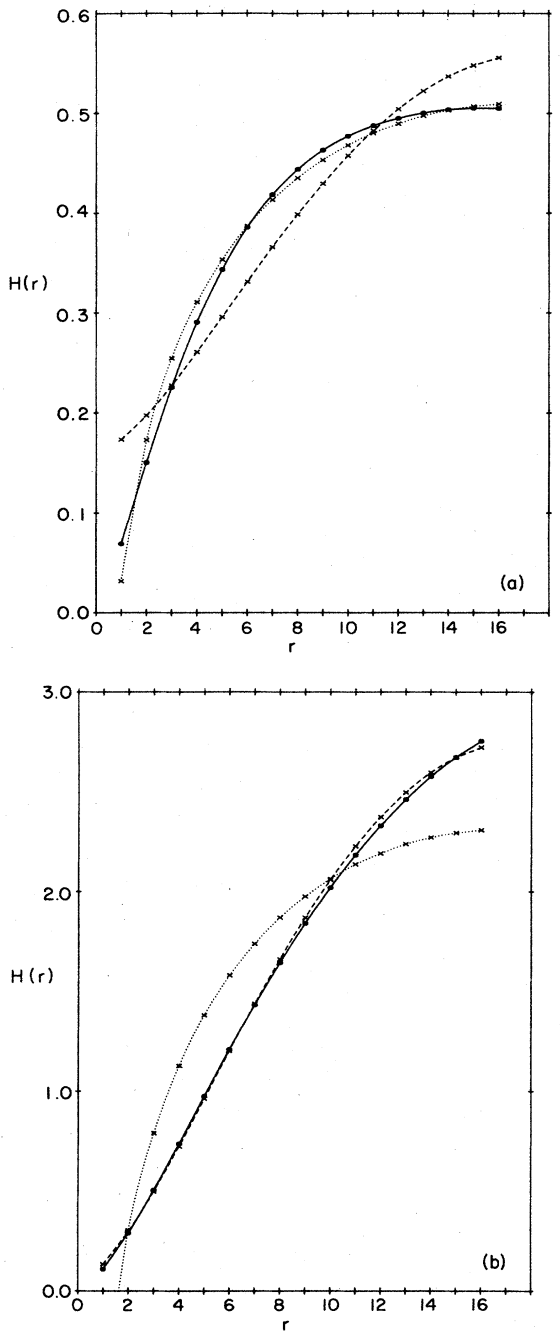

FIG. 11. Height-height correlation functions for the Laplacian roughening model in the (a) intermediate and (b) high-temperature phases. Shown in the figure are the Monte Carlo data (—·—·—·), and fits to the predicted KTHNY forms for the intermediate (× ··· × ··· ×) and high-temperature (× — — × — — ×) phases (Strandburg, Solla, and Chester, 1983).

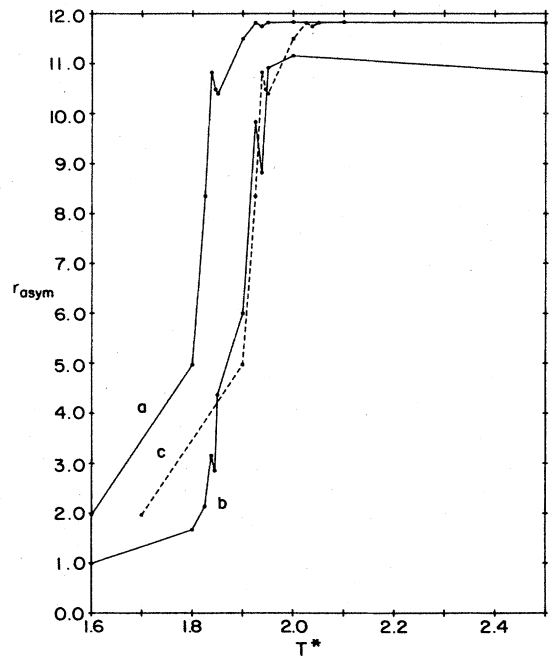

FIG. 12. r_{asym} as a function of temperature for the Laplacian roughening model as derived from the (a) height-height and (b) tilt-tilt correlation functions. An intermediate, rough, oriented phase is clearly observed. Curve *c* shows the data derived from the height-height correlations shifted in temperature by an amount $\Delta T^* = 0.1$ (Strandburg, Solla, and Chester, 1983).

are present in the Laplacian roughening model, the distance between them is only about 5% in temperature. The thermodynamic quantities show a rather sharp increase that might mislead one into thinking that the transition is first order. The KTHNY theory predicts that thermodynamic quantities will remain smooth throughout the transition, but this prediction does not preclude fairly sharp behavior, especially as the crossover to a first-order transition is neared.

Janke and Kleinert (1980, 1984) and Janke and Toussaint (1986) have argued that a first-order transition is observed in the Laplacian roughening model. Simulations of a model that is exactly equivalent to the Laplacian roughening model on a square lattice were interpreted as displaying a first-order transition. However, Janke and Kleinert caution that the natural core energy depends on the lattice structure, and the nature of the transition is expected to change with core energy. The transition may simply be different on the square lattice from the Strandburg, Solla, and Chester results for a triangular lattice.

Janke and Kleinert present as evidence of a first-order transition the apparent stability of both low- and high-temperature phases at the transition temperature. They quench a random system to the transition temperature and find that it does not order during their Monte Carlo run. Similarly, a completely ordered system, heated instantaneously to the transition temperature, does not disorder during the run. This method of determination of the order of the transition is equivalent to assuming that the observation of hysteresis in a simulation implies a first-order transition. The use of hysteresis in determining the order of a transition by computer simulation is extremely dangerous due to the fact that hysteresis may be an artifact of a simulation that heats or cools too quickly through a continuous transition and is therefore not in equilibrium in the transition region. This danger is exacerbated by critical slowing-down effects that may occur near continuous transitions.

A study by Janke and Toussaint of the system size dependence of the height of the specific-heat peak in a LRM on a triangular lattice claims that the peak height increases linearly with the size of the system for three sizes studied, implying a first-order transition. The Janke and Toussiant curve for a system of size 37×37 reaches a height of only 8 while the results of Strandburg, Solla, and Chester for a smaller system of size 32×32 reach a considerably greater height of about 14.

The methods used to obtain the specific heat in these systems (numerical differentiation of the energy and energy fluctuations) can only underestimate the specific heat. A possible explanation for the discrepancy is that Janke and Toussaint may have inadvertently missed the specific-heat peak by taking temperature increments that were too large. Indeed, the entire peak observed by Strandburg, Solla, and Chester fits between data points on the Janke and Toussiant plot. Figure 13 shows the specific-heat data of Strandburg, Solla, and Chester. The increment between data points on the Janke and Toussaint curve for size 37×37 near the peak is indicated. Perhaps the size dependence observed by Janke and Toussaint is explained by the fact that they have taken progressively closer temperature increments as the system size is increased. In fact, the peak height and width at their largest system size (smallest sampling interval) of 58×58 agree rather well with the value obtained by Strandburg, Solla, and Chester for the 32×32 lattice, suggesting a size-independent specific-heat peak consistent with the KTHNY theory.

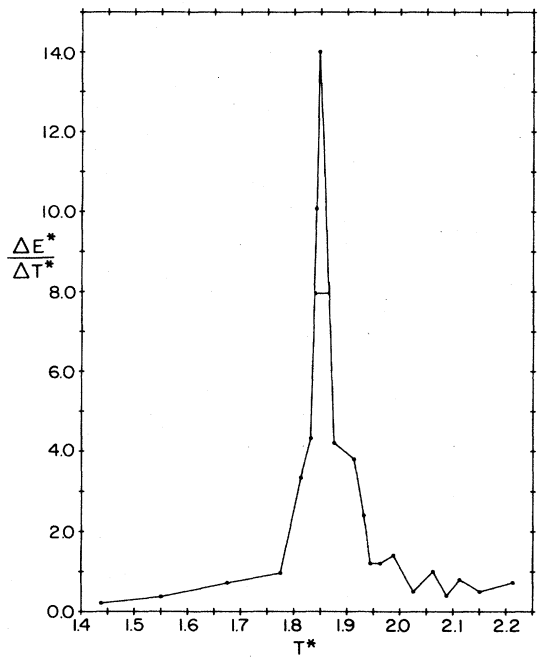

FIG. 13. Specific heat as a function of temperature for the Laplacian roughening model (Strandburg, Solla, and Chester, 1983). The temperature interval between data points for the Janke and Toussaint calculation is also shown (—), located near their peak height of about 8.

3. Laplacian roughening model with other core energies

Strandburg (1986) modified the Laplacian roughening model to allow changes in the disclination core energy. Because the change from the natural core energy leads to long-range interactions in the corresponding Laplacian roughening model, an approximate model was derived with short-range interactions. This model, valid in the limit of small deviations, δE_c, from the natural core energy is given by

$$H_{MLR}=\frac{1}{2T^*}\sum_{\mathbf{q}}[G^{-2}(\mathbf{q})-\gamma G^{-4}(\mathbf{q})]h(\mathbf{q})h(-\mathbf{q}) , \tag{23}$$

where

$$G(\mathbf{q})=\left[4-\tfrac{2}{3}\sum_j \cos(\mathbf{q}\cdot\hat{\delta}_j)\right]^{-1}$$

and

$$\gamma=\frac{\sqrt{3}}{32\pi}\delta E_c$$

in momentum space. In real space the interactions extend out to fourth neighbors in the triangular lattice. This model was analyzed using the correlation function methods described above to yield the phase diagram shown in Fig. 14. This phase diagram and the apparent divergence of the specific-heat maximum (see inset in Fig. 14) near a core energy of 2.7 give evidence of a core-energy-dependent crossover from KTHNY-type behavior to a first-order transition. The melting temperatures obtained from this simulation were in reasonably good agreement with the predictions of the KTHNY recursion relations for core energies below the natural core energy down to 2.7, indicating that the approximation of small core energy change is not seriously wrong in that region.

For technical reasons the approximate model breaks down rather catastrophically at short distances for core energies above the natural core energy, leading to higher effective core energies and eventually to a nonphysical interaction. Fortunately, these problems are confined to the less interesting region above the natural core energy and do not affect the study of the crossover behavior.

Finite-size scaling analysis was performed for several core energies. The dependence of three thermodynamic quantities on system size was investigated. At the highest core energy investigated all three quantities displayed the behavior predicted by the KTHNY theory. At the lowest core energy investigated the behavior was as expected for a first-order transition, confirming the crossover from KTHNY to first-order behavior as core energy is decreased, which had been inferred from the correlation function study.

The behavior of the specific heat at two intermediate core energies is shown in Fig. 15. At a core energy of 3.5, behavior characteristic of the crossover multicritical point is observed. At 2.7, multicritical behavior is observed at the smallest sizes, with a crossover to first-order behavior evident at the largest size. The multicritical exponents obtained from the two core energies are in extremely good agreement. Assuming hyperscaling ($d\nu=2-\alpha$), the exponents are $\nu=0.58\pm0.03$, $\alpha=0.85\pm0.06$.

It is interesting to compare these results to those of Saito (1982a, 1982b). The transition temperature of Saito's higher core energy is in good agreement with the Laplacian roughening model results and with the KTHNY recursion relations. At Saito's lower core energy, however, the Laplacian roughening model gives a sequence of two continuous transitions at a temperature that is not in agreement with Saito's results (see Fig. 14). It is quite possible that the crossover core energy is dependent on details of the model and that the value is simply different in the dislocation simulation. It is also possible that Saito's effective core energy is lower than the quoted value due to the same effect that gives higher effective core energies for Laplacian roughening model core energies above the natural value. (The sign of this effect is reversed due to the duality transformation.)

Janke and Kleinert (1984) have also investigated a variation of the Laplacian roughening model on a square lattice (in a different but equivalent language). They have found a tricritical point at the natural core energy. The term which they have added to the Hamiltonian in an attempt to change the core energy is (in Laplacian roughening language)

$$[h(\mathbf{r})-h(\mathbf{r}+\hat{x})]^2[h(\mathbf{r})-h(\mathbf{r}-\hat{y})]^2 . \quad (24)$$

This term, however, does not preserve the tilt symmetry of the original Hamiltonian since, when $h(\mathbf{r})\rightarrow h(\mathbf{r})+1/2\pi\mathbf{G}\cdot\mathbf{r}$, the energy is changed. This symmetry violation corresponds, in the dislocation model, to al-

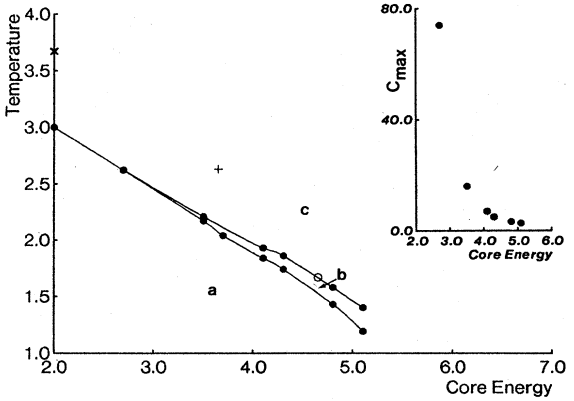

FIG. 14. Phase diagram of the Laplacian-roughening model in the core-energy-temperature plane showing the transition temperatures T_1 and T_2. These transitions separate the (a) flat, oriented, (b) rough, oriented, and (c) rough, unoriented phases. Also shown are Saito's results for T_2 for two core energies at which he observed continuous (0) and first-order (+) transitions, respectively. The HN prediction for the location of the transition at $E_c=2.0$ is also shown (×). The lines are simply a guide to the eye. Inset shows the maximum specific heat C_{max} as a function of core energy E_c (Strandburg, 1986).

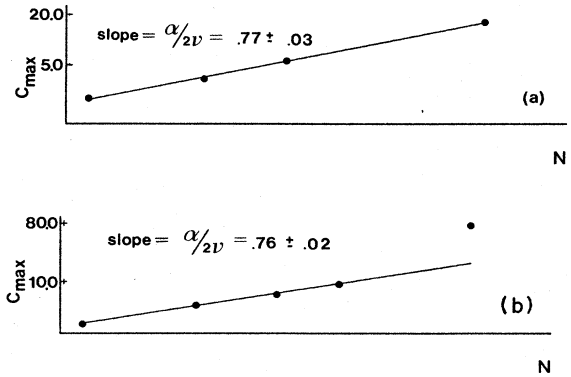

FIG. 15. Logarithm of C_{max} vs logarithm of system size N at $E_c=$(a) 3.5 and (b) 2.7 (Strandburg, 1986).

lowing isolated dislocations at low temperatures in the solid. Qualitative change is thus expected when this term is added.

IV. EXPERIMENTAL INVESTIGATIONS OF THE TWO-DIMENSIONAL MELTING TRANSITION

A. Introduction

Four categories of experimental systems have been studied in order to probe the nature of the 2D melting transition: (a) layered liquid-crystal phases, (b) electrons on the surface of liquid helium, (c) various gases adsorbed on graphite, and (d) a colloidal suspension of charged submicron-sized spheres. The comparison of these experiments with theories for two-dimensional melting is difficult both because the experiments in themselves are difficult and because the most revealing theoretical quantities are hard to measure. In addition, most of the experimental systems are not ideal two-dimensional systems. The effects of this nonideality on the transition behavior may in principle be substantial.

Adsorbed gases and liquid-crystal films may be explored in great detail by high-resolution x-ray diffraction measurements, heat capacity and isotherm measurements, and, in the case of liquid-crystal films, mechanical measurements of elastic response. The development of high-intensity synchrotron x-ray sources and of well-oriented single-crystal samples has even allowed investigations of bond-orientational ordering in these systems. However, the number of substances for which a complete set of measurements has been made is still limited. Determining the order of the melting transition is surprisingly difficult, and the results for most systems are still quite controversial.

The adsorbed gas systems depart from ideal two-dimensional systems in two respects: They have important interactions with the substrates, and they display phenomena associated with the formation of more than one layer of adsorbate. Liquid-crystal films, while devoid of substrate effects, are complicated by interlayer couplings and, even in the thinnest films, by couplings of bond-orientational order to order in the molecular orientation or "tilt." These complicating factors give rise to rich phase diagrams in the adsorbed gas and liquid-crystal systems. They also contribute to the difficulties in interpretation mentioned above.

The system of electrons suspended above the surface of liquid helium provides, on the other hand, a nearly ideal example of a simple 2D system. The liquid-helium substrate provides no ordering potential and the behavior is classical in the appropriate density regimes. All available experimental results on this system favor the Kosterlitz-Thouless melting theory. However, the range of measurements available for these systems is limited to dynamic measurements of coupled electron-helium modes. Interpretation of these measurements requires a large amount of theoretical input. No direct structural measurements are available and, in particular, none of the experiments are sensitive to bond-orientational order.

The system of submicron-sized charged spheres provides in some respects a bridge between experiment and simulation. Because the spheres are macroscopic their motions may be directly observed and correlation functions, for example, computed from photographs.

In spite of the difficulties inherent in most of the experimental systems, the experimental results on two-dimensional melting are extremely interesting. Apparently continuous transitions have been observed in a number of systems and evidence for the hexatic to isotropic transition exists in some. In this brief review we concentrate on those experiments that show behavior differing from the strong first-order transitions typical of three-dimensional melting. Interestingly, the number of systems that belong in this category has continued to increase as more and more detailed experiments have been done.

B. Experimental studies of liquid-crystal films

Liquid-crystal materials are composed of anisotropic molecules. These molecules are generally of a very complicated chemical makeup. One example of such a compound is 4-*n*-pentylbensenethio-4′-*n*′-tetradecyloxybenzoate. Luckily, the details of the composition of these molecules are irrelevant for the phase transitions that concern us. We will therefore refer to them by their shorthand names (14S5 in the case cited) and visualize them as rods. There are also liquid crystals composed of flat, disklike molecules. We do not discuss them here. A typical size of the molecules that are discussed in this section is $25\times5\times5$ Å^3.

Although there is still need for considerable study in these liquid-crystal systems, the evidence is mounting that, at least in some thin films, the KTHNY phase sequence has been observed (Collett *et al.*, 1984; Davey *et al.*, 1984; Sirota *et al.*, 1985; Dierker *et al.*, 1986). Whether the transitions themselves obey the KTHNY predictions is open to further study (Davey *et al.*, 1984; Dierker *et al.*, 1986). In addition, the KTHNY picture, developed to describe behavior of two-dimensional systems, has proved useful in gaining insight into some interesting three-dimensional phases.

1. Summary of liquid-crystal phases

The combinations of positional, molecular-orientational, and nearest-neighbor-bond-orientational orderings possible in liquid-crystal systems lead to a rich variety of phases and phase transitions. Of particular interest in the study of two-dimensional phase transitions are the smectic phases. These phases are illustrated in Fig. 16. In these phases a standing density wave along one direction produces a "layered" system that can often be thought of as a stack of weakly coupled two-dimensional

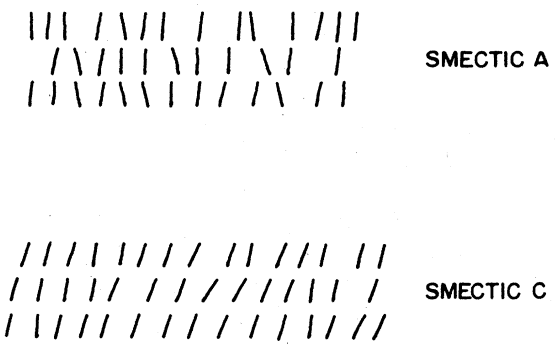

FIG. 16. Schematic representation of the liquid-crystal phases smectic A and smectic C.

layers. The density wave in these phases possesses quasi-long-range order. Both bulk smectic systems and thin films consisting of as few as two molecular layers have been studied. In the smectic-A phase the molecules exhibit liquidlike ordering within the layers, while the molecular long axes are perpendicular to the layers. In the smectic-C phases the molecular axes assume an overall "tilt" with respect to the layer normal. These phases are often characterized by chirality (i.e., the direction of molecular tilt rotates as one proceeds from layer to layer).

Upon cooling, the smectic-A phase may undergo a transition to a phase in which some hexagonal order appears within the layers. These phases have been known as B phases and it has recently been shown that they are of two types—the hexatic-B and crystalline-B phases. The crystalline-B phase is actually a solid displaying long-range positional and bond-orientational order in three dimensions. Such a phase may be thought of as a stack of two-dimensional crystals. Since the two-dimensional crystal displays quasi-long-ranged positional order, its susceptibility to a positional ordering field is infinite. Interlayer forces provide such a field and the positional order in the stacked layers is long range in three dimensions. As the number of layers is decreased there should be a crossover to two-dimensional behavior characterized by quasi-long-range positional order. Experiments described in Sec. IV.B.3 show that very thin films of the crystalline-B phase display power-law structure factors characteristic of 2D solids.

Birgeneau and Litster (1978) suggested the possibility of a "stacked hexatic" phase. Such a phase may be viewed as a stack of 2D hexatic layers characterized by short-range positional order and by quasi-long-range bond-orientational order. These layers thus have an infinite susceptibility to a bond-angle ordering field, and the stacked hexatic will display long-range bond-orientational order while maintaining short-range positional order within the layers. We will refer to these phases as long-range hexatics to distinguish them from the two-dimensional hexatics with which we are primarily concerned in the rest of this article. An order-parameter theory of these long-range hexatics has been worked out by Bruinsma and Nelson (1981) and by Aeppli and Bruinsma (1984). Again, one may hope that very thin films of materials that display a three-dimensional hexatic-B phase (with long-range bond-orientational order) will cross over to 2D hexatics as the number of layers is decreased. Evidence for such behavior is described below.

Materials that display smectic-C (tilted molecular axes) phases also may have long-range hexatic phases. The possible phase diagrams for these materials are even more complicated than for materials in which the molecular axes remain perpendicular to the layers. Two distinct three-dimensional long-range hexatic phases are observed in these materials. Smectic-I and smectic-F are distinguished by the direction of molecular tilt with respect to the local positional structure of the system.

A theoretical discussion of the expected phase diagram of a two-dimensional system with molecular tilt was provided by Nelson and Halperin (1980). The resulting phase diagram is shown in Fig. 17. Additional defects associated with ordering of the molecular tilt are added to the usual KTHNY theory. The molecular tilt may be thought of as providing an orienting field, similar to that produced by a substrate. In the presence of molecular tilt ordering, quasi-long-range bond-orientational order is always present. Thus no true liquid should occur in "tilted" systems.

According to this theory, the smectic-C phase should actually be a stack of bond-orientationally ordered layers, rather than a stack of fluid layers as has been previously supposed. The bond-orientational order should be rather weak, however, since it is induced by the tilt ordering. Such a phase would differ from a true hexatic since the orientational susceptibility would remain finite and the Frank constant K_A would remain small. The smectic-C phase is comparable to the liquid phase in an adsorbed system. There, weak bond-orientational order is always induced by the substrate. In this picture, no real transi-

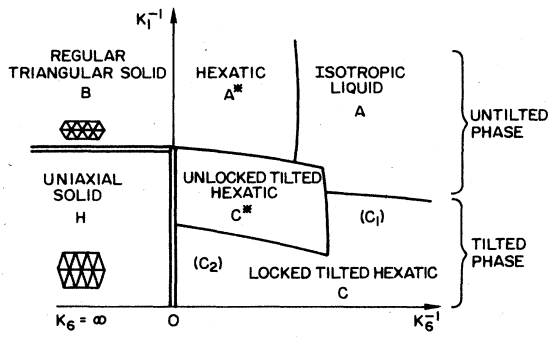

FIG. 17. Phase diagram for smectic liquid-crystal layers, as a function of the inverse temperature-dependent Frank coefficients $K_1^{-1}(T)$ and $K_6^{-1}(T)$. Both solid and fluid phases are shown, and these can be either tilted or untilted. The Frank constant K_6 is infinite in the solid phases. Experiments with varying temperature might trace a path from the lower-left to the upper-right portion of the figure, with increasing temperatures (Nelson and Bruinsma, 1980).

tion would separate the smectic-*C* and long-range hexatic phases. Indeed, synchrotron x-ray studies of a material previously thought to have displayed a smectic-*C* to hexatic transition have shown that no true phase transition occurs (Brock *et al.*, 1986). However, if the coupling of bond-orientational order and molecular tilt is sufficiently weak, the observed behavior may be experimentally indistinguishable from the zero-coupling behavior.

2. Experimental methods

As mentioned above, three methods have primarily been used in the experimental study of liquid-crystal phases. Thermodynamic measurements are used to map out the phase diagrams and to investigate the order of the transition and the appropriate critical exponents. Measurements of the in-plane shear modulus are made using a torsional oscillator technique. An annular film of a controlled thickness is drawn between the edges of two disks. The top disk is a torsional oscillator whose resonant period may be accurately measured. As the resistance to shear of the suspended film changes, the resonant period of the oscillator changes in a manner proportional to the in-plane shear modulus. Using this method the change in period may be measured as a function of temperature and the shear modulus determined.

The development of synchrotron radiation facilities and techniques has allowed for extensive high-resolution x-ray diffraction studies that probe the structure of these materials. Because these free-standing liquid-crystal films have no substrate to produce extra background scattering, they make particularly good subjects for x-ray scattering studies. Very thin films of the crystalline phases will be expected to show the power-law structure factors characteristic of two-dimensional solids.

Bulk long-range hexatic phases will be expected to show square-root Lorentzian line shapes (Aeppli and Bruinsma, 1984). Spots will be observed, rather than rings, due to the long-range bond-orientational order. Such spots will be observed if the orientational domains within the sample are large enough. An infinite 2D hexatic phase, on the other hand, would be expected to show a liquidlike diffuse ring of scattering due to the algebraic decay of the bond-angular order. In any real experiment, however, angular correlations extending the length of the sample will provide a modulation of the ring, leading to a pattern of six asymmetric spots whose broadening in the angular direction grows with sample size. The radial spot width will be determined by positional correlations, and the angular width by orientational fluctuations.

Recently, a clever experiment exploiting the link between bond-orientational order and molecular tilt order in materials forming smectic-*C* ("tilted") phases has been performed by Dierker *et al.* (1986). They used light scattering to observe the defect structure in the molecular tilt ordering and then used the observed structure to infer information about the bond-orientational order. Their results are discussed below.

3. Experimental results

Untilted systems. The long-range hexatic-*B* phase was first observed in the liquid crystal 650BC (Huang *et al.*, 1981). The hexatic-*B* phase is characterized in x-ray scattering experiments by short-range liquidlike positional order accompanied by long-range orientational order within the layers. The positional correlation length in this phase, while finite, is quite long ($\sim$100 A), corresponding to approximately 20 atomic spacings (Huang *et al.*, 1981; Davey *et al.*, 1984). The long-range hexatic-*B* phase does not support an in-plane shear, as is expected from the lack of positional order (Pindak *et al.*, 1982).

Neither the smectic-*A* ("layered liquid") to long-range hexatic-*B* nor the hexatic-*B* to crystal phase transition is expected to be of the Kosterlitz-Thouless type in these three-dimensional phases. Indeed the hexatic-*B* to crystal transition is strongly first order. The critical behavior near the long-range hexatic to layered liquid transitions appears to vary depending upon the system studied in a way which is not yet understood (Huang *et al.*, 1981; Viner *et al.*, 1983; Davey *et al.*, 1984; Huang *et al.*, 1986). It is often characterized by a specific-heat exponent near 0.5, possibly indicating the presence of a Gaussian tricritical point (Huang *et al.*, 1981; Bruinsma and Aeppli, 1982; Viner *et al.*, 1983; Davey *et al.*, 1984; Huang *et al.*, 1986). A general argument has been proposed to explain the appearance of this tricritical point (Aharony *et al.*, 1986).

An important observation with probable implications for two-dimensional systems is that the layered liquid to long-range hexatic transition is accompanied by a rapid increase in positional order as evidenced by a sharpened radial width of the structure factor, as well as by the appearance of the angular modulations of the scattering, which characterize the long-range hexatic ordering. The theoretical calculation of Aeppli and Bruinsma (1984) related this increased positional order to the bond-orientational order. The radial width of the structure factor was given in terms of the specific-heat exponent and amplitude. The experimental results show a good fit to this theoretical relationship (Davey *et al.*, 1984).

An apparently continuous hexatic to liquid transition in a two-layer film has been observed in one of these untilted materials, suggesting that the two-dimensional behavior of that material may conform to KTHNY predictions (Davey *et al.*, 1984). In the very thinnest of the hexatic films (two or three molecular layers) the sixfold modulation of the structure factor is no longer observable, although the increase in positional correlations characteristic of the long-range hexatic to layered liquid transition is observed. The disappearance of the structure factor modulation is consistent with a crossover from long-range to quasi-long-range bond-orientational order and the appearance of the large angular fluctuations expected in two dimensions.

Tilted systems. Long-range hexatic phases are also ob-

served in systems with molecular tilt ordering (Pindak *et al.*, 1982). Bond-orientational order is observed in these phases and has recently been observed in a smectic-C (tilted layered liquid) phase as well (Brock *et al.*, 1986). Presumably the bond-orientational order in the observed long-range hexatic phase is intrinsic, rather than induced by the tilt, and is thus much stronger than the induced bond-orientational order of the smectic-C phase.

Thus, the behavior of these systems is very similar to that observed for the materials forming smectic-A phases. At high temperatures the layers show fluidlike ordering. There is an apparent transition to a phase with long but still finite positional correlations and long-range bond-orientational order, and then a first-order freezing transition (Sirota *et al.*, 1985). The behavior of these tilted systems as a function of film thickness has also been studied. In some systems the long-range hexatic phases only appear as film thickness is decreased (Sirota *et al.*, 1985).

Exploiting the locking in the long-range tilted hexatic phase of the bond-angle field to the director field of the molecular axes, Dierker *et al.* (1986) use the structure of disclinations observed in light scattering experiments to deduce information about the relative strengths of the elastic constants related to director twist and bond-angle twist (K_A). A defect structure observed in the long-range tilted hexatic phases is shown in Fig. 18.

In the hexatic phase a "star" appears whose arms separate regions in which the molecular axes (and hence the bond orientations) remain ordered. The sudden 60° shifts in orientation of the director at the boundaries of these regions are made so as to preserve the bond-orientational order. The appearance of this structure implies a dominance of the bond-angle elastic constant over that associated with director twist. The fact that these arms appear at the smectic-C to long-range tilted hexatic transition indicates that bond-orientational order that is not induced by the coupling to the molecular tilt has occurred. An elastic calculation relates the length and number of the "arms" to the value of K_A. The five arms observed at the transition are the number that would be expected for a value of K_A of $72/\pi$, the value predicted by the KTHNY theory.

The hexatic to crystal transition in very thin films has not been studied in detail in untilted systems. In systems in which the molecular axes are tilted, however, the long-range hexatic to three-dimensional crystal transition has been studied as a function of film thickness. The transition was found to grow less abrupt as the film thickness decreased. For example, in one system the first-order jump in the positional correlations decreased as the number of layers decreased to 5 (Sirota *et al.*, 1985). The Dierker *et al.* (1986) experiment provides information about this transition as well. Since the arm length of the "star" observed in the center of the disclinations can be related to the bond-orientational elastic coupling K_A, it can be used to measure the behavior of K_A near the long-range tilted hexatic to crystalline transition. The arm length appears to diverge as the transition is approached. A fit of this divergence to a form predicted by KTHNY,

$$K_A \sim \exp[c/(T-T_m)^{\nu}] , \tag{25}$$

gives an exponent in good agreement with the KTHNY theory.

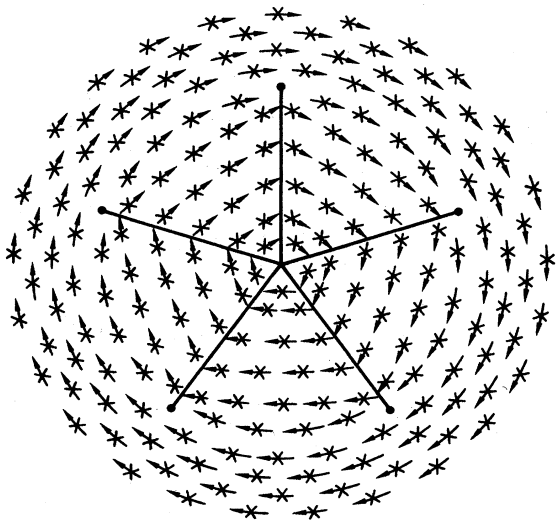

FIG. 18. Point disclination of $S=+1$ in the smectic-C^* phase of a two-layer film develops, upon cooling, in the hexatic-I^* phase five straight radial disclination arms. The calculated director- and bond-orientation pattern about the five-armed star defect is shown. The arrows indicate the local orientation of the director; the crosses, the local orientation of the sixfold symmetric bonds (Dierker, Pindak, and Meyer, 1986).

C. Electrons on the surface of liquid helium

The classical freezing transition of electrons on the surface of liquid helium was first observed by Grimes and Adams (1979). An electric field was set up perpendicular to the helium surface by means of a capacitor that had the positive plate submerged in the helium. The force thus applied was balanced by the repulsion between the electrons and the helium. The distance between electrons in these experiments was large, so the electrons behave classically.

Because the electron Boltzmann factor is given by $\exp(-V/k_B T)$, where V is a sum of pair potentials,

$$v(r_{ij}) = \frac{e^2}{r_{ij}} , \tag{26}$$

the phase diagram may be expressed in terms of one combined density-temperature parameter Γ (proportional to the square root of the density divided by the temperature). The densities accessible at a temperature of 0.5 K

($10^5 < n < 10^9$ cm^{-2}) corresponded to a range of Γ of $2 < \Gamma < 200$. The electron system forms a gas for $\Gamma < 1$ and a liquid for $1 < \Gamma < 100$. Observations of the electron system were made by measuring the density dependence of coupled modes of the electron system and helium capillary waves. These modes appear when the electron system crystallizes, because the repulsion between the electrons and the helium produces a small ($\frac{1}{10}$ Å deep) dimple under each electron, thus coupling the phonons of the electron system to capillary waves or "ripplons" on the helium surface. The appearance of these coupled resonances signals the onset of freezing.

The mobility of the electrons in a 2D lattice was measured by Mehrotra, Guenin, and Dahm (1982). An ac voltage was applied to one end of the submerged capacitor plate, which was divided into three electrically isolated segments. The response was measured at the other end. The time delay between applied signal and response reflected the electron mobility. A measure of "excess scattering" was obtained by subtracting a background determined by the known behavior for the liquid and for the low-temperature crystal. A peak in excess scattering was observed near the melting transition. The authors conjectured that this excess scattering was due to the dissociation of dislocation pairs. The value of Γ at melting ($\Gamma = 124 \pm 4$) was consistent with values obtained from the KT theory and from Monte Carlo simulations (Fisher *et al.*, 1979; Gann *et al.*, 1979; Morf, 1979).

Guo *et al.* (1983) performed a similar experiment. They probed the frequency dependence of the excess scattering. They compared this frequency dependence to an adaptation of the Ambegaokar *et al.* (1980) theory for the dynamics of the KT transition in 2D superfluids, and obtained good agreement with the KT theory.

Gallet *et al.* (1982) deduced values for the shear modulus μ from the coupled electron-helium modes, by relating the shear modulus to the effective mass of the "dimple." They found good agreement with the KT prediction for the value of μ at melting.

Thus all available experimental data on the 2D electron system supports the KTHNY melting theory. Unfortunately, these experiments contain no information about bond-orientational order and thus can make no comment concerning the HNY predictions for the hexatic phase.

D. Adsorbed gases

1. Introduction

Adsorbed gases provide an almost inexhaustible number of possible combinations of substrate and adsorbate and there have been many, many studies of such systems. Here, we concentrate on systems physisorbed on graphite substrates. In particular, we are interested in the phases that are incommensurate with the graphite substrate, in which the approximation to a strictly two-dimensional system is closest.

These systems often have phase diagrams which, in the appropriate regions, look very much like the phase diagrams of their three-dimensional counterparts. The phase diagram of xenon on graphite, for example, is shown in Fig. 19. As the amount of gas adsorbed on the substrate increases, however, these systems can show interesting layering effects including roughening transitions and wetting transitions. We will not discuss these phase transitions here.

While the substrate does not impose positional order on these incommensurate phases, the ground states of these solids have a preferred orientation with respect to the graphite crystal axes. Novaco and McTague predicted this "orientational epitaxy" (Novaco and McTague, 1977; McTague and Novaco, 1979). When the lattice constant is not commensurate with the graphite substrate, the zero-temperature state may not be aligned with the graphite axes, but it may be rotated by some finite angle. These systems may undergo a transition from the rotated state to a state aligned with the substrate symmetry axes. In the aligned state the adsorbate is believed to be described as a collection of commensurate patches separated by domain walls (Shiba, 1980; Gordon and Villain, 1982). Depending upon the ordering of the domain walls, the aligned state may be either solid or liquid.

Long-range bond-orientational ordering is always imposed by the substrate. The effect of the long-range bond-orientational ordering is to smear out any possible hexatic to isotropic transition. The two-dimensional liquid phases in these systems always have substrate-induced long-range bond-orientational order. However, if an adsorbed system passes near the point at which a substrate-free hexatic to isotropic transition would occur, some remnant of the transition may be observed (just as in the case of a ferromagnet in a small magnetic field, one

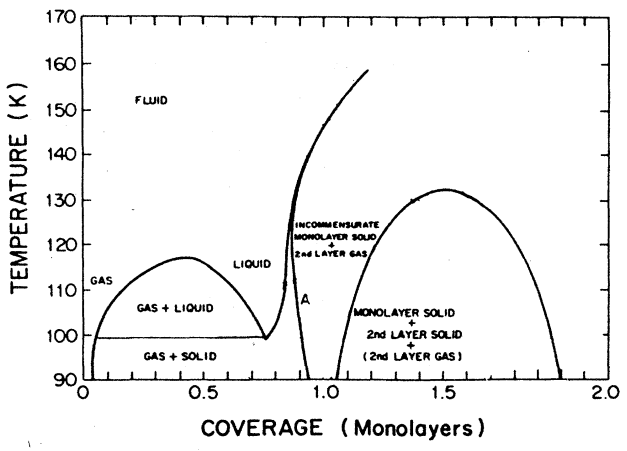

FIG. 19. Phase diagram of xenon on graphite between 0 and 2 monolayers (Heiney *et al.*, 1983).

may observe a remnant of critical behavior when passing near the zero-field critical point). Indeed, the effect of the substrate may be modeled by a sixfold field h_6, which couples to the bond-orientational order.

2. Experiments on specific systems

Rather than attempt an exhaustive review of experiments on systems physisorbed on graphite, we will briefly discuss some systems in which unusual melting behavior has been observed with emphasis on recent, high-resolution experiments. These systems include the noble gases xenon, krypton, argon, and helium as well as ethylene and CF_4. Experimental phase diagrams are shown in Figs. 19–24.

a. Krypton, xenon, and argon on graphite

Comparisons of the xenon, krypton, and argon phase diagram are interesting because these systems are all rather well described by a Lennard-Jones potential. Their bulk phase diagrams are essentially the same when scaled by the appropriate Lennard-Jones parameters. The differences in the two-dimensional phase diagrams must be due to differences in their interactions with the graphite substrate.

Krypton on graphite. The size of krypton is such that its substrate-free lattice spacing is similar to the spacing that would be imposed by the graphite substrate. Thus, krypton at monolayer densities freezes into a commensurate solid whose melting properties may be described by lattice models. As the density is increased, krypton on graphite exhibits a novel transition into a reentrant fluid phase that may be described as a domain-wall fluid (Birgeneau *et al.*, 1981; Coppersmith *et al.*, 1981; Abraham *et al.*, 1982). At yet higher densities krypton on graphite forms an incommensurate solid (Butler *et al.*, 1980; Specht *et al.*, 1984). The melting of the incommensurate solid is of interest for this discussion.

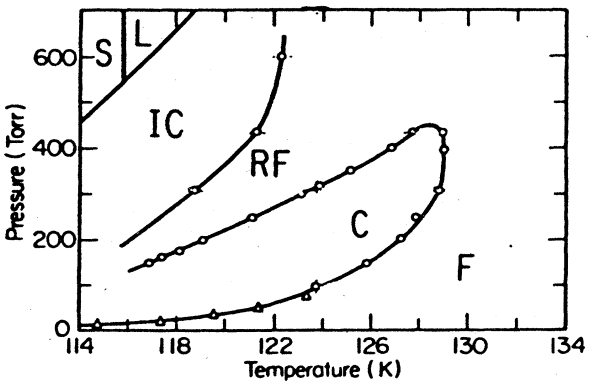

FIG. 20. Phase diagram of near-monolayer krypton: *F*, fluid; *C*, commensurate solid; RF, reentrant fluid; IC, incommensurate solid; *S*, bulk solid; *L*, bulk liquid (Specht *et al.*, 1984).

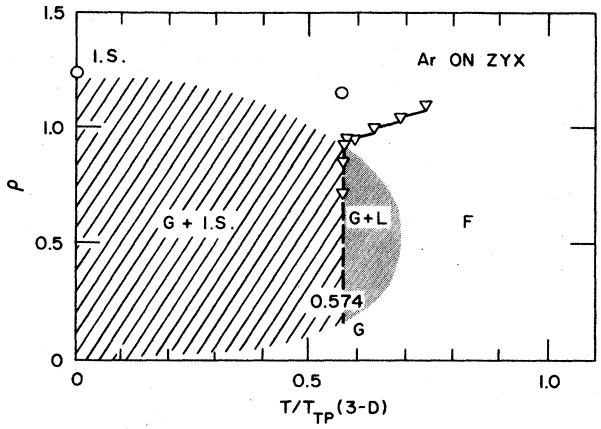

FIG. 21. Experimental phase diagram of argon on graphite. Phases shown are gas (*G*), fluid (*F*), and incommensurate solid (IS) (McTague *et al.*, 1982).

Specht *et al.* (1984) have performed synchroton x-ray studies that indicate that the incommensurate melting is continuous. These transitions are very broad, in contrast to the melting of incommensurate xenon, and there is as yet no connection of the observed continuous melting to any theory. A transition to a rotated state occurs well inside the solid and therefore is not a factor in the melting transition. The incommensurate melting occurs at coverages well above one monolayer. The effect of the second layer on the melting transition is not known.

Argon on graphite. The argon atom is smaller than the krypton atom and its natural lattice spacing is 8% smaller. This spacing is different enough from that of the graphite substrate that argon always forms an incommensurate solid structure. Until recently it was believed that argon on graphite always melts continuously, even in the submonolayer region. The evidence for this belief was derived from x-ray scattering studies (McTague *et al.*, 1982) and from measurements of heat capacity (Chung, 1979). Vapor-pressure isotherm measurements

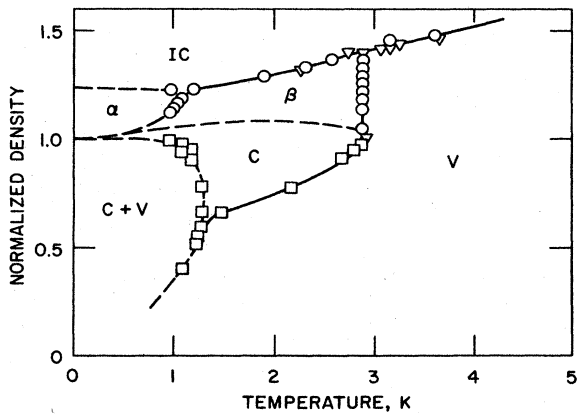

FIG. 22. Phase diagram of ^{4}He on graphite. Solid lines indicate well-defined phase boundaries. Dashed lines indicate suspected phase boundaries (Motteler, 1985).

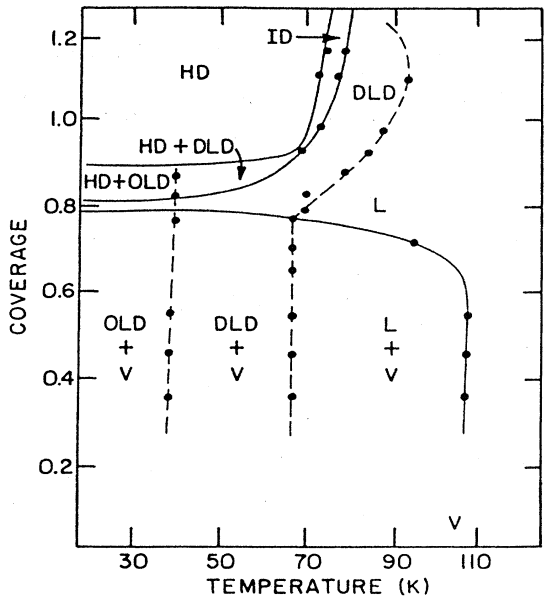

FIG. 23. Experimental phase diagram for ethylene on graphite. Phases shown are liquid (L), vapor (V), high-density solid (HD), ordered low-density solid (OLD), disordered low-density solid (DLD), and intermediate density solid (ID). "Ordered" and "disordered" refer to the orientations of the molecular axes, which are thought to lie in a plane in these low-density phases (Kim, Zhang, and Chan, 1986).

(Larher, 1983) also showed a broad melting region. McTague *et al.* (1982) found a gradual continuous increase of the positional correlations near melting in a synchroton x-ray study of submonolayer argon. The form of the variation of correlation length with temperature was shown to be consistent with a prediction of the KTHNY theory over a rather broader temperature interval than was expected from calculations of the width of the KTHNY critical region. There was also a broad specific-heat peak centered just above the temperature at which the correlation length diverged, consistent with the KTHNY predictions.

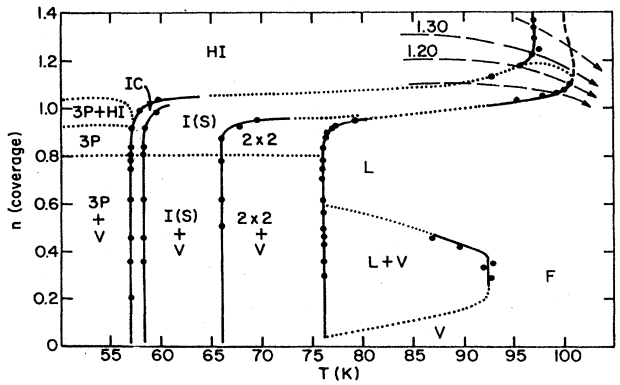

FIG. 24. Experimental phase diagram of CF_4 on graphite. Phases shown are liquid (L); fluid (F); vapor (V); hexagonal incommensurate (HI); two commensurate phases (2×2 and $3P$); and two phases, whose identification is uncertain and is discussed in the text [$I(S)$ and IC] (Zhang, Kim, and Chan, 1986).

More detailed recent heat-capacity studies in the submonolayer region by Migone *et al.* (1984) reveal a small, rather sharp ($\sim$0.3 K in width) heat-capacity peak that had previously been buried in the broad peak mentioned above. The broad peak is centered at a temperature about 6% above that of the sharp peak. The sharp peak occurs at a coverage-independent temperature, consistent with the melting temperature observed in the scattering studies. It is identified by Migone *et al.* as a signature of first-order, triple-point melting. If this interpretation is correct, the broad peak may well be a remnant of the hexatic to isotropic transition. It is also possible that the small sharp peak is due to continuous KTHNY melting, since the KTHNY theory does not predict the width or height of the specific-heat peak, but only states that it does not diverge.

Indeed, recent synchroton x-ray experiments by Nielsen *et al.* (1987) contest the conclusion of Migone *et al.* (1984) that the melting of submonolayer argon is first order. Nielsen *et al.* observe a continuous evolution from liquid to solid, with liquid correlation lengths reaching approximately 1000 Å. Over a temperature interval comparable to the width of the sharp heat-capacity peak, they observe a continuous evolution of the correlation length from 200 to 900 Å. These recent x-ray studies continue to be consistent with predictions of the KTHNY theory for the temperature evolution of the correlation length and diffraction peak intensities. Indeed, they probe an effective temperature region closer to the transition than is the case for xenon on graphite.

Unfortunately, systematic errors prevent a comparison of absolute temperature scales between the x-ray and heat-capacity data, and thus it is not possible to test the relative positions of the heat-capacity anomalies and apparent correlation length divergence.

The entropy change due to the higher temperature, broad heat-capacity peak is much greater than that due to the lower temperature, sharp peak. Liquid-crystal studies find that most of the entropy change occurs at the hexatic to layered liquid transition (Viner *et al.*, 1983). This finding is consistent with the interpretation of the broad heat-capacity peak observed in argon as due to the hexatic-isotropic transition. If so, one might expect (in analogy to the liquid-crystal systems) to see a sharp increase in positional correlations (stopping short of divergence) associated with the broad upper peak. No such increase has been observed in the x-ray studies. Because of the differing temperature scales, it is not certain whether the appropriate temperature region has been examined.

Another possibility is that the broad peak is due to a rotational transition. The argon system has been shown to display an unusual melting transition from a rotated solid to a rotated liquid (D'Amico *et al.*, 1986). The rotational transition occurs above melting as does the broad specific-heat peak. This rotational transition is expected to be of Ising type and thus have $\alpha=0$, consistent

with a rounded peak.

At monolayer coverages and above, all extant evidence is consistent with continuous melting transitions. However, the experimental evidence at these higher coverages is not nearly as complete as in the submonolayer regime.

Xenon on graphite. The natural lattice spacing of xenon is approximately 8% larger than that of krypton. It forms a triangular incommensurate solid for temperatures above 65 K. The melting of xenon on graphite is probably the most studied of all two-dimensional melting transitions. The melting of submonolayer xenon on graphite is strongly first order [(Litzinger and Stewart, 1980; Heiney *et al.*, 1983 and references therein)]. There is substantial agreement, however, that at higher coverages the melting transition becomes continuous (Heiney *et al.*, 1983; Rosenbaum *et al.*, 1983; Dimon *et al.*, 1984; Nagler *et al.*, 1985; Specht *et al.*, 1985; Colella and Suter, 1986).

X-ray diffraction studies find positional correlation lengths that diverge as the transition is approached from the liquid, with lengths up to 2000 Å actually observed (Heiney *et al.*, 1982, 1983; Dimon *et al.*, 1984; Specht *et al.*, 1984, 1985; Nagler *et al.*, 1985). Continuous melting is said to occur for temperatures above 125 K. Vapor-pressure isotherms indicate a crossover from first order to continuous melting above 150 K (Colella and Suter, 1986). The continuous transition is, in both studies, and in contrast to the case of argon on graphite, extremely sharp. The disagreement between these experiments as to the location of the crossover point demonstrates the difficulty in distinguishing between a continuous transition and a weakly first-order transition.

The compressibility, found in the vapor-pressure isotherm experiments (Colella and Suter, 1986), could be decomposed into two pieces (see Fig. 25): a sharp peak corresponding well to a resolution-limited δ function and a broad, temperature-independent peak fit well by a Lorentzian. The sharp peak was interpreted as due to a first-order transition. It shrinks as temperature is increased until it disappears at a temperature of about 150 K. The broad peak is then the only signature of the melting transition at higher temperatures.

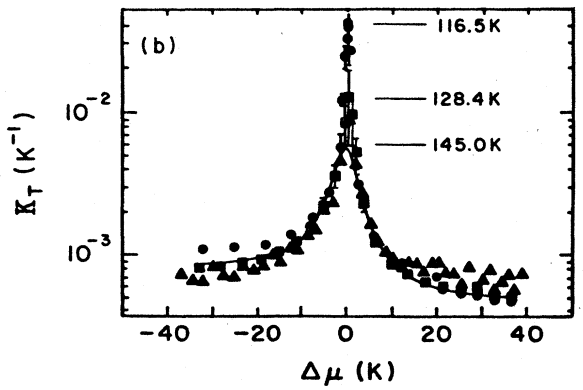

FIG. 25. Compressibility as a function of chemical potential for the xenon-on-graphite system. Data are shown for isotherms measured at 116.5, 128.4, and 145.0 (Colella and Suter, 1986).

It would be tempting to interpret the broad peak as the nonsingular anomaly predicted by the KTHNY melting theory. In that case its presence below the multicritical point would be a signature of the beginning of a KTHNY transition which is then preempted by a first-order transition. Alternatively, the broad peak may be the characteristic behavior of the multicritical point itself. If so, this multicritical point is of a novel character. In particular, its behavior is different from that found in computer simulations of the crossover from first-order to continuous transitions in the Laplacian roughening model, dual to the disclination gas (Strandburg, 1986).

As is to be expected from the sixfold substrate field, the xenon liquid is orientationally ordered. Above melting, x-ray diffraction on single-crystal samples show broadened sixfold spots rather than the ring usually seen in a liquid. The presence of spots indicates the existence of long-range bond-orientational order. In other words, the system exhibits some stiffness with respect to bond-orientational fluctuations. This stiffness may be provided solely by the hexagonal substrate field h_6, or there may be a nonzero intrinsic elastic constant K_A. A nonzero value of K_A is a signature of a hexatic phase.

Rosenbaum *et al.* (1983) compared the observed behavior of the spot width to predictions of a harmonic theory allowing for nonzero substrate field h_6 and Frank constant K_A. Using the KTHNY prediction that, near melting, K_A is proportional to the square of the positional correlation length, they compared their results with predictions for the behavior of the angular width at various values of h_6. For reasonable values of h_6 they found that a nonzero K_A was required to explain their data. In order to explain their results by substrate effects alone, values of h_6 3 orders of magnitude larger than previous estimates for xenon on graphite were required.

Recent synchrotron studies of xenon on the (111) face of silver (Greiser *et al.*, 1987) provide further evidence that xenon melts into an intrinsic hexatic phase. Xenon on silver does not orient according to the Novaco and McTague predictions (1977), indicating that the substrate field is extremely small and that the orientation of the overlayer is determined by pinning at the edges or steps on the substrate surface. [For a discussion of the role of defects in determining the structure of adsorbed layers see, for example, the work of Kern *et al.* (1986).] The value of h_6 for xenon on silver is estimated to be approximately $\frac{1}{10}$ that for xenon on graphite.

Surprisingly, since the substrates are so different, the behavior of the xenon-on-silver system is essentially identical to that of xenon on graphite. The melting temperatures coincide, as do the values of K_A required to explain the angular spot width data above melting. While the spot width data can also be fit by a model involving strong step spinning, the quantitative agreement of the results for xenon on two very different substrates implies

that the hexatic ordering is indeed intrinsic to the adsorbate.

The low-temperature phase observed, however, is not a true, quasi-long-range solid. Some frozen-in disorder remains, and the narrowest line widths observed in scattering studies are wider than would be expected from the experimental resolution or from substrate irregularities (Nagler *et al.*, 1985; Specht *et al.*, 1985; Greiser *et al.*, 1987). Greiser *et al.* argue that a plausible source of the disorder is the pinning of dislocations to grain boundaries or steps.

Comparison of xenon and argon on graphite. The xenon and argon systems, although displaying approximately the same magnitude of incommensurability with the graphite substrate, have very different melting behavior. These differences are almost certainly due to interactions with the substrate, since xenon and argon are both well described by Lennard-Jones potentials. The substrate tends to expand the argon lattice from its preferred separation. The potential well is relatively soft in the direction of expansion and one might expect substrate effects to be fairly significant. In contrast, in trying to contract the xenon lattice, the substrate potential is working against the strong hard-core repulsion and therefore, may be expected to be less effective. Abraham (1983a) points out two factors that may be useful in understanding the difference between the Ar and Xe melting transitions: The argon melting temperature in the submonolayer regime is comparable to the corrugation of the substrate potential (probably the reason that argon melts into a rotated fluid). Also, the argon fluid density in the submonolayer region is roughly equal to the commensurate density, again indicating the importance of substrate effects in the submonolayer melting.

b. Helium on graphite

The phase diagram of ^{4}He on graphite is shown in Fig. 22 (Motteler, 1985). Both ^{4}He and ^{3}He have been studied and their melting behavior is qualitatively the same. The phase diagram of helium is also very similar to that of hydrogen and deuterium, with phase boundaries differing only by a temperature scaling (Freimuth and Wiehert, 1985; Motteler, 1985; Dash, 1987). On the basis of the analogy between helium and these systems, the phases labeled α and β are identified as an incommensurate solid with "striped" domain walls, and a hexagonal domain-wall liquid similar to that observed in krypton on graphite. In this case the line between the regions β and V shows the location of heat-capacity maxima related to the change from the domain-wall liquid to an ordinary disordered liquid but does not denote a true phase boundary. It is surprising to see how similar the phase diagram of helium on graphite is to that of krypton on graphite considering the vast differences in temperature scales and in the respective atomic sizes.

Because of its magnetic properties, ^{3}He may be studied with nuclear magnetic resonance. Widom *et al.* (1979) performed an NMR study of the melting transition of incommensurate ^{3}He on graphite. They observed evidence of two transitions. One of these transitions was associated with slow motions, which they hypothesized were the motions of unbound dislocations. The second was associated with the fast atomic motions characteristic of the fluid phase. The first transition seemed to correspond well to predictions of the location of the KTHNY melting transition assuming that renormalizations of the elastic constants are small (essentially a large core energy limit). The second transition was correlated with peaks in the specific heat.

Thermodynamic measurements have also been used to study the melting of the incommensurate helium solid. In particular, Ecke and Dash (1983) analyzed the excess specific heat near melting in terms of defect generation. They were unable to distinguish between various potential thermally excited defects. However, they were able to obtain a single defect activation energy over a temperature range up to within a few percent of the melting temperature. If this defect is interpreted as a tightly bound dislocation pair, then the core energy in units of the peak temperature would be between 3.5 and 5 depending on the density. The defect energy measured by Ecke and Dash is quite similar to defect energies obtained by Feile *et al.* (1982) by neutron scattering measurements on ^{3}He (Feile *et al.*, 1982). Whether these defect energies can be taken as core energies for the application of the KTHNY theory depends on how well dislocations can be described by elastic theory in this system at these short distances.

Ecke and Dash (1983) improved the calculation of Widom *et al.* (1979) of the predicted KTHNY melting temperature by using the Greif and Goodstein (1981) elastic constant values, which take into account substrate effects, finite-pressure corrections, and the breakdown of the Cauchy approximation for the relationships of the elastic constants. They include "phonon-renormalization" effects in a rough way by using a temperature dependence indicated by computer simulations of a Lennard-Jones potential system. These calculations place the specific-heat peak temperature below the predicted melting temperature and hence contradict the KTHNY predictions. However, better calculations, using the HN recursion relations, should be performed for a more meaningful comparison.

The density of defects present near melting in the helium-on-graphite system is similar to that for the 2D XY model (0.3%; see Tobochnik and Chester, 1979) and considerably smaller than that generally observed in simulations of 2D melting for stiff-core potentials (approximately 2%; see Tobochnik and Chester, 1982). The width of the helium specific-heat peak is, however, considerably narrower than that observed for the 2D XY model. Dash and Ecke conclude that the shape of their specific-heat peak is consistent with either a KTHNY transition or a substrate-heterogeneity-broadened first-order transition.

Hurlbut and Dash (1984), however, argued that their measurements of the temperature dependence of the 2D pressure in ^{4}He monolayers show that the melting transition is first order. Near melting, the shape of the temperature derivative of the pressure as a function of temperature should be the same as the shape of the heat capacity. We therefore discuss (as they did) their results in terms of heat capacity.

The experimental data of Hurlbut and Dash (1984) could be explained equally well by a broadened first-order model or by the smooth behavior predicted by KTHNY. Hurlbut and Dash concluded that the transition was first order on the basis of the narrowness of the peak width as compared to widths obtained in the XY model (Tobochnik and Chester, 1979) and dislocation gas calculations (Saito, 1982a, 1982b). Strandburg *et al.* (1985; see also Hurlbut and Dash, 1985) pointed out, however, that the specific-heat peak width is nonuniversal and that, both experimental (xenon on graphite; see Colella and Suter, 1986) and model (Laplacian roughening model; see Strandburg *et al.*, 1983) systems exist in which the peak width is extremely narrow and yet the transition is continuous. Indeed, the continuous Laplacian roughening transition at core energies comparable to those obtained for helium on graphite shows a specific-heat peak width remarkly close to that observed by Hurlbut and Dash.

An interesting observation of Ecke and Dash (1983) is that at certain coverages a second small specific-heat peak is seen at temperatures about 7% higher than the melting peak. Ecke and Dash speculate that this peak is due to a substrate-induced rotational transition. It is interesting to compare this observation with the observation of two peaks in argon on graphite. In argon the relative sizes of the two peaks are reversed, with the melting peak being considerably smaller than the broad second peak.

c. Ethylene on graphite

Recent heat-capacity experiments of Kim *et al.* (1986) show evidence for continuous melting of ethylene on graphite at all coverages. Zhang *et al.* (1986) extended this work to higher coverages and found that the melting of the bilayer solid was also continuous. This continuous melting is characterized not by divergences but by broad rounded anomalies (Kim *et al.*, 1986). In this case the anomalies are about 5% wide in temperature. The phase diagram of ethylene on graphite according to these measurements is shown in Fig. 23.

The solid from which the melting takes place is thought to have a structure such that the ethylene molecules are lying with their long axis parallel to the substrate. The orientations of these axes are, however, disordered at these temperatures. The effect of this additional molecular structure on the melting transition and, in particular, on the bond-orientational order is not known, but it is unlikely to be substantial since the molecular axis directions are random.

The defect activation energy was also determined (as for helium on graphite) in the monolayer and submonolayer regime (Kim *et al.*, 1986). If these defects are interpreted to be dislocation pairs, then the core energies, in units of the transition temperature, were on the order of 20. For such high core energies the renormalization of the coupling constant should be very small. The measured core energy may therefore be compared to the "unrenormalized" values used in defect simulation studies. The simulations indicate that such high core energies would certainly put the system in the continuous regime (Saito, 1982a, 1982b; Strandburg *et al.*, 1983; Strandburg, 1986). However, it is not known whether the measured defects actually are dislocation pairs.

d. CF_4 on graphite

Recently very intriguing results have been obtained by Zhang *et al.* (1986) for the melting of CF_4 on graphite. An experimental phase diagram for CF_4 is shown in Fig. 24. This system has a very complicated phase diagram, which has been the subject of considerable study (Kjaer *et al.*, 1982; Nagler *et al.*, 1985). We concentrate here on results for the melting of the hexagonal incommensurate solid (HI in the figure). Synchrotron x-ray measurements have been interpreted in terms of a continuous melting of the HI phase (Kjaer *et al.*, 1982).

At high temperatures, where the phase boundary is perpendicular to the temperature axis, the specific-heat measurements show a small sharp peak and a broad peak about 5% above it in temperature. This heat-capacity signature is remarkably like that of argon on graphite at submonolayer coverages. Bak and Bohr (1983) have suggested a theory for the transitions of CF_4, which includes the effects of domain walls and of dislocations. They suggest that the melting of the HI phase is of the KTHNY type and that the phase into which the HI solid melts is a phase with Ising symmetry. A further Ising-type transition is required to drive the system into the disordered fluid phase. It seems plausible that the two specific-heat peaks observed are the signatures of these two transitions.

There has been some controversy as to the identification of the phase marked $I(s)$ in the figure. It has been generally believed to be a "striped" phase with uniaxial ordering of domain walls. Some experimental results have indicated, however, that this phase may be a fluid (Nagler *et al.*, 1985). Zhang *et al.* (1986) have identified a new phase (labeled *IC* in the diagram). They do not offer a conjecture as to the structure of this phase.

We offer our own guess here. Bohr and Bak have performed calculations that predict the intervention of a phase with 2×1 symmetry between the 2×2 commensurate and striped phases. The situation is similar to that of Kr on graphite in which the weakly incommensurate solid is unstable to the unbinding of dislocations to form a reentrant domain wall liquid. In the case of CF_4, how-

ever, the domain-wall liquid is anisotropic, remaining ordered in one direction. Perhaps the phase labeled $I(S)$ is the predicted anisotropic fluid phase. In that case IC may well be the striped phase.

It is not at all clear as yet how all these phases connect up in the phase diagram. Vapor-pressure isotherm measurements would be valuable in order to investigate the region in which the phase boundaries are parallel to the temperature axis (where specific-heat measurements are insensitive to details of the transition).

As the above examples demonstrate, the situation in the melting of physisorbed overlayers is quite intriguing and far from well understood. Further theoretical and simulational work in light of these recent experimental advances is certainly called for.

E. Charged submicron-sized spheres

Recent experiments (Murray and Van Winkle, 1987) have probed the melting transition of submicron-sized charged spheres suspended in water and confined between glass plates. These spheres interact primarily with a screened Coulomb potential. Since the spheres are repelled by the plates, squeezing the plates closer together lowers the sphere density. The experiments were performed in a glass wedge. Photographs were taken at various points along the wedge in order to obtain data for a variety of densities. Each photograph contained about 2000 spheres.

The photographs were analyzed in terms of correlation functions and defect structure. The results indicated the presence of two separate transitions characterized by the sudden increase of the orientational and translational correlation lengths, respectively. These transitions were separated by a region approximately 5% wide in density, which appears to be a hexatic phase.

The defect structure in this system was probed using the Voronoi polygon construction (see Sec. V.C.3). As has been the case in simulation studies as well, the picture obtained by such an analysis is complex, and comparison with the KTHNY picture of defect pairs is not straightforward. Section V.C.3 contains a discussion of some of the difficulties involved in such comparisons.

Because a hexatic phase is apparently observed in this system, it should be able to provide insight into the question of what a hexatic phase "looks like." The KTHNY theory describes behavior at large length scales and there has not been a clear picture of how a hexatic phase should appear on an atomic scale. The lack of such a picture has hindered the resolution of the issue of whether the intermediate region observed in some simulations is a hexatic phase or a coexistence region (see Sec. V.B.2.a). On the whole, the charged sphere system is very promising for the investigation of the two-dimensional melting problem in real time and space in an experimental system.

V. COMPUTER SIMULATIONS OF ATOMIC SYSTEMS

A. Introduction

Ever since the discovery by Alder and Wainwright (1962) of a liquid-solid phase transition in the hard-disk system, computer simulations have been used to study the melting of two-dimensional atomic systems having many different potentials. In this section we review these simulations and suggest some useful avenues for further research. We begin with a general introduction to the simulation methods. The advantages and disadvantages of various choices of simulation procedure for the study of the melting transition are discussed and some cautions regarding interpretation are advanced. Included in this introduction are comments on finite size and time effects and on the difficulty of distinguishing a hexatic phase from a two-phase coexistence region.

We next discuss the results of specific simulations. We expect that the melting behavior may depend on the interaction potential. For example, the defect core energy may vary as the potential is changed. Section V.C includes a discussion of results for systems interacting with relatively hard core potentials. These systems include hard disks, Lennard-Jones potential, $1/r^{12}$ potential, and the Gaussian core model. In Sec. V.D we discuss systems with intermediate strength potentials—$1/r^6$, $1/r^5$, and $1/r^3$. Section V.E contains a description of simulations of the soft $1/r$ and 2D Coulomb potential systems. Weeks (1981) has shown that, for potentials of the form $1/r^n$ in 2D, there can be no volume change upon melting for $n<2$. This finding indicates that there may be something special about the melting of these systems. In particular, they might be expected to display weaker melting transitions. Simulations of particles on a substrate are included in Sec. V.F and compared with experiments on adsorbed gases. Finally, we offer general conclusions regarding the simulation results and suggest future directions for further simulation study.

B. General considerations

1. Methods

Two methods of simulation are used: the Monte Carlo and molecular dynamics methods. In both methods results for quantities of interest are obtained as averages over configurations generated by the repeated application of a simple algorithm which governs the motions of the particles.

a. Molecular dynamics

The molecular dynamics method (Rahman, 1965; Verlet, 1967; Kushik and Berne, 1977; Andersen, 1980) simulates the dynamics of Newtonian motion while the Monte Carlo method simulates the configuration sums of statis-

tical mechanics. The particle motions in a molecular dynamics simulation are determined by numerically integrating the equations of motion. The time increments in the integration are called time steps and involve moving each particle a small distance. The choice of the length of these time steps must be made so that they are on the order of real microscopic time scales of the system. Molecular dynamics has the advantage of allowing investigations of realistic dynamics.

The molecular dynamics (MD) method operates most naturally in the microcanonical (constant energy) ensemble. Extensions of this method to other ensembles have been introduced in recent years (Andersen, 1980). For example, a canonical ensemble may be simulated through coupling to a heat bath. One method of implementing such a coupling is to occasionally randomize the velocity of a given particle according to a Boltzmann distribution. A constant pressure ensemble may be implemented by coupling the system to a hydrostatic "piston." The mass of the piston is arbitrary and must be chosen so as to produce volume fluctuations over a physically reasonable time scale. Questions regarding the method of enforcing a given ensemble are discussed below as they arise for specific simulations.

b. Monte Carlo

The Monte Carlo method (Binder, 1979) relies, as its name implies, upon moves chosen from a random distribution. These moves are accepted or rejected according to a comparison of the appropriate statistical probability with a random number. For example, in the canonical ensemble $\exp(-\beta\delta v)$ (where δv is the change in energy due to the proposed move) is compared to a random number between 0 and 1. If it is greater than the random number the move is accepted. In theory, the Monte Carlo method offers considerably more flexibility in implementation than the molecular dynamics method. Straightforward implementation of various ensembles is possible simply by modifying the types of moves used and using the appropriate statistical weight. For example, a constant pressure ensemble may be implemented by using changes in the volume of the system as attempted moves and using the appropriate isobaric statistical weight to determine whether the changes are accepted or rejected.

There is considerable freedom in choosing the atomic moves as well. Any combination of moves may be used as long as the transition probabilities satisfy detailed balance. The usual method is to move one atom at a time to some position chosen randomly from a circle of arbitrary size around the present position. The size of this circle is arbitrary and is usually chosen to give a reasonable probability of accepted moves (around 30–50 %). In the constant pressure simulation, there is also a choice to be made in the size of the attempted volume changes and the frequency of attempting volume changes. There are no clear guidelines as to how to make these choices and they are usually made heuristically.

While many choices of Monte Carlo (MC) procedure will give the correct results in the limit of infinite simulation time, there can be considerable differences in equilibration rates for various procedures. For example, an XY spin system studied by Swendsen (1982) undergoes two transitions. A standard MC procedure, in which one spin at a time was flipped, implied one first-order transition with a large hysteresis loop. Only when a MC procedure involving the flipping of whole rows of spins at a time was used were the two transitions observed. These results suggest the importance of investigations into variations on the "one particle at a time" traditional MC method in order to probe modes that are of importance for phase transitions.

Because of the flexibility in choosing the Monte Carlo procedure, the Monte Carlo method provides in principle a better chance for determining phase transition behavior than molecular dynamics, since a clever choice of Monte Carlo move may considerably shorten equilibration times. The loss of dynamic information is not unimportant, however. In any event, since the simulations described here have not taken advantage of this flexibility, there is probably no reason to prefer the molecular dynamics or Monte Carlo results and we will treat them as equivalent.

c. Monte Carlo renormalization group

The Monte Carlo renormalization-group (MCRG) method (Swendsen, 1982) is an extension of the Monte Carlo method to take advantage of renormalization-group ideas. It has not yet been applied to the problem of two-dimensional melting. It has, however, been extremely successful in investigations of phase transitions in spin systems. The method allows the calculation of long-distance properties of the system, such as critical exponents, by computations of local correlation functions. Applications of this method to the defect systems discussed in Sec. III (which reside on a lattice) should be straightforward. The question of how to perform renormalization transformations for atomic systems is still open. Tobochnik (1982) employed the MCRG method for the q-state clock model, whose phase diagram for $q=5,6$ is rather similar to the KTHNY predicted melting phase diagram. Using MCRG he found three phases—an ordered phase, a disordered phase, and an intermediate critical phase. He pointed out that standard MC alone gave a confusing picture of the transition structure, showing hysteresis and large fluctuations.

2. Implications of the choice of ensemble

The choice of ensemble is also, in principle, arbitrary. In finite simulations, however, these choices can have important effects on the results. Most simulations of two-dimensional melting have been performed in the constant temperature, density, and number-of-particles ensemble.

A few simulations have been performed in a constant temperature, pressure, and number-of-particles ensemble.

a. Constant density ensemble

Constant density simulations have the disadvantage that local density fluctuations (and hence local defects such as vacancies) are suppressed in finite systems. These density fluctuations may be very important for the two-dimensional melting transition.

Two-phase coexistence or hexatic phase? The existence of a two-phase coexistence region at a first-order transition in the constant density ensemble provides both advantages and disadvantages. If a coexistence region can be identified, it provides good evidence of a first-order transition. However, distinguishing a coexistence region from a hexatic phase has proved a somewhat difficult task.

Particle trajectory maps are often invoked to demonstrate coexistence (Abraham, 1980, 1981; Koch and Abraham, 1983). True phase separation is not observed in the simulations. Rather (see Fig. 26) the existence of solidlike and liquidlike patches is interpreted as evidence for coexistence. Perhaps the simulation time scales are too short to allow complete phase separation. Periodic boundary conditions also mitigate against large-scale rearrangements such as phase separation. It may be, however, that the absence of phase separation is an indication of a vanishing interfacial energy, and that the patches are the critical fluctuation characteristic of the hexatic phase. Since no one knows for certain how a hexatic phase would appear in such maps, it is rather difficult to draw convincing conclusions from the observation of these patches.

Broughton, Gilmer, and Weeks (1982) simulated the stability of a phase-separated system prepared at the apparent coexistence temperature in a $1/r^{12}$ system. The system was stable over long periods of time. However, the solid melted and reformed during the simulation, indicating that the boundary between solid and liquid has a low interfacial energy. Melting and reformation does not occur in the simulation of three-dimensional coexistence. Broughton *et al.* thus conclude that their evidence favors a first-order interpretation, but they cannot rule out the possibility that the observed melting and reforming is an indication of critical fluctuations.

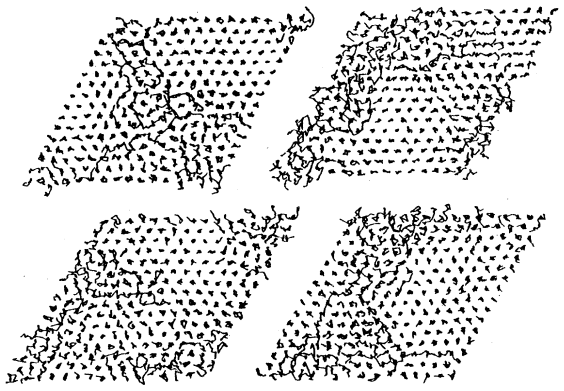

FIG. 26. Particle trajectory plots showing apparent two-phase equilibrium in a Lennard-Jones potential system (Abraham, 1981).

The long-distance behavior of the bond-angular correlation function will in principle distinguish between a hexatic phase and a region of two-phase coexistence. However, in a finite system, especially when the coexistence region consists of patches of fluid and solid rather than a true phase separation, a coexistence region may be characterized by a slow decay of bond-orientational order very similar to that characterizing a hexatic phase (Tobochnik and Chester, 1982). The long-distance behavior is very difficult to extract due to periodic boundary conditions and also because the bond-angular correlation function is an oscillating function of distance.

Therefore Strandburg, Zollweg, and Chester (1984) have investigated the local bond-orientational order on various length scales for Lennard-Jones and hard-disk systems and shown good agreement with a coexistence model in which the coexisting phases consist of patches of approximately 50 particles. The agreement with the coexistence model was quantitative at short length scales with computations using the expected fractions of liquid and solid. Udink and van der Elsken (1987) have criticized the inference of coexistence from these results, demonstrating that the solid fractions calculated from various moments of the bond-orientational order parameter are not in agreement except for very small systems. They conclude that this disagreement rules out a coexistence interpretation. In their discussion, however, they neglect the fact that in a system of coexisting patches (as opposed to a phase-separated system) the size dependences of the various moments of the order parameter differ, leading to differences in the apparent solid fraction.

Udink and van der Elsken are certainly correct, however, in noting that the existence of inhomogeneities on a local scale does not imply global inhomogeneity. The appearance of coexisting patches of solid and liquid rather than true phase separation must be an artifact of computer simulation due to some combination of low interfacial energy and the short times probed in simulations.

Alternatively, the solidlike and liquidlike patches may be the signatures of critical fluctuations expected in a hexatic phase. Strandburg, Zollweg, and Chester (1984) used the low-temperature phase of the two-dimensional XY model (which has spin order analogous to the bond-angle order in a hexatic phase) to model the expected hexatic behavior. This phase was homogeneous down to the lowest length scales. However, it is becoming clear that the local defect structure observed near melting even in those systems for which other evidence points to KTHNY melting (Murray and Van Winkle, 1987; Udink and van der Elsken, 1987) is considerably more complex

than that in the XY model, rendering this comparison less than satisfactory. Indeed, Udink and van der Elsken (1987) have recently argued that this patchy intermediate region exhibits the algebraic bond-orientational order characteristic of a hexatic phase (see Sec. V.C).

Even if it is certain that a coexistence region is observed, a study of size dependence is needed to show that this coexistence persists in the thermodynamic limit. The probability of observing the "wrong" phase at a given temperature is proportional to

$$\exp(-\beta N \delta f) , \tag{27}$$

where N is the size of the system and δf is the free-energy difference between the two phases.

In a finite system there will always be a region near the transition where both phases are observed. If N and δf are both small, this region may be fairly wide. An example of this effect is given by Landau and Swendsen (1981) in a study of tricritical behavior in spin systems. A histogram of values of thermodynamic quantities showed a double-peak structure at the transition, an indication of coexistence. However, MCRG calculations showed that the transition was, in fact, continuous. A slight tendency of the peaks to merge with increasing size was evident in the standard Monte Carlo simulation, once again indicating the importance of the study of size effects.

To add to the confusion still further, there is also the possibility of first-order melting into a hexatic phase, which would produce, in a constant density simulation, a region of solid/hexatic coexistence and a hexatic region. An exercise that might prove very useful would be to attempt to create a hexatic by application of a sixfold bond-angle field and then to remove the field to test the stability of the phase.

b. Constant pressure ensemble

Constant pressure simulations should display no region of coexistence to muddy the question of a hexatic phase. The fact that no hexatic phase has been observed in constant pressure simulations is an argument in favor of interpretation of the "intermediate region" observed at constant density as a coexistence region. Even this argument is not conclusive, however, since the width of a hexatic phase could be quite different depending on what path one uses to traverse it. Abraham (1981) has performed a constant pressure simulation for a Lennard-Jones system beginning with a configuration obtained from a constant density simulation in the intermediate region. He found that the system quickly adopted behavior characteristic of the appropriate single phase, good evidence in this case of two-phase coexistence.

Determining the order of a phase transition in a constant pressure simulation is not easy either. Distinguishing a discontinuous jump at the transition from a steep but continuous rise is very difficult, and questions of equilibration near the transition must always be raised. While the overall density may fluctuate in a constant pressure simulation, local density fluctuations are still rather difficult to excite.

Technical controversies concerning the method of implementing a constant pressure ensemble have arisen. The questions involve the frequency with which area changes are attempted and the method by which the new particle positions inside the larger volume are obtained. Toxvaerd (1984) has argued that in a simulation by Abraham and Koch (1984), using a combination of Monte Carlo tests for area changes and molecular dynamics for particle motions, the times between attempts to change the area were too short to allow for the transient effects of the induced pressure wave to die away and equilibrium to be reached. Pressure waves are only a problem for molecular dynamics simulations.

Another point made by Toxvaerd (1984) has implications for both Monte Carlo and molecular dynamics (MD). He criticizes Abraham and Koch for using an overall length rescaling as the means of changing the volume. He argues that the Monte Carlo acceptance or rejection probability should then reflect changes in the surface free energy between coexisting phases and the defect density. Toxvaerd claims that the neglect of these effects will lead to a bias in the density fluctuations. Rull *et al.* (1985) concur in Toxvaerd's analysis, adding that constant-temperature MD calculations are also questionable because of the velocity rescaling involved.

Broughton, Gilmer, and Weeks (1981) have performed a molecular dynamics simulation in which constant pressure was enforced by a directed rescaling of all lengths to ensure that the virial pressure would agree with the imposed pressure, rather than by a Monte Carlo test. One may still worry that the method of imposing this pressure may bias the configurations explored. Abraham and Koch (1984) and Broughton, Gilmer, and Weeks have performed checks of their constant pressure results against constant density results and found no cause for alarm. However, it is certainly reasonable to keep Toxvaerd's comments in mind for future implementations of the constant pressure ensemble.

c. Constant chemical potential ensemble

The constant chemical potential ensemble is rather attractive, in principle, for the study of melting, since it allows easily for the important local density fluctuations. Indeed, Fisher and Husė (1982) have pointed out that use of a constant N ensemble will tend to make a transition look "sharper" in a finite system than it is in the thermodynamic limit. A study of the hard hexagon lattice gas for a small system showed regions of apparent coexistence or hysteresis even when the transition was known to be continuous.

However, implementation of the constant chemical potential ensemble for dense systems has not been successful as yet. The difficulties arise in attempts to insert a particle. If the attempt is made at a random position in the system, the chance of acceptance is extremely low. Some work has been done on methods to choose the in-

sertion position cleverly, but there is a clear need for more research into this issue. The simulation of adsorbed systems (allowing motion in the third dimension) may be closely related to simulations in which the number of particles is allowed to fluctuate. Some such simulations have been performed (see Sec. V.E). It is interesting to note that these simulations, even on a flat substrate, reproduce the experimental results for the continuous melting of xenon on graphite extremely well, although the order of the transition remains a matter of dispute.

3. Choice of boundary conditions

In addition to the choice of ensemble, the choice of boundary conditions is also open. With very few exceptions the simulation studies of two-dimensional melting have been performed with periodic boundary conditions. Periodic boundary conditions have the advantage of eliminating edge effects, which can completely dominate the behavior of very small systems. However, periodic boundary conditions have disadvantages, as well. The most noticeable disadvantage of periodic boundary conditions is that they tend to stabilize the solid. This stabilization has been argued to make the system mimic the KTHNY predictions by allowing the solid to superheat until the stability limit represented by the attaining of the value 16π for the elastic constant K is reached (Abraham, 1981).

Another very important effect of periodic boundary conditions (at least in systems with a constant number of particles) is the tendency to inhibit both large-scale particle rearrangements and the formation of point defects such as vacancies. As mentioned in Sec. II.A simulations designed to test this effect by adjusting the system size so as not to accommodate a triangular lattice (and thus inserting a vacancy), found significant differences between these results and those for a solid which fits exactly into the system (Stillinger and Weber, 1981; Broughton *et al.*, 1982).

A simulation of the $\ln r$ potential system on a circle with free boundary conditions has been performed by Choquard and Clerouin (1983). The system size used in this simulation was very small, however. Further investigations of the effects of boundary conditions would certainly be of interest.

4. Finite-size effects

Surprisingly, very little study of size dependence has been done for the melting of 2D atomic systems. As has been discussed above in Sec. II.A, what little study has been done has indicated the existence of strong finite-size effects. In particular, if the defect cores are extended, as they seem to be in the Lennard-Jones system (Joos and Duesbery, 1985) where they appear to be about 30 lattice spacings in extent, finite-size effects may be absolutely dominant at sizes below the size of the defect cores. Toxvaerd (1981, 1983) observed significant size dependence of the defect density and elastic constants in the solid near melting.

Udink and van der Elsken (1987) have recently used finite-size scaling to study the positional and bond-orientational order in a Lennard-Jones system. Their results (see Sec. V.C) provide evidence, contrary to the conclusions of most single-size simulations of this system, for the KTHNY melting sequence.

An approximate calculation by Novaco and Shea (1982) for a 256-particle $1/r^5$ potential system finds that the density fluctuations corresponding to longer wavelengths than available in their finite-size system were about twice as large as the density difference between the lowest density equilibrium solid and the highest density equilibrium liquid in their simulation. This calculation also highlights the importance of studies of size dependence. While some very large systems have been simulated (Bakker *et al.*, 1984), the systematic effects of changes in size were not addressed in these simulations.

The most obvious effect of finite size is to blur the distinction between first-order and continuous transitions. First-order transitions are no longer sharp. The long-wavelength modes that are crucial for continuous transitions are truncated. Even continuous transitions will exhibit coexistence over some region [see Eq. (27)], and will certainly not exhibit any true divergences. Since in a finite system the specific heat will always be rounded, a study of size dependence must be done in order to distinguish, for example, between the "sharp" specific-heat peak expected at a first-order transition and the "rounded" peak expected at a KTHNY transition.

Another important finite-size effect is the observation of a van der Waals–type loop in a graph of pressure versus density when a first-order transition is traversed. This loop has been explained by Mayer and Wood (1965). It may replace a flat coexistence region in a small enough system. The interface energy required to form coexisting phases is proportional to the length of the interface. At a first-order transition in an infinite system, this interface energy will always be negligible when compared to the free energy gained by having the coexistence. In a finite system, however, the free energy may be lowered over a certain region by maintaining the pure phase, since the interface energy may be significant. This effect may be especially pronounced in a simulation with period boundary conditions and short-time scales, where complete phase separation, which minimizes the interface length, does not have time to occur. It will be useful for the reader to keep the possible effects of finite systems size in mind when reading the discussions of individual simulations below.

5. Effects of finite simulation time

A crucial question in computer simulations is whether the system reaches equilibrium. This question is especially important near the melting transition where large pre-

transitional fluctuations on the fluid side and fluctuations in the intermediate region have been observed. The attainment of equilibrium is usually determined by watching the value of various quantities as a function of time (here meaning either MD time steps or Monte Carlo attempted moves) and determining when a plateau has been reached. Metastability is a serious concern in simulations, as are the critical slowing-down effects known to exist near a continuous phase transition. The times involved in computer simulations are very short compared to experimental time scales, and defect equilibration times are expected to be very long. An encouraging note is the attainment by Zollweg (1984) of a nearly defect-free solid by compressing a hard-disk liquid through the freezing transition.

Because simulation time scales are so short, hysteresis is not a useful indicator of a first-order transition. Hysteresis may be due to heating or cooling too quickly through the transition. For example, a straightforward Monte Carlo simulation by Tobochnik (1982) of the clock spin models found hysteresis where his more reliable MCRG studies found an intermediate critical phase rather analogous to the predicted hexatic phase.

Very little detailed investigation of finite-time effects has been done. Novaco and Shea (1982) have studied these effects in detail for the $1/r^5$ potential system. They studied a system of 256 particles using a constant energy MD method. In order to obtain a more quantitative understanding of the approach to equilibrium, they computed the time dependence of autocorrelation functions of various quantities. In the transition region they observed relaxation times longer than their longest runs (approximately 100 000 time steps). In addition to the increase of relaxation times near the transition, an increase in the amplitude of fluctuations in quantities such as the temperature was seen. Novaco and Shea interpreted these effects as evidence for "critical slowing down" and thus for a continuous transition.

Koch and Abraham (1983) argue that these effects are an artifact of the constant density simulation and that they indicate fluctuations of the liquid-solid ratio in a coexistence region. Indeed constant pressure simulations by Koch and Abraham of a Lennard-Jones system show much shorter relaxation times than their constant density simulations of the same system. Since the Koch and Abraham and Novaco and Shea (1982) results are observed for different systems, there is no reason to assume that they are in conflict. In any case, the point made by Novaco and Shea is that careful investigation of correlation times is crucial in the study of possibly continuous transitions.

In light of the above discussion of problems with the use of computer simulation for the study of melting the reader may be wondering whether the technique has any use at all in this area. There remain several advantages of computer simulations for the study of 2D melting. Simulations allow a direct "tuning" of particle interactions so as to investigate the dependence of the melting behavior on the potential. Simulations also allow studies of strictly two-dimensional systems, as well as of the effects of allowing motion in the third dimension. The effects of substrate ordering fields may also be studied and distinguished from the effects of motion in the third dimension. Finally, simulations allow direct access to the microscopic configurations, eliminating much of the guesswork required in interpretation of most experimental results. For example, bond-orientational correlation functions are directly measurable in simulations. A microscopic view of crystal defects and particle motions may also be obtained.

C. Simulation studies of systems with hard-core potentials

In 1962 Alder and Wainwright reported a simulation of the melting of a system of 870 hard disks using the MD technique. Using runs extending to 20 000 collisions per particle they determined the pressure as a function of density at constant temperature. In a finite system undergoing a first-order transition one expects to see a "loop" in the density versus pressure curve, rather than the jump in density one would expect for an infinite system (Mayer and Wood, 1965). Alder and Wainwright (1962) concluded from their observation of such a loop that the melting transition was a first-order transition. They also studied particle trajectories in the transition region. These displayed solidlike and liquidlike regions and were thus interpreted as evidence of two-phase coexistence. Later simulations confirmed this picture of a conventional first-order transition in two dimensions. In response to suggestions that dislocations might be important for melting in two- and three-dimensional systems, Cotterill and Pederson (1972) noted that dislocations were present near melting in a "by eye" study of particle maps.

Of course, at the time of these simulations, no detailed theory of dislocation-mediated melting existed and, in particular, no suggestion that the transition might be continuous in two dimensions had been made. Following the announcement of the KTHNY theory of two-dimensional melting, a series of detailed simulations of two-dimensional melting have been and continue to be reported. The first of these reported the observation of three regions, which were interpreted as evidence for the KTHNY theory (Frenkel and McTague, 1979). However, Toxvaerd (1980) noted that the density which Frenkel and McTague simulated was in the solid-vapor coexistence region at low temperatures. The three regions are explained as liquid, liquid-solid coexistence, and an overexpanded solid characterized by negative pressures and induced by the periodic boundary conditions. The sixfold anisotropy of the intermediate region may be explained by the anisotropy of the coexisting solid phase, which maintains its alignment with the periodic box in this finite system.

Many of the simulations reported since have also been

performed at densities where the ground state is a coexisting solid and vapor. The minimum density of the zero-temperature solid is $\rho^*=0.9165$ for Lennard-Jones systems. However, the triple-point density is estimated to be ρ^* approximately equal to 0.81–0.82, so that by the time melting is reached a single-phase solid is the equilibrium phase. The fact that the simulations do not reproduce the solid-vapor coexistence region at very low temperatures is probably not significant for the interpretation of the melting of systems with densities reasonably greater than 0.82.

Since the time of the Frenkel and McTague (1979) study most workers have reported the observation of first-order transitions in the hard-core systems. The first-order transition observed, however, is acknowledged by most to be weak. There is evidence of low interface free energies in the coexistence region (Toxvaerd, 1980; Broughton *et al.*, 1982). The computed differences in free energy between solid and liquid at the transition are small (Toxvaerd, 1978; Barker *et al.*, 1981; Phillips *et al.*, 1981; Broughton *et al.*, 1982). Significant precursors of melting and freezing are observed. In particular, the fluid before freezing is surprisingly ordered. The first peak of the structure factor of a 2D $1/r^{12}$ potential system has a height of about 5.5 compared to a height of 2.85 for a 3D system (Broughton *et al.*, 1982). Considerable bond-orientational ordering has also been observed in the hard-core liquids near freezing (Strandburg *et al.*, 1984).

Studies of size dependence of various quantities have cast doubt on the conclusion of first-order melting (Toxvaerd, 1981, 1983; Udink and van der Elsken, 1987). In particular, finite-size scaling studies of the Lennard-Jones system lend support to the KTHNY melting theory (Udink and van der Elsken, 1987).

Figure 27 sketches the phase diagram obtained from simulations for the Lennard-Jones potential system (Abraham, 1983, 1984). The exact positions of the phase boundaries are still a subject of some dispute. The order of the melting transition (depicted here as first order) will be discussed below. The Lennard-Jones potential is

$$v(r)=4\varepsilon\left[\left[\frac{\sigma}{r}\right]^{12}-\left[\frac{\sigma}{r}\right]^{6}\right]. \tag{28}$$

The phase diagram is plotted in units of $\rho^*=\rho\sigma^2$, $T^*=k_BT/\varepsilon$. At sufficiently high densities one expects the Lennard-Jones system to show similar transition behavior to the $1/r^{12}$ system.

The transition from uniform solid to solid-vapor coexistence in the Lennard-Jones system occurs at a density in good agreement with the zero-temperature calculations of Joos and Duesbery (1985). An important point to note is that the melting transition line of the Lennard-Jones system is more or less parallel to the temperature axis. Thus, isotherm measurements will provide a much better test than isochores in determining the order of the transition. The basic outlines of the Lennard-Jones phase diagram are in rather good agreement with the xenon-

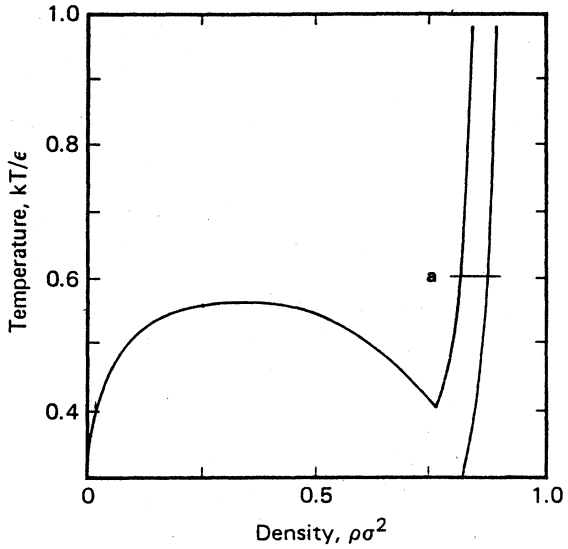

FIG. 27. Phase diagram of the Lennard-Jones potential system as obtained from simulations by Abraham (1981). The approximate location of the experimental xenon-on-graphite tricritical point is also indicated (a).

on-graphite phase diagram, thus illustrating the relatively minor influence of substrate effects in the xenon system. The approximate position of the xenon tricritical point is noted on the Lennard-Jones phase diagram. In the next few sections we describe the simulations of the Lennard-Jones system as well as simulations for the hard-disk and Gaussian core model systems. We review the evidence concerning the order of the melting transition.

1. Thermodynamic quantities

Barker, Henderson, and Abraham (1981), Phillips, Bruch, and Murphy (1981), Toxvaerd (1978), Broughton, Gilmer, and Weeks (1982), and Udink and Frenkel (1987) have performed free-energy computations for hard-core systems. These methods generally entail an analytic or perturbation calculation of a reference free energy for both solid and liquid branches followed by integration of simulation data into the phase transition region. The double tangent method is then used to determine the nature and position of the transition from the crossing of the solid and fluid free-energy curves. These methods are biased in favor of first-order transitions since they assume that the solid and fluid equations of state remain smooth near the transition. These calculations lead to the conclusion that the transition is weakly first order. The free-energy differences at melting are small. Because the transition is so weakly first order, the determination of the order of the transition is not unambiguous. The finite-size and simulation time effects mentioned earlier deserve more careful consideration in interpreting free-energy calculations.

Since free-energy calculations are computation inten-

sive, it is reasonable to try to use raw thermodynamic data to extract information about the nature of the transition. Until recently, estimates of the melting temperature from raw thermodynamic data differed quite significantly from those obtained using free-energy calculations. It was suggested that the raw thermodynamic data reflected the mechanical instability of a superheated solid (Abraham, 1981). Recent improved free-energy calculations, however, are in good agreement with the melting temperatures deduced from raw thermodynamic quantities (Udink and Frenkel, 1987). Disagreement persists, however, over the location of the fluid end of the intermediate region, even among those who believe they observe first-order melting.

Several workers have obtained data for density versus pressure along an isotherm (Tsien and Valleau, 1974; Toxvaerd, 1980, 1981; Broughton *et al.*, 1982; Evans, 1982). In most of these simulations, the density and temperature are held fixed and the pressure is measured. The results of a careful simulation of this nature will show a van der Waals-type "loop" in the P vs ρ graph if the transition is first order (see Fig. 28).

Loops were observed in all of these studies. Again, a study of the system size dependence of these loops seems to be called for. A demonstration of the effect of periodic boundary conditions on these loops was provided by Broughton *et al.* (1982), who simulated two systems of particles interacting with a $1/r^{12}$ potential. In one system the number of particles was chosen so that a triangular lattice would fit exactly into the periodic cell. The other system included a vacancy. The loop on the solid side was much larger for the system which fit perfectly into the cell, showing the stabilizing effect of the periodic boundary conditions on the solid. The system with a vacancy included also showed a loop, which was smaller and more symmetric and thus possibly representative of the actual transition behavior.

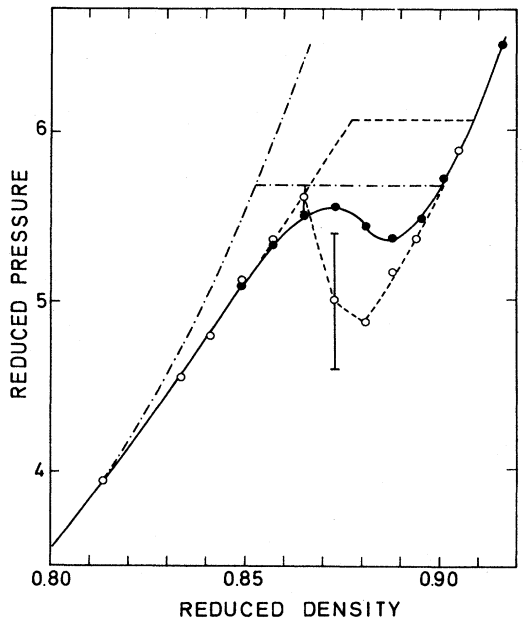

FIG. 28. Pressure as a function of density for the Lennard-Jones potential system at a temperature $T^*=1.0$. Results for sizes $N=3600$ (—·—·—·) and $N=256$ (○---○) are shown, and the Mayer and Wood "loop" is observed (Toxvaerd, 1981).

Data for thermodynamic quantities along an isochore has also been obtained for these systems by several workers. Such data is considerably less useful, since, as may be seen from the phase diagram in Fig. 27, the melting line is essentially parallel to the temperature axis. Thus the transition will be especially smeared in this direction. In addition, many of the simulations have been performed very near the triple point density, where solid-vapor coexistence is also expected over some portion of the phase diagram, thus confusing matters further.

Also, no "loop" is observed in the constant density simulations. It is thus very difficult to distinguish a coexistence region from a continuous transition. Tobochnik and Chester (1982), for example, identified two changes in slope in plots of thermodynamic quantities along an isochore at densities of 0.856 and 0.888. They suggested that these might possibly mark the boundaries of a hexatic phase on the basis of measurements of other quantities, discussed below. Later analysis showed that the intermediate region was well described as a coexistence region containing patches of liquid and solid (Strandburg *et al.*, 1984). However, recent finite-size scaling studies lend support to the hexatic interpretation of this intermediate region (Udink and van der Elsken, 1987).

The single specific-heat peak for a first-order transition should be characterized by a flat top as one crosses a coexistence region. This flat behavior within the coexistence region is indeed consistent with the observations of Tobochnik and Chester (1982) at the two densities mentioned. At a density of 1.14, the energy versus temperature data (shown in Fig. 29) indicates a strikingly different specific-heat behavior. The specific heat derived from this data will display two separated peaks corresponding to the two regions of increased slope near t $[=(T-T_m)/T_m]=0.0$ and 0.18. Tobochnik and Chester believed that the transition at this density was first order since the transition was much more abrupt than at the lower densities and did not accord with the KTHNY predictions in various respects. They did not show a specific-heat curve. However, recent experimental evidence from xenon on graphite indicates that the crossover to continuous melting occurs as the density is increased, and that the continuous transition is very sharp. A reinvestigation of the melting of the Lennard-Jones system at high densities would seem to be in order.

Constant pressure simulations have also been used to study the melting of hard-core systems. The authors of these simulations have come to the conclusion that the transition is first order from the observation of hysteresis, metastability, and nucleation (Abraham, 1980, 1981; Broughton *et al.*, 1981). The problems with determining the order of the transition by observation of hysteresis

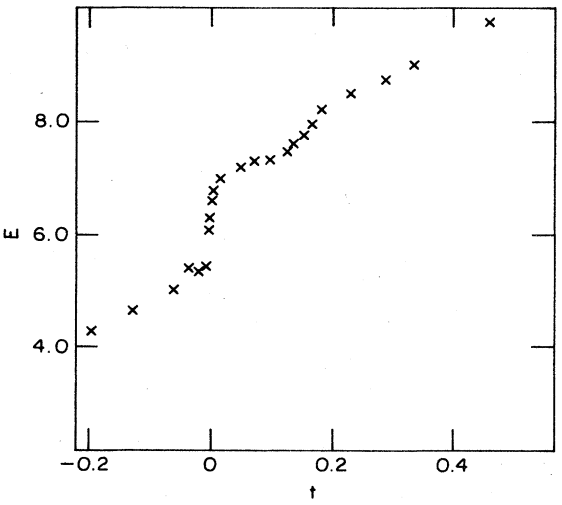

FIG. 29. Energy vs temperature for a Lennard-Jones system at $\rho\sigma^2=1.14$. The temperature is plotted in units of $t=T-T_m/T_m$, where T_m is the melting temperature (Tobochnik and Chester, 1982).

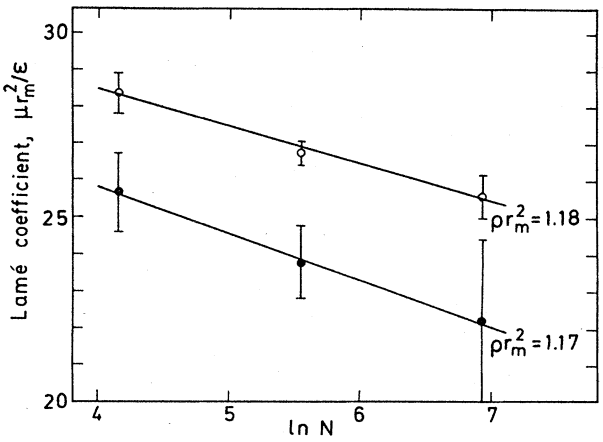

FIG. 30. Shear modulus as a function of logarithm of system size for a Lennard-Jones system (Toxvaerd, 1983).

have been mentioned already. Distinguishing a discontinuous jump from a sharp but continuous rise in density is also difficult.

Because of the difficulty in distinguishing a first-order transition from a KTHNY transition using these simple thermodynamic probes, researchers have turned to other methods of investigating melting in these systems. In particular, efforts have been made to check the specific predictions of the KTHNY theory.

2. Elastic constants

One very simple prediction of the KT melting theory is that the combination of elastic constants

$$K_R=\frac{4\mu(\mu+\lambda)}{2\mu+\lambda} \tag{29}$$

should show a universal temperature dependence as melting is approached, and that it should decrease to the value 16π and then drop to zero at melting. Such a drop has been observed in a number of simulations (Abraham, 1981; Broughton *et al.*, 1982; Tobochnik and Chester, 1982). Statistical errors in the determination of K are typically of the order of 10–20 % near melting.

In spite of this frequently good agreement with the KTHNY prediction for K, most researchers have concluded that the transitions in these systems are first order on other grounds (primarily the observation of either hysteresis or coexistence). Perhaps the KTHNY mechanism is barely preempted by a weakly first-order transition. In this case the value of K obtained near the transition may be very close to the predicted value of 16π. Alternatively, Abraham (1981) proposed that the observation of melting when $K=16\pi$ is really the melting of a superheated solid. He drew this conclusion on the basis of free-energy calculations that placed the transition at a lower temperature. More recent free-energy calculations, however, give melting temperatures very near the temperatures at which $K\approx 16\pi$ was observed (Udink and Frenkel, 1987).

Tobochnik and Chester (1982) observed differences in the behavior of K near melting depending on the density of their Lennard-Jones system. At low densities (near the triple point) the value of K at melting was approximately 16π. At a higher density the value was much higher (about 60). They suggested that perhaps the transition changes from KTHNY-like to first order as density is increased. Ironically this suggestion is exactly the opposite of the trend observed in experiments on xenon on graphite and of the trend suggested above by analysis of the Tobochnik and Chester specific heats. Further simulations will be required to solve this puzzle.

One possible clue is provided by Toxvaerd's observation of strong size dependence of the shear modulus in a Lennard-Jones system near melting (Toxvaerd, 1983). His data (see Fig. 30) show a decrease in shear modulus as a function of increasing system size. The elastic constant K is strongly influenced by the shear modulus. Perhaps a study of size dependence of K at the Tobochnik and Chester higher density would uncover a decrease to a value consistent with the KTHNY prediction as system size is increased.

The effect of a substrate potential on the KTHNY elastic constant prediction may be included by defining another elastic constant to describe the resistance to shear imposed by the substrate. Possibly a similar term should be included to account for the stiffening effect of the periodic boundary conditions.

3. Defect analysis

Investigations of the microscopic defect structure of these systems are possible using the Voronoi polygon method, pioneered for this purpose by McTague *et al.* (1980). Voronoi polygons are a generalization of the

Wigner-Seitz cell to a system not on a lattice. The system is divided into contiguous polygonal cells, one for each particle. Disclinations are manifested as polygons with numbers of sides other than six (usually five or seven). Dislocations are made up of pairs of disclinations. In principle, they will show up in a Voronoi polygon analysis as pairs of five- and seven-sided polygons. Dislocation pairs would then be pairs of these 5–7 disclination pairs. Grain boundaries show up as alternating strings of five- and seven-sided polygons. Primarily, these defects are studied simply by eyeballing maps of their location.

The KTHNY melting theory describes the solid as a dilute gas of dislocation pairs that dissociate at the transition to form a dilute gas of pairs of disclinations (the hexatic phase). The XY model, which is known to undergo a KT transition through the unbinding of vortex pairs, has a population of vortex pairs near the transition of 0.3% of the number of spins (Tobochnik and Chester, 1979). The melting transition of hard-core systems is clearly more complicated with a 2% population of dislocation pairs at melting (Tobochnik and Chester, 1982). Dislocations are also observed to cluster and to form grain boundary loops (Toxvaerd, 1981; Broughton *et al.*, 1982; Tobochnik and Chester, 1982).

This clustering has led many researchers to conclude that the melting of two-dimensional hard-core systems is first order and is associated with a proliferation of grain boundaries as proposed by Chui (1982, 1983). There are several problems with coming to such a conclusion. Complex defect structures have been observed even in studies (Murray and Van Winkle, 1987; Udink and van der Elsken, 1987) where other evidence is strongly in favor of the KTHNY picture. The Voronoi polygon analysis deals with the structure in the immediate neighborhood of a particle. The KTHNY theory deals with the long-distance interactions of defects. If extended defect cores exist in these systems [as the Joos and Duesbery (1985, 1986) calculations indicate], then much of what is observed in Voronoi polygon analysis should be more properly subsumed in the defect core. Indeed the short lifetime of some of these defects suggests that this is the case, as does the observation by Toxvaerd (1981) of an increase in defect density as the system size is increased.

Another complication in interpreting these Voronoi polygon maps exists. The logarithmic interaction of disclinations in the hexatic phase is due to screening by dislocations. These dislocations are "invisible" in the KTHNY calculation, but they will not be invisible in our Voronoi maps. Indeed, these dislocations are predicted to have correlations in the hexatic phase very like the grain boundary loops observed (Halperin and Nelson, 1978; Fisher *et al.*, 1979).

Correlation functions between defects of various types have been studied only for the Gaussian core model (Stillinger and Weber, 1981; Weber and Stillinger, 1981). Initially, one might expect that the short-range behavior of these correlation functions might be sensitive to the defect unbinding transitions. If, however, the defect cores are extended, the information obtained from these correlation functions will be much less direct. Examples of the defect correlations obtained by Stillinger and Weber are shown in Fig. 31. No simple pattern of behavior was observed. An asymmetry between the 5-5 and 7-7 correlation functions due to the presence of a significant number of defect configurations other than simple pairs was observed.

It is thus not clear what is the best way to interpret the information obtained by Voronoi polygon analysis. Perhaps some type of MCRG procedure applied to the defects would be informative. Unfortunately, it is very difficult to get good statistics on defect quantities, since the number of defects (even near melting) is such a small fraction of the number of particles.

4. Nearest-neighbor-bond-orientational order

The most distinctive predictions of the KTHNY theory concern the behavior of the nearest-neighbor-bond-orientational order. The two-dimensional solid shows long-range bond-orientational order and quasi-long-range positional order, and the fluid is characterized by short-range exponentially decaying order in both position and bond angle. The KTHNY theory predicts algebraic decay of bond-angular order accompanied by short-range positional order in the intermediate hexatic phase. Attempts to fit the angular correlation function to a power-law form in the intermediate (hexatic or coexistence) region for hard-core systems have usually led to values of η greater than 0.25 (the upper limit for stability of the hexatic phase), implying either that the behavior observed in these systems is not really power-law decay but some combination of fluidlike and solidlike behavior characteristic of two-phase coexistence (Tobochnik and Chester, 1982), or that the long-distance limit has not yet been reached. The angular correlation function is generally characterized by long-time scale fluctuations and

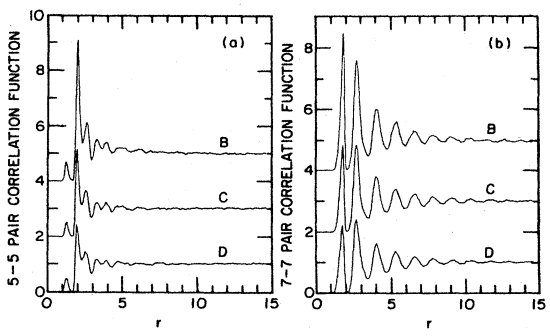

FIG. 31. Defect correlation functions for the Gaussian core model in the (B) coexistence, (C) cold fluid, and (D) warm fluid regions: (a) function g_{55}; (b) function g_{77} (Weber and Stillinger, 1981).

the uncertainties in η are quite large. The behavior of the orientational correlation function $g_6(r)$ in the solid phase is as expected, showing long-range bond-angular order. The HN theory predicts that the angular correlation length will diverge as the fluid-hexatic transition is approached from the fluid side. Almost all simulations of hard-core systems find the angular correlation length reaching the size of the system before the first-order transition occurred (Frenkel and McTague, 1979; Zollweg, 1980, 1984; Broughton *et al.*, 1982; Tobochnik and Chester, 1982). It is impossible to judge from these results whether it would have diverged in an infinite system.

Two simulations of very large Lennard-Jones systems have addressed the bond-orientational correlation functions. In these large systems, one might hope to probe the asymptotic regime. Bakker *et al.* (1984) have performed an MD simulation of 10 000 particles interacting via a Lennard-Jones potential at a density of 0.88. Fits of the bond-angular correlation function to an exponentially decaying form in the fluid region led to the conclusion that the orientational correlation length saturated near $T=1.11$ at a value of about 20 lattice spacings, before reaching the size of the system. Bakker *et al.* concluded therefore that the transition is first order and that the intermediate region bounded by changes in slope of the energy versus temperature curve (see Fig. 32) corresponds to a two-phase coexistence region.

The form of the correlation function $g_6(r)$ did not show any appreciable change in behavior when proceeding from the solid into the intermediate region, at $T=0.88$. This fact is consistent with the picture of a two-phase region with a small amount of fluid present. Between $T=0.99$ and $T=1.02$ a marked change in the behavior of the bond-orientational correlation functions is observed. Rather than the rapid saturation to a constant observed at lower temperatures, a slow decay was seen (see Fig. 33). This behavior is interpreted by Bakker *et al.* (1984) as consistent with a coexistence region in which the liquid spans the entire system.

One might argue, however, that these observations are also consistent with the existence of a hexatic phase in the region between $T=0.99$ and $T=1.11$. Bakker *et al.* observed that the data at $T=1.02$ and $T=1.08$ may be fit to a power-law decay with decay exponent, $\eta_6=0.22$ for $T=1.08$ (very close to the predicted value of 0.25 at a hexatic to isotropic transition). Is it possible that they have observed a hexatic phase bounded by first-order transitions? Or, possibly, that the divergence of the orientational correlation length occurred between $T=1.11$ and $T=1.08$? The critical region for these transitions is predicted to be very narrow (Cardy, 1982; Greif *et al.*, 1982; Dahm, 1984).

Udink and van der Elsken (1987) have studied the function $g_6(r)$ in a system of 12480 Lennard-Jones particles. They simulated at a reduced density of 0.873, near that studied by Bakker *et al.* Udink and van der Elsken, however, found no saturation of the angular correlation length upon approaching the intermediate region from the liquid. Their observed correlation lengths reached the size of the system. In addition, they obtained a good fit of the temperature dependence of the correlation length to the exponential form predicted by the KTHNY theory.

The reasons for this disagreement are unclear. It seems unlikely that the small difference in simulation density is sufficient to explain it. A more likely possibility is that the fitting procedures employed by the two groups led to disparate results. Since the orientational correlation function is an oscillating function, a smoothing procedure is required before a correlation length may

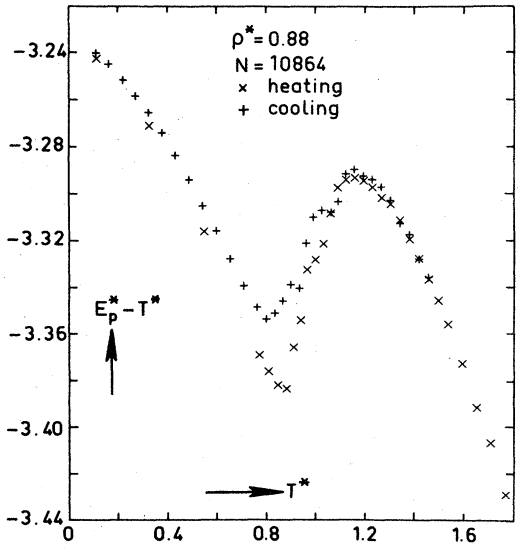

FIG. 32. Reduced potential minus kinetic energy vs reduced temperature (Bakker, Bruin, and Hilhorst, 1984).

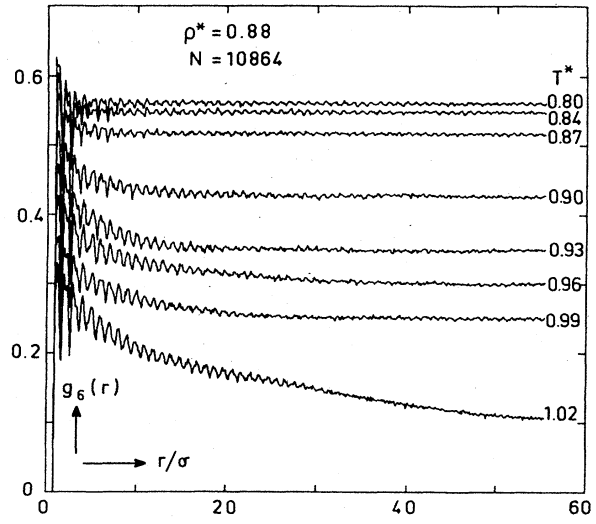

FIG. 33. Orientational correlation function for various temperatures in the solid and intermediate regions (Bakker, Bruin, and Hilhorst, 1984).

be extracted (Zollweg, 1980). The correlation length obtained may also depend on the interval of r over which the fit is performed. Currently the results of Bakker *et al.* and those of Udink and van der Elsken simply stand unreconciled.

Udink and van der Elsken (1987) do not report fits of their correlation functions to a power-law form in the intermediate region. Instead, they have employed finite-size scaling to obtain the decay exponents from the appropriate order parameters. This work is described in the following section.

5. Local bond-orientational order

Because of the difficulty in determining the long-distance behavior of the orientational correlation function, Strandburg, Zollweg, and Chester (1984) have used a local measure of bond-orientational order on various length scales to investigate the orientational order of the intermediate region in both Lennard-Jones and hard-disk systems. They studied the angular susceptibility of subsystems of particles. In this study χ_6 was defined as

$$\chi_6 = \langle |\psi_6|^2 \rangle - \langle |\psi_6| \rangle^2 ,$$

where (30)

$$\psi_6 = \frac{1}{N} \sum_l \frac{1}{n_l} \sum_j \exp(i 6 \theta_{lj})$$

and where the sum on l is over all particles, the sum on j is over the nearest neighbors of particle l, nl is the number of nearest neighbors of particles l, and θ_{lj} is the angle made with a fixed axis by the bond joining particles l and j.

If the system is made up of coexisting phases and the subsystems are small enough, one would expect most subsystems to be either solid or liquid. The solidlike regions seen in particle trajectory plots near the middle of the intermediate region are of size on the order of 100 particles. However, particle trajectory plots primarily give a sense of the extent of positional order. The work of Strandburg, Zollweg, and Chester tests whether the bond-orientational order is also explained by coexisting patches of solid and liquid. If so, the distribution of values of χ_6 for sufficiently small subsystems should then be given by a sum of the distributions of χ_6 in the solid near melting and the fluid near freezing. The results of Strandburg *et al.* are in quantitative agreement with predictions based on two-phase coexistence in both the hard-disk and Lennard-Jones systems. The results show the existence of solidlike and liquidlike patches of size on the order of 50 particles in bond-angular as well as in positional order.

The Lennard-Jones system investigated was at a density $\rho^* = 0.856$ equal to one of the lower-density system of Tobochnik and Chester (1982). The hard-disk system should correspond to a very high-density Lennard-Jones system. The similarity of the low-density Lennard-Jones and hard-disk results therefore contradicts the distinction between low- and high-density Lennard-Jones systems made by Tobochnik and Chester. A van der Waals theory (Weeks and Broughton, 1983) of the Lennard-Jones system also finds no distinction between the melting behavior of a purely repulsive Lennard-Jones potential and the full Lennard-Jones potential with an attractive part in this region of the phase diagram.

Unfortunately, an accurate model of the subsystem distribution of χ_6 for a hexatic phase is not available. In the work of Strandburg, Zollweg, and Chester (1984), the angular behavior of the low-temperature phase of the XY model was used as a model. This analogy is suggestive but may not apply precisely, especially since the defect structure in the particle systems is considerably more complex than that in the XY model. Since macroscopic phase separation is not observed, it is possible that the solid and liquid patches observed are critical fluctuations that would be expected throughout a hexatic phase.

Recent finite-size scaling studies of the positional and bond-orientational order parameters at a reduced density of 0.873 strongly suggest that despite the apparent agreement of the distributions of local bond-orientational order with a coexistence model, the intermediate region is actually a hexatic phase.

Udink and van der Elsken (1987) performed calculations of the translational and bond-orientational order parameters and their second- and fourth-order moments as a function of system size. The exponents η and η_6 were then obtained from fits to log-log plots of these quantities as a function of system size. They found that the translational exponent η showed a sharp increase at a temperature corresponding to the melting temperature inferred from, for example, a plot of energy versus temperature. At that temperature, η also passed the value of $\frac{1}{3}$, which is the upper limit for mechanical stability of the solid.

The bond-orientational exponent η_6 also displayed a dramatic increase at a distinctly higher temperature. This temperature corresponded extremely well to the hexatic-liquid transition temperature from a fit of the temperature dependence of the orientational correlation length. These results demonstrate the existence of an orientationally ordered, positionally disordered phase over a region approximately 10% wide in temperature.

The hexatic melting temperature deduced from these studies is somewhat below the fluid-intermediate region boundary deduced from changes of slope in plots of thermodynamic quantities. Such a result is not surprising since the KTHNY transition is not predicted to be associated with any singularities in thermodynamic quantities. Indeed the specific-heat maximum associated with defect unbinding is predicted to occur above the transition temperature. It is interesting to note that the melting transition at this density occurs well above the reduced temperature at which a crossover to continuous melting occurs in the xenon-on-graphite system.

6. Particle motions

Particle motions are studied by measuring the average squared displacement of particles from their lattice sites and by observation of trajectory maps. Trajectory maps may provide evidence for two-phase coexistence.

Generally, melting is associated with a dramatic increase in the average squared displacement. Toxvaerd (1983) has reported some rather disturbing studies of size dependence of this quantity. He found that, at a temperature that had apparently been in the solid region for a system of size 1024, diffusion set in for a system of 8100 particles. He interpreted this as evidence that the system melted as its size was increased. In several cases the onset of diffusion occurred when u^2 reached the value 0.18. He compared this to the Lindemann criterion for three-dimensional melting and suggested that melting may always occur at this value of u^2. As Toxvaerd points out, since u^2 goes as $\ln N$ in 2D in the low-temperature harmonic solid, u^2 will reach the value 0.18 for some system size at any low temperature.

Koch and Abraham (1983), however, reported an observation of solid state stability for values of u^2 larger than 0.18. They also pointed out that the onset of diffusion does not necessarily signify melting. Diffusion may occur in the equilibrium solid and, indeed, does in the 3D solid. Toxvaerd argues that the onset of diffusion at a particular value of u^2 and the observed frequency of consecutive hops are evidence against the interpretation of this diffusion as an equilibrium solid property.

Another interesting observation about particle motions is the report by Alder and Ceperley (Alder *et al.*, 1982) for the hard-disk system of the observation of cyclic permutations of on the order of 10 particles just prior to melting. Interestingly, similar behavior has been reported for the $\ln r$ potential system (Choquard and Clerouin, 1983). The significance of these cyclic motions is not known.

7. Summary of simulations of hard-core systems

Taken together the above results lead to the following conclusions: Free-energy studies indicate that the strictly two-dimensional hard-core potential systems melt via weak first-order transitions. Most studies of other quantities have been consistent with first-order transitions. However, the fluid near freezing is characterized by long orientational correlation lengths. While Bakker *et al.* (1984) argue that these correlation lengths do not diverge, Udink and van der Elsken (1987) find correlation lengths approaching the size of the system even in a very large system. Very long runs are necessary to obtain equilibrium in the cold fluid and transition regions. Fluctuations are significant in these regions.

Until recently the intermediate region has been most consistently interpreted in terms of two-phase coexistence. It displays a high density of defects with a prevalence of grain boundaries and clusters. A visual perusal of trajectory plots shows solidlike and liquidlike patches. The local bond-orientational order parameter distribution may be quantitatively reproduced by a coexistence model. However, the finite-size scaling studies of Udink and van der Elsken demonstrate that the intermediate region is an orientationally ordered, positionally disordered phase, bounded by transitions that are in accord with the KTHNY predictions inasmuch as these have been tested. These results highlight the extreme importance of studies of size dependence for the interpretation of computer simulation results.

While Udink and van der Elsken have been reluctant to label this orientationally ordered phase hexatic, their reluctance is based primarily on the discrepancy between the defect-rich structures observed in Voronoi polygon analysis of their configurations and the dilute gas of dislocations described in the KTHNY theory. As has been discussed in Sec. V.C.3, one should be careful about taking this picture too literally as a description for local particle configurations. The KTHNY theory describes the behavior at length scales greater than a defect core radius, which may in fact be very large in these systems. The large length scale behavior has been shown, by the finite-size scaling analysis, to be quite consistent with the KTHNY theory. Why this phase is so well modeled on shorter length scales by a coexistence model remains puzzling.

One final suggestion for future simulations of the Lennard-Jones system may be given. Most simulations to date have been carried out along isochores. Thus the path taken in the simulations runs nearly parallel to the phase boundary. Such a path will tend to "smear out" the transition region. An isothermal path may provide cleaner transition behavior.

D. Intermediate strength interactions

While most simulation studies of 2D melting have been carried out for the hard-core systems described above, there is also great interest in the study of 2D melting for softer potentials. The defect core energy may be expected to vary depending on the potential. In this section we review results for the intermediate potentials. In particular, studies have been performed for the $1/r^6, 1/r^5$, and $1/r^3$ potentials.

The $1/r^6$ potential system has been studied in detail by Allen *et al.* (1983). They studied a system of 2500 particles using reasonably long runs (40 000 MC steps per particle or passes near the transition). Their study ranged from an investigation of the microscopic defect structure to a determination of the free energy. Their results are rather similar to those for the hard-core potential systems. The free-energy computation indicated a first-order transition with $\delta v/v = 0.7\%$. They had significant equilibration problems in the transition region, characterized by slow energy fluctuations, superheating, and supercooling if great care was not taken in moving slowly through the transition region, and an inability to cool to a defect-free solid in the computer time available. They

also observed a sharp rise in defect density at the transition with a relatively high density of defects across the transition region.

The transition region was most consistently described as a two-phase region. The elastic constant K, while approaching 16π near melting, declined gradually across the transition region rather than jumping to zero at melting. Since K should be 0 in a fluid or hexatic phase and $>16\pi$ in solid, these intermediate values probably indicate two-phase coexistence. Although finite-size effects would also give nonzero values for K in a hexatic phase, one would expect these values to be small. Trajectory plots were "patchy" and consistent with two-phase coexistence. In addition, while it was possible to fit the correlation function g_6 to a power-law form in this region, the exponents η_6 characterizing the decay were all $(1.12<\eta_6<1.15)$ considerably larger than $\frac{1}{4}$ (the upper limit for stability of the hexatic phase).

In spite of these indications of two-phase coexistence, the long time fluctuations present in this region and the significant pretransitional effects observed left Allen *et al.* (1983) unwilling to draw a conclusion as to the nature of the transition in the long-time, large system limit. The pretransitional effects included a rapid increase of the angular correlation length as the freezing transition was approached from above, similar to that observed in the hard-core systems. Thus, except for added difficulties in equilibration and in recooling the solid, the results for the $1/r^6$ potential are very similar to those for hard-core potentials. A weak first-order transition was observed in the simulation. Significant pretransitional effects left open the question of finite-size and time effects on the nature of the transition.

The detailed study of finite-time effects by Novaco and Shea (1982) for a constant energy molecular dynamics simulation of the $1/r^5$ potential system has been discussed above. In the transition region they observed relaxation times longer than their longest runs (100 000 time steps), leading them to conclude that data obtained in this transition region should clearly be regarded as nonequilibrium data. A cautionary note: this nonequilibrium data forms a loop in the ρ-P plane, and in the absence of information concerning relaxation times the transition would certainly be interpreted to be first order. The time dependence of the autocorrelation functions was quite similar for every quantity for which it was computed, including such dissimilar quantities as the internal energy and the local-angular-order parameter ψ_6. In addition to the increase of relaxation times near the transition, an increase in the amplitude of fluctuations in quantities, such as the temperature, was seen.

Novaco and Shea interpreted these effects as evidence of critical slowing down. Koch and Abraham (1983) argued that the long relaxation times were simply an artifact of the constant density simulation and characterized a two-phase region. In any event, in the absence of equilibrium, Novaco and Shea concluded that it was not possible to determine the order of the transition.

In a molecular dynamics study of the 2D dipole system ($1/r^3$ interaction) at constant energy, Kalia and Vashishta (Kalia and Vashishta, 1981; Vashishta and Kalia, 1982) reported the observation of a first-order transition in a 256 particle system. They based their conclusion on the observation of superheating and supercooling and a latent heat of melting. This latent heat was found to be $<1\%$ of the energy of the solid phase. They used the pair correlation functions to demonstrate that the superheated and supercooled states correspond to solid and liquid, respectively, and that they are stable in runs of 40 000 time steps. In addition, they observed homogeneous nucleation when an energy equal to the latent heat was subtracted from the supercooled liquid. Their results for this system were essentially equivalent to those they obtained for the electron system (see next section). Since the system was rather small, a study of size dependence would seem to be in order.

Bedanov and Gadijak (1982), while concurring in the diagnosis of the $1/r^3$ transition as first order, found significant differences between the $1/r^3$ and $1/r$ systems. They observed that the orientational correlation length and the positional correlation length diverged at the same temperature for the $1/r^3$ system, but that these divergences were separated in the electron system. Their system contained 504 particles, and they do not describe the length of their molecular dynamics runs.

In summary, studies of systems interacting with intermediate potentials find weak first-order transitions, as do most studies of the hard-core potentials. However, the findings of Allen *et al.* (1983) and of Novaco and Shea (1982) emphasize the importance of finite-size and time effects in these systems, and none of the statements regarding the order of the transition can be considered to be definitive.

E. Soft interaction potentials

As mentioned above, Weeks (1981) has shown through an examination of the Clausius-Clapeyron equation that, for potentials of the form $1/r^n$ if $n<d$ (where d is the dimensionality of the system), there can be no density discontinuity at melting and thus no two-phase coexistence. This proof is consistent with the empirical observation that the first-order character is weakened as the potential is softened. Of course a first-order transition, characterized by an entropy discontinuity, can certainly still occur in these systems.

The earliest simulation of the 2D electron system was that by Hockney and Brown in 1975. They found melting distinguished by a λ-like transition at $\Gamma=95$. This finding has, however, not been corroborated by any of the simulations that followed nor by any of the experiments on 2D electron systems. Since Hockney and Brown had very short simulation times it is considered

likely that they were observing nonequilibrium effects.

At about the same time as the development of the KTHNY theory for 2D melting, Gann, Chakravarty, and Chester (1979) completed a Monte Carlo study of the melting of a 100-particle 2D electron system. Their conclusions were based on a free-energy calculation. They concluded from this study that melting was characterized by a first-order transition at $\Gamma = 130$. This value of Γ is in good agreement with the concurrent experimental determination by Grimes and Adams (1979). Grimes and Adams, however, found a transition in agreement with KTHNY predictions, in as many respects as could be tested. The difference in slope of the computed solid and liquid free-energy curves of Gann, Chakravarty, and Chester was only approximately 0.03%. They noted that the free-energy method is biased toward a first-order interpretation, and that they cannot rule out a continuous transition within the accuracy of their computation. They also noted that the fluid before freezing was quite well ordered, as evidenced by the observation of significant structure in the pair correlation function.

Kalia, Vashishta, and de Leeuw (1981; see also Vashishta and Kalia, 1982) have performed a molecular dynamics simulation of the electron system for various system sizes. For a system of 100 particles they observed a rather wide (10%) region of hysteresis in the energy. They also observed homogeneous nucleation on a time scale of 10 000 time steps. In light of this observation they concluded that their 40 000 time-step runs are indeed sufficiently long. The width of the hysteresis region decreased with system size to about 4% for 500 particles, but the magnitude of the jump in entropy across the transitions did not decrease. The magnitude of this jump is in agreement with the density wave theory of Ramakrishnan (1982), which predicts a first-order transition. Since the Ramakrishnan theory is a mean-field treatment, however, it is possible that the theory may correctly predict the approximate magnitude of the entropy difference between the solid and fluid without correctly predicting the details of the transition.

Assertions of first-order melting of the 2D electron system have been challenged by the most extensive set of simulations for this system, those of Morf (Fisher *et al.*, 1979; Morf, 1979, 1981). Morf reports several equilibration problems in studying the melting transition of the 2D electron system. In particular, it was not possible even in long runs to cool the system back into a defect-free solid. None of the other simulations of the electron system studied defects. Morf suggests that this difficulty may be due to very long defect relaxation times associated with the KTHNY transition.

As mentioned previously, calculations of the energies of various defects have been performed for the 2D electron system. The dislocations are seen to follow the predictions of elastic theory down to distances of two or three lattice spacings. Because of the ambiguity in the choice of core diameter, these results can be applied only approximately to the prediction of the melting temperature. However, when a core diameter of 1 to 2 times the lattice constant was assumed, and when renormalization of the shear modulus by phonons was accounted for by Monte Carlo measurements at low temperatures, Morf obtained from the KTHNY theory a predicted melting value of $\Gamma = 137$, in good agreement with simulation and experimental results.

In addition, Morf obtained good agreement for the behavior of the shear modulus near freezing with predictions obtained from the HN recursion relations. He also observed the onset of particle diffusion and a drop in shear wave frequency for $140 > \Gamma > 120$ as melting occurred. Power-law decay of the orientational correlation function with $\eta_6 < \frac{1}{4}$ was observed for $134 > \Gamma > 130$, strongly suggesting the identification of this region as a hexatic phase.

Unfortunately, the inability to obtain reversibility through the transition makes the drawing of firm conclusions as to the nature of the transition impossible. In an attempt to address this issue, Morf (1983) has investigated the effects of adding a small hexatic field term to the Hamiltonian. This field has an effect similar to that of a hexagonal substrate, stabilizing the long-range angular order and thus precluding the observation of a hexatic to fluid transition. However, the addition of this field allowed Morf to obtain reversibility through the transition and to study the phase diagram as a function of h_6. The melting curve as a function of the hexatic field h_6 for small h_6 was consistent with the HN predictions and inconsistent with the predictions of the Clausius-Clapeyron-type relation $dT_m/dh_6 = \delta M_6/\delta S$. The transition was studied for $\frac{1}{24}k_B T_m < h_6 < \frac{1}{3}k_B T_m$. It is still possible, however, that for $h_6 < \frac{1}{24}k_B T_m$ the transition crosses over to first order.

For the still softer $\ln r$ potential (2D one-component plasma with a uniform neutralizing background), the evidence is limited. Choquard and Clerouin (1983) reported a simulation of this system in which they found a weak first-order transition characterized by premelting effects described as cyclic permutations of six or more particles. As mentioned above, similar effects have been observed for the hard-disk system. Choquard and Clerouin observed little hysteresis and a very narrow transition region (less than a percent wide). They argued for a first-order transition on the basis of the observed hysteresis and the observation of solidlike and liquidlike patches in a trajectory plot in the transition region. Neither of these pieces of evidence is conclusive.

Perhaps most importantly, the Choquard and Clerouin effective system size was very small since they used free boundary conditions. They used 511 particles on a disk with free boundary conditions, analyzing only the particles within a radius $1/2R$ (about 125 particles) in order to avoid surface effects. While the idea of using free boundary conditions is certainly of interest, studies of finite-size effects are of crucial importance in such systems.

F. Adsorbed systems

In order to provide a detailed comparison with experiment, and especially to understand the discrepancy between the continuous transitions observed in some experimental systems and the first-order transitions observed in simulations of the corresponding two-dimensional systems, simulations of particles on a substrate have been performed. In recent years, the phase diagrams of xenon, krypton, and argon on graphite have been studied in detail by computer simulation. Remarkably good agreement with experimental results has been obtained, although differences in interpretation persist. Krypton on graphite has not been studied in the range of incommensurate melting, so we will not discuss the simulation results here. Xenon and argon on graphite have been simulated by using a Lennard-Jones potential to model the various atomic interactions, adjusting the parameters to experimentally determined values. Molecular dynamics methods were used with a constant number of atoms enclosed in a three-dimensional "box" with periodic boundary conditions in two dimensions, a graphite substrate on the "bottom" and a reflecting wall on the "top."

A simulation study of submonolayer argon on graphite by Abraham (1983a) found a continuous melting transition. This finding is in accord with all experimental evidence but the most recent heat-capacity results, which indicate a very weak first-order transition. 1680 argon atoms were used in the simulation and the size of the graphite substrate was about 400 Å^2. Since this broad, continuous transition differs markedly from the behavior of the corresponding 2D Lennard-Jones system, in which the system melts over a much smaller temperature range, it is clear that substrate effects are significant for this system. Abraham points out two reasons for this to be so. The submonolayer argon melting temperature is about 47 K. However, the corrugation of the graphite substrate potential is about 50 K. Also, the density of the liquid into which the submonolayer argon system melts is very close to the commensurate density for argon. Trajectory plots show a gradual growth of liquidlike regions over a greater than 10% region in temperature.

The melting of argon near and above one monolayer has not been studied in recent computer simulations. The extant experimental evidence is in favor of continuous melting at the higher coverages. The relationship of the argon on graphite melting to any of the two-dimensional melting theories is not clear, but it is certain that the substrate plays an important role in the melting transition.

Xenon on graphite is considerably less influenced by the substrate ordering field. Since the optimal xenon spacing is 8% larger than the commensurate spacing, the substrate has the effect of compressing it. In trying to compress the xenon adlayer, however, the substrate is working against the stiff $1/r^{12}$ repulsive part of the potential and hence is relatively ineffective. Submonolayer xenon on graphite melts with a relatively strong first-order transition.

As the coverage is increased, however, the xenon on-graphite-transition becomes continuous in the experiments, as evidenced both by x-ray scattering and by isotherm measurements [see (iii) in Sec. IV.D.2.a]. Abraham (1983, 1984) and Koch and Abraham (1983) have simulated xenon on graphite in the coverage regime covered by the scattering experiments. The experimental results were reproduced extraordinarily well. A very interesting aspect of the simulations is that the transition appeared continuous even when a smooth substrate (rather than a graphite substrate) was used (Abraham, 1984). These results confirm the picture of xenon as relatively uninfluenced by the graphite ordering field.

Abraham takes strong exception, however, to the interpretation of the experimental and simulational results as evidence of a true continuous melting transition. X-ray diffraction studies have been performed both at constant coverage and at constant chemical potential. In both types of experiments the xenon melting appeared continuous with positional correlation lengths on the best substrates extending to 2000 Å (Heiney *et al.*, 1983; Rosenbaum *et al.*, 1983; Dimon *et al.*, 1984; Nagler *et al.*, 1985; Specht *et al.*, 1985). Abraham has performed constant coverage simulations that reproduce the experimental constant coverage results extremely closely (Abraham, 1984). He has also performed a constant two-dimensional pressure simulation in which he observed a discontinuity in the density as a function of temperature or pressure and thus concludes that the transition is actually first order.

Abraham explains the apparently continuous transition observed in the constant coverage experiment and simulation as due to the presence of a region of coexistence between solid and fluid. Note that earlier results of Abraham (1983) in which what was called a "temporal bifurcation" coexistence (in which the system jumped back and forth from solid to liquid as a function of time) was observed were not borne out in his simulation of a larger system. In the larger system the first layer density remained reasonably constant in time. The two-phase coexistence posited for this larger system is of the conventional type. The number of xenon atoms in the larger system was 2304 and the largest length scale thus around 200 Å.

The experimentalists argue that their data may only conceivably be fit by a coexistence hypothesis over a 0.4-K range (where $T_m = 152$ K) where the evidence was inconclusive. In contrast, Abraham concluded from an analysis of trajectory plots that coexistence extends for several degrees. Trajectory plots are perhaps a rather misleading tool, since they do not allow quantitative comparisons, and since critical fluctuations might be expected to look very much like coexistence over short time scales.

At constant chemical potential or pressure, a first-order transition will not be characterized by coexistence but by discontinuities in thermodynamic quantities. In an early constant pressure simulation of xenon on graph-

ite by Koch and Abraham (1983), hysteresis and discontinuities were observed and interpreted as evidence of a first-order melting transition. Later comparison with experiment, however, demonstrated that the simulations had in fact missed the very narrow region over which the continuous transition was observed experimentally. The hysteresis and density jumps were due to nonequilibrium effects.

In the later study by Abraham (1984) a much finer grid of temperatures was investigated and a discontinuity was still observed at constant pressure. Abraham suggested that the continuous transition observed experimentally at constant chemical potential was an artifact of substrate inhomogeneities. At least as plausible, however, is that Abraham's simulation study is still missing the continuous transition. The width of a transition is sensitive to the axis along which the phase boundary is crossed. The constant pressure transition may be more abrupt than the transition at constant density or chemical potential. The extremely long correlation lengths observed experimentally indicate that if a first-order transition is actually observed in the simulation, it may very well be a result of finite-size effects. The experimental correlation lengths also indicate a long substrate coherence length, and suggest that the smearing due to substrate inhomogeneities should be minimal.

The development of single-crystal graphite substrates allowed the study by x-ray diffraction of the bond-orientational order. A system in which angular order is long range, while positional order is short range, will generate an x-ray diffraction pattern characterized by asymmetric spots whose radial width measures the positional correlation length and whose angular width is related to the mean-square fluctuation θ^2 of the bond angles. θ^2 is a quantity similar in concept to the mean-squared displacement u^2 in a crystal, and measures the fluctuations in bond angle in the ordered phase.

In an infinite, substrate-free hexatic or fluid phase there will be no preferred bond orientation and so the asymmetric spot will broaden to form a diffuse ring. Substrate fields lead to long-range bond-orientational order in a fluid or hexatic and thus spots will be observed. Finite system size effects will also produce spots in a hexatic phase, or even in a liquid whose bond-angular correlation length approaches the size of the system.

Rosenbaum *et al.* (1983) plotted the radial width versus the angular width as obtained from the experimental diffraction patterns. The dependence of the angular spot width on the radial spot width in a long-range hexatic has been predicted (Aeppli and Bruinsma, 1984) to be linear if the hexatic ordering is intrinsic rather than substrate induced. Rosenbaum *et al.* found a region of linear dependence just above the melting temperature and hypothesize that this behavior indicates hexatic ordering that is not simply an artifact of the substrate.

Abraham compares the Rosenbaum *et al.* (1983) data to his results for the variation of the inverse bond-orientational correlation length with the inverse positional correlation length. These correlation lengths were obtained by performing exponential fits to the positional and bond-orientational correlation functions obtained from his xenon-on-graphite simulations. He finds a dependence of the inverse bond-orientational correlation length on the inverse positional correlation length consistent (after arbitrary normalization) with the experimentally determined dependence of θ^2 on the inverse positional correlation length.

The meaning of this comparison is obscure, however. The observation of spots in the experimental diffraction pattern shows the existence of bond-orientational order on lengths comparable to the sample size (approximately 4000 Å). Abraham's orientational correlation lengths are much shorter (about 40 Å), while his system size is about 200 Å. These two findings are not at all consistent. Since, on a graphite substrate, long-range bond-orientational order must be present, the angular correlation lengths quoted by Abraham must characterize a short-distance transient in the bond-orientational correlations. None of his bond-angular correlation functions are shown in his paper; therefore one cannot judge the quality of the fits.

The xenon-on-graphite simulations of Abraham do not resolve conclusively the question of the order of the melting transition, or of the possible existence of a non-substrate-induced hexatic ordering above the transition. However, in spite of disagreement over interpretation of the results, they do show that impressively good quantitative agreement between experiment and simulation may be obtained. They also show that the corrugation of the graphite substrate is not crucial in determining the nature of the xenon-on-graphite melting in the near-monolayer regime.

An important question that remains unresolved is why standard simulations of xenon on graphite are able to reproduce the experimental observations so well. By contrast, very large system sizes and detailed finite-size scaling studies are required in the strictly two-dimensional systems. That the apparently continuous transitions are not caused by the sixfold substrate field is clear from Abraham's results for a smooth substrate.

Apparently the possibility of motion in the third dimension is crucial in these simulations. Probably this fact is an indication that density fluctuations are not being equilibrated as well in strictly two-dimensional systems. It is also a possibility that the continuous transition is inherently related to the presence of a second layer of atoms (since the crossover to continuous melting in xenon occurs near monolayer coverages).

VI. CONCLUSIONS

The nature of the two-dimensional melting transition remains an open and fascinating question. At this point the stage is set for further experimental, theoretical, and simulational work.

The primary task for theorists at this juncture is to

provide calculations that make more direct contact with specific experimental systems. In the realm of adsorbed systems particularly, the experimental observations remain virtually unexplained in the incommensurate melting regime. An understanding of the relationship between the defects in real systems and the idealized dislocations and disclinations of the defect-mediated melting theories is also lacking. Theories are also needed to describe the continuous to first-order crossover observed in the defect simulations and the xenon-on-graphite system.

Experimentally, there is also much to be done. For liquid-crystal systems a picture is emerging in which the KTHNY theory plays a significant and useful role. Further experimental studies, particularly of very thin films, will be required in order to complete our understanding. For electrons on helium, clever means need to be devised by which the structure, and especially the bond-orientational order may be observed. Determination of the ways in which bond-orientational order is manifest in measurable quantities is a challenge to theorists as well. The phase diagrams of the recently studied adsorbed systems still contain notable ambiguities (such as the position of the xenon-on-graphite multicritical point). Additionally, there are many incommensurate physisorbed systems whose melting transitions have never been studied using today's better substrates and synchrotron x-ray facilities. While one hesitates to recommend adding to the collection of unexplained phase diagrams, it seems likely that as more systems are given careful study, trends will appear that will lead to general insights. Finally, the influence of the substrate on melting may be better understood if alternative, high-quality substrates are developed that produce ordering fields of different strengths and symmetries. The recent studies of xenon on silver (Greiser *et al.*, 1987) illustrate the usefulness of such an approach.

Particular directions that might be fruitful for simulation work include more direct contact with experiment, including in particular more simulations in regions of the Lennard-Jones phase diagram that have displayed interesting behavior in experiments; further systematic study of size dependence and the effects of finite time scales; the exploration of possible multiparticle Monte Carlo moves that might expedite equilibration of defects and density fluctuations; the development of practical constant chemical potential simulation methods; further simulations on a flat substrate; and the application of MCRG methods to the study of two-dimensional melting.

ACKNOWLEDGMENTS

Many colleagues have contributed to my understanding of two-dimensional melting through seminars, correspondence, and personal conversations. In particular, I would like to thank G. V. Chester for introducing me to the problem and directing my thesis work on this topic and for many useful discussions; P. M. Horn for getting me started on this article; S. A. Solla and J. A. Zollweg for fruitful collaborations; and M. W. Chan, N. J. Collela, R. B. Griffiths, H. Kleinert, R. H. Morf, R. A. Suter, and R. H. Swendsen for stimulating discussions and correspondence. I am also grateful to J. G. Dash, H. Hilhorst, B. Joos, J. P. McTague, D. R. Nelson, Y. Saito, and F. A. Stillinger for comments on the manuscript. This work was supported primarily by the Carnegie-Mellon University Center for the Study of Materials through the Materials Research Laboratory Section, National Science Foundation, under Grant No. DMR-8417821. Partial support was also provided by National Science Foundation Grant No. DMR-79-24008-A02, administered by the Materials Science Center at Cornell University, and by the U.S. Department of Energy BES-Materials Sciences, under Contract No. W-31-109-ENG-38.

REFERENCES

Abraham, F. F., 1980, Phys. Rev. Lett. **44**, 463.
Abraham, F. F., 1981a, Phys. Rep. **80**, 339.
Abraham, F. F., 1981b, Phys. Rev. B **23**, 6145.
Abraham, F. F., 1983a, Phys. Rev. B **28**, 7338.
Abraham, F. F., 1983b, Phys. Rev. Lett. **50**, 978.
Abraham, F. F., 1984, Phys. Rev. B **29**, 2606.
Abraham, F. F., and S. W. Koch, 1984, Phys. Rev. B **29**, 2824.
Abraham, F. F., S. W. Koch, and W. E. Rudge, 1982, Phys. Rev. Lett. **49**, 1830.
Aeppli, G., and R. Bruinsma, 1984, Phys. Rev. Lett. **22**, 2133.
Aharony, A., R. J. Birgeneau, J. D. Brock, and J. D. Litster, 1986, Phys. Rev. Lett. **57**, 1012.
Alder, B. J., D. M. Ceperley, and E. L. Pollock, 1982, Int. J. Quantum Chem. Symp. **16**, 49.
Alder, B. J., and T. E. Wainwright, 1962, Phys. Rev. **127**, 359.
Allen, M. P., D. Frenkel, and W. Gignac, 1983, J. Chem. Phys. **78**, 4206.
Ambegaokar, V., B. I. Halperin, D. R. Nelson, and E. D. Siggia, 1980, Phys. Rev. B **21**, 1806.
Andersen, H. C., 1980, J. Chem. Phys. **72**, 2384.
Bak, P., and T. Bohr, 1983, Phys. Rev. B **27**, 591.
Bakker, A. F., C. Bruin, and H. J. Hilhorst, 1984, Phys. Rev. Lett. **52**, 449.
Barker, J. A., D. Henderson, and F. F. Abraham, 1981, Physica A **106**, 226.
Bedanov, V. M., and G. V. Gadijak, 1982, Phys. Lett. A **92**, 400.
Binder, K., 1979, Ed., *Monte Carlo Methods in Statistical Physics,* Topics in Current Physics, Vol. 7 (Springer, New York).
Binder, K., 1984, Ed., *Applications of the Monte Carlo Method in Statistical Physics,* Topics in Current Physics, Vol. 36 (Springer, New York).
Birgeneau, R. J., G. S. Brown, P. M. Horn, D. E. Moncton, and P. W. Stephens, 1981, J. Phys. C **14**, L49.
Birgeneau, R. J., and J. D. Litster, 1978, J. Phys. (Paris), Lett. **39**, 399.
Bishop, D. J., W. O. Sprenger, R. Pindak, and M. E. Neubert, 1982, Phys. Rev. Lett. **49**, 1861.
Brock, J. D., A. Aharony, R. J. Birgeneau, K. W. Evans-Lutterody, J. D. Litster, P. M. Horn, G. B. Stephenson, and A. R. Tajbakhsh, 1986, Phys. Rev. Lett. **57**, 98.
Broughton, J. Q., G. H. Gilmer, and J. D. Weeks, 1981, J. Chem. Phys. **75**, 5128.

Broughton, J. Q., G. H. Gilmer, and J. D. Weeks, 1982, Phys. Rev. B **25**, 4651.
Bruinsma, R., and G. Aeppli, 1982, Phys. Rev. Lett. **48**, 1625.
Bruinsma, R., and D. R. Nelson, 1981, Phys. Rev. B **23**, 402.
Butler, D. M., J. A. Litzinger, and G. A. Stewart, 1980, Phys. Rev. Lett. **44**, 466.
Cardy, J. L., 1982, Phys. Rev. B **26**, 6311.
Choquard, Ph., and J. Clerouin, 1983, Phys. Rev. Lett. **50**, 2086.
Chui, S. T., 1982, Phys. Rev. Lett. **48**, 933.
Chui, S. T., 1983, Phys. Rev. B **28**, 178.
Chung, T. T., 1979, Surf. Sci. **87**, 348.
Colella, N. J., and R. M. Suter, 1986, Phys. Rev. B **34**, 2052.
Collett, J., P. S. Pershan, E. B. Sirota, and L. B. Sorensen, 1984, Phys. Rev. Lett. **52**, 356.
Coppersmith, S. M., D. S. Fisher, B. I. Halperin, P. A. Lee, and W. F. Brinkman, 1981, Phys. Rev. Lett. **46**, 549.
Cotterill, R. M. J., and L. B. Pederson, 1972, Solid State Commun. **10**, 439.
D'Amico, K. L., J. Bohr, D. E. Moncton, and D. Gibbs, 1986, Bull. Am. Phys. Soc. **31**, 376.
Dahm, A. J., 1984, Phys. Rev. B **29**, 484.
Dash, J. G., 1987, private communication.
Davey, S. C., J. Budai, J. W. Goodby, R. Pindak, and D. E. Moncton, 1984, Phys. Rev. Lett. **53**, 2129.
Dierker, S. B., R. Pindak, and R. B. Meyer, 1986, Phys. Rev. Lett. **56**, 1819.
Dimon, P., P. M. Horn, M. Sutton, R. J. Birgeneau, and D. E. Moncton, 1984, Phys. Rev. B **31**, 437.
Domany, E., M. Schick, and R. H. Swendsen, 1984, Phys. Rev. Lett. **52**, 1535.
Ecke, R. E., and J. G. Dash, 1983, Phys. Rev. B **28**, 3738.
Evans, D. J., 1982, Phys. Lett. A **88**, 48.
Feile, R., H. Wiechert, and H.-J. Lauter, 1982, Phys. Rev. B **25**, 3410.
Fernandez, J. F., and M. F. Ferreira, 1986, Phys. Rev. B **34**, 292.
Fisher, D. S., B. I. Halperin, and R. Morf, 1979, Phys. Rev. B **20**, 4692.
Fisher, M. E., and D. A. Huse, 1982, in *Melting, Localization, and Chaos,* edited by R. K. Kalia and P. Vashishta (North-Holland, Amsterdam), p. 259.
Freimuth, H., and H. Wiehert, 1985, Surf. Sci. **167**, 432.
Frenkel, D., and J. P. McTague, 1979, Phys. Rev. Lett. **42**, 1632.
Gallet, F., G. Deville, A. Valdes, and F. I. B. Williams, 1982, Phys. Rev. Lett. **49**, 212.
Gann, R. C., S. Chakravarty, and G. V. Chester, 1979, Phys. Rev. B **20**, 326.
Gordon, M. B., and J. Villain, 1982, J. Phys. C **15**, 1817.
Greif, J. M., and D. L. Goodstein, 1981, J. Low Temp. Phys. **44**, 347.
Greif, J. M., D. L. Goodstein, and A. F. Silva-Moreira, 1982, Phys. Rev. B **25**, 6838.
Greiser, N., G. A. Held, R. Frahm, R. L. Greene, P. M. Horn, and R. M. Suter, 1987, Phys. Rev. Lett. **59**, 1625.
Grimes, C. C., and G. Adams, 1979, Phys. Rev. Lett. **42**, 795.
Guo, C. J., D. B. Mast, Y.-Z. Ruan, M. A. Stan, and A. J. Dahm, 1983, Phys. Rev. Lett. **51**, 1461.
Halperin, B. I., and D. R. Nelson, 1978, Phys. Rev. Lett. **41**, 121.
Heiney, P. A., R. J. Birgeneau, G. S. Brown, P. M. Horn, D. E. Moncton, and P. W. Stephens, 1982, Phys. Rev. Lett. **48**, 104.
Heiney, P. A., P. W. Stephens, R. J. Birgeneau, P. M. Horn, and D. E. Moncton, 1983, Phys. Rev. B **28**, 6416.
Hockney, R. W., and T. R. Brown, 1975, J. Phys. C **8**, 1813.
Hoover, W. G., J. A. Combs, and C. Massobrio, 1984, Phys. Rev. Lett. **53**, 2351.
Hoover, W. G., N. E. Hoover, and W. C. Moss, 1979, J. Appl. Phys. **50**, 829.
Huang, C. C., G. Nounesis, and D. Guillon, 1986, Phys. Rev. A **33**, 2602.
Huang, C. C., J. M. Viner, R. Pindak, and J. W. Goodby, 1981, Phys. Rev. Lett. **46**, 1289.
Hurlbut, S. B., and J. G. Dash, 1984, Phys. Rev. Lett. **53**, 1931.
Hurlbut, S. B., and J. G. Dash, 1985, Phys. Rev. Lett. **55**, 2227.
Janke, W., and H. Kleinert, 1980, Phys. Lett. A **114**, 255.
Janke, W., and H. Kleinert, 1984, Phys. Lett. A **105**, 134.
Janke, W., and D. Toussaint, 1986, Phys. Lett. A **116**, 387.
Joos, B., and M. S. Duesbery, 1985, Phys. Rev. Lett. **55**, 1997.
Joos, B., and M. S. Duesbery, 1986, Phys. Rev. B **33**, 8632.
Kalia, R. K., and P. Vashishta, 1981, J. Phys. C **14**, L643.
Kalia, R. K., P. Vashishta, and S. W. deLeeuw, 1981, Phys. Rev. B **23**, 4794.
Kern, K., P. Zeppenfeld, R. David, R. L. Palmer, and G. Comsa, 1986, Phys. Rev. Lett. **57**, 3187.
Kim, H. K., Q. M. Zhang, and M. H. W. Chan, 1986, Phys. Rev. Lett. **56**, 1579.
Kjaer, K., M. Nielsen, J. Bohr, H. J. Lauter, and J. P. McTague, 1982, Phys. Rev. B **26**, 5168.
Kleinert, H., 1983, Phys. Lett. A **95**, 381.
Koch, S. W., and F. F. Abraham, 1983, Phys. Rev. B **27**, 2964.
Kosterlitz, J. M., and D. J. Thouless, 1978, in *Progress in Low Temperature Physics,* Vol. VII-B, edited by D. F. Brewer (North-Holland, Amsterdam), p. 373.
Kosterlitz, J. M., and D. J. Thouless, 1973, J. Phys. C **6**, 1181.
Kuchik, J., and B. J. Berne, 1977, in *Statistical Mechanics, Part B: Time-Dependent Processes,* edited by B. J. Berne (Plenum, New York).
Ladd, A. J. C., and W. G. Hoover, 1982, Phys. Rev. B **26**, 5469.
Landau, D. P., and R. H. Swendsen, 1981, Phys. Rev. Lett. **46**, 1437.
Larher, Y., 1983, Surf. Sci. **134**, 469.
Litzinger, J. A., and G. A. Stewart, 1980, in *Ordering in Two Dimensions,* edited by S. K. Sinha (North-Holland, New York), p. 267.
Mayer, J. E., and W. W. Wood, 1965, J. Chem. Phys. **42**, 4268.
McTague, J. P., J. Als-Nielsen, J. Bohr, and M. Nielsen, 1982, Phys. Rev. B **25**, 7765.
McTague, J. P., D. Frenkel, and M. P. Allen, 1980, in *Ordering in Two Dimensions,* edited by S. K. Sinha (North-Holland, Amsterdam), p. 147.
McTague, J. P., and A. D. Novaco, 1979, Phys. Rev. B **19**, 5299.
Mehrotra, R., B. M. Guenin, and A. J. Dahm, 1982, Phys. Rev. Lett. **48**, 641.
Mermin, N. D., and H. Wagner, 1966, Phys. Rev. Lett. **17**, 1133.
Migone, A. D., Z. R. Li, and M. H. W. Chan, 1984, Phys. Rev. Lett. **53**, 810.
Moncton, D. E., and R. Pindak, 1979, Phys. Rev. Lett. **48**, 701.
Moncton, D. E., R. Pindak, S. C. Davey, and G. S. Brown, 1982, Phys. Rev. Lett. **49**, 1861.
Morf, R. H., 1979a, Phys. Rev. Lett. **43**, 931.
Morf, R. H., 1979b, Phys. Rev. Lett. **54**, 931.
Morf, R. H., 1981, in *Physics of Intercalation Compounds,* edited by L. Pietronero and E. Tosatti, Springer Series in Solid State Sciences, Vol. 38 (Springer, New York), p. 252.
Morf, R. H., 1983, Helv. Phys. Acta **56**, 743.
Motteler, F. C., 1985, Ph.D. thesis (University of Washington).

Murray, C. A., and D. H. Van Winkle, 1987, Phys. Rev. Lett. **58**, 1200.
Nagler, S. E., P. Dutta, P. M. Horn, S. K. Sinha, and D. E. Moncton, 1985, Bull. Am. Phys. Soc. **30**, 334.
Nagler, S. E., P. M. Horn, T. F. Rosenbaum, R. J. Birgeneau, M. Sutton, S. G. J. Mochrie, D. E. Moncton, and R. Clarke, 1983, Phys. Rev. B **32**, 7373.
Nelson, D. R., 1980, in *Fundamental Problems in Statistical Mechanics V,* Proceedings of the Fifth International Summer School on Fundamental Problems in Statistical Mechanics, Enschede, Netherlands, edited by E. G. D. Cohen (North-Holland, Amsterdam), p. 53.
Nelson, D. R., 1982, Phys. Rev. B **26**, 269.
Nelson, D. R., and B. I. Halperin, 1979, Phys. Rev. B **19**, 2457.
Nelson, D. R., and B. I. Halperin, 1980, Phys. Rev. B **21**, 5312.
Nielsen, M., J. Als-Nielsen, J. Bohr, J. P. McTague, D. E. Moncton, and P. W. Stephens, 1987, Phys. Rev. B **35**, 1419.
Novaco, A. D., and J. P. McTague, 1977, Phys. Rev. Lett. **38**, 1286.
Novaco, A. D., and P. A. Shea, 1982, Phys. Rev. B **26**, 284.
Phillips, J. M., L. W. Bruch, and R. D. Murphy, 1981, J. Chem. Phys. **75**, 5097.
Pindak, R., D. J. Bishop, and W. O. Sprenger, 1980, Phys. Rev. Lett. **44**, 1461.
Pindak, R., D. E. Moncton, S. C. Davey, and J. W. Goodby, 1981, Phys. Rev. Lett. **46**, 1135.
Pindak, R., W. O. Sprenger, D. J. Bishop, D. D. Osheroff, and J. W. Goodby, 1982, Phys. Rev. Lett. **48**, 173.
Rahman, A., 1964, Phys. Rev. **136**, A405.
Ramakrishnan, T. V., 1982, Phys. Rev. Lett. **48**, 541.
Rull, L. F., J. J. Morales, and F. Cuadros, 1985, Phys. Rev. B **32**, 6050.
Saito, Y., 1982a, Phys. Rev. B **26**, 6239.
Saito, Y., 1982b, Phys. Rev. Lett. **48**, 1114.
Saito, Y., and H. Muller-Krumbhaar, 1984, in *Applications of the Monte Carlo Method in Statistical Physics,* edited by K. Binder, Topics in Current Physics, Vol. 36 (Springer, New York), p. 223.
Shiba, H. J., 1980, J. Phys. Soc. Jpn. **48**, 211.
Sirota, E. B., P. S. Pershan, L. B. Sorensen, and J. Collett, 1985, Phys. Rev. Lett. **55**, 2039.
Specht, E. D., R. J. Birgeneau, K. L. D'Amico, D. E. Moncton, S. E. Nagler, and P. M. Horn, 1985, J. Phys. (Paris), Lett. **45**, L561.
Specht, E. D., M. Sutton, R. J. Birgeneau, D. E. Moncton, and P. M. Horn, 1984, Phys. Rev. B **30**, 1589.
Squire, D. R., A. C. Host, and W. G. Hoover, 1968, Physica (Utrecht) **42**, 388.
Stewart, A., 1974, Phys. Rev. A **10**, 671.
Stillinger, F. H., and T. A. Weber, 1981, J. Chem. Phys. **74**, 4015.
Strandburg, K. J., 1986, Phys. Rev. B **34**, 3536.
Strandburg, K. J., 1987, Phys. Rev. B **35**, 7161.
Strandburg, K. J., S. A. Solla, and G. V. Chester, 1983, Phys. Rev. B **28**, 2717.
Strandburg, K. J., R. M. Suter, N. J. Colella, P. M. Horn, S. A. Solla, R. J. Birgeneau, S. G. J. Mochrie, E. D. Specht, K. L. D'Amico, and D. E. Moncton, 1985, Phys. Rev. Lett. **55**, 2226.
Strandburg, K. J., J. A. Zollweg, and G. V. Chester, 1984, Phys. Rev. B **30**, 2755.
Swendsen, R. H., 1982a, Phys. Rev. Lett. **49**, 1302.
Swendsen, R. H., 1982b, in *Real-space Renormalization,* edited by T. W. Burkhardt and J. M. J. van Leeuwen, Topics in Current Physics, Vol. 30 (Springer, Berlin), p. 57.
Tobochnik, J., 1982, Phys. Rev. B **26**, 6201.
Tobochnik, J., and G. V. Chester, 1979, Phys. Rev. B **20**, 3761.
Tobochnik, J., and G. V. Chester, 1982a, Phys. Rev. B **25**, 6778.
Tobochnik, J., and G. V. Chester, 1982b, Phys. Rev. B **25**, 6778.
Toxvaerd, S., 1978, J. Chem. Phys. **69**, 4750.
Toxvaerd, S., 1980, Phys. Rev. Lett. **44**, 1002.
Toxvaerd, S., 1981, Phys. Rev. A **24**, 2735.
Toxvaerd, S., 1983, Phys. Rev. Lett. **51**, 1971.
Toxvaerd, S., 1984a, Phys. Rev. Lett. **53**, 2352.
Toxvaerd, S., 1984b, Phys. Rev. B **29**, 2821.
Tsien, F., and J. P. Valleau, 1974, Mol. Phys. **27**, 177.
Udink, C., and D. Frenkel, 1987, Phys. Rev. B **35**, 6933.
Udink, C., and J. van der Elsken, 1987, Phys. Rev. B **35**, 279.
Van Himbergen, J. E., 1984, Phys. Rev. Lett. **53**, 5.
Vashishta, P., and R. K. Kalia, 1982, in *Melting, Localization, and Chaos,* edited by R. K. Kalia and P. Vashishta (North-Holland, New York), p. 43.
Verlet, L., 1967, Phys. Rev. **159**, 98.
Viner, J. M., D. Lamey, C. C. Huang, R. Pindak, and J. W. Goodby, 1983, Phys. Rev. A **28**, 2433.
Weber, T. A., and F. H. Stillinger, 1981, J. Chem. Phys. **74**, 4020.
Weeks, J. D., 1981, Phys. Rev. B **24**, 1530.
Weeks, J. D., and J. Q. Broughton, 1983, J. Chem. Phys. **78**, 4197.
Widom, A., J. R. Owers-Bradley, and M. G. Richards, 1979, Phys. Rev. Lett. **43**, 1340.
Young, A. P., 1979, Phys. Rev. B **19**, 1855.
Young, D. A., and B. J. Alder, 1974, J. Chem. Phys. **60**, 1254.
Zhang, Q. M., Y. P. Feng, H. K. Kim, and M. H. W. Chan, 1986, Phys. Rev. Lett. **57**, 1456.
Zhang, Q. M., H. K. Kim, and M. H. W. Chan, 1986, Phys. Rev. B **33**, 5149.
Zollweg, J. A., 1980, in *Ordering in Two Dimensions,* edited by S. K. Sinha (North-Holland, Amsterdam), p. 331.
Zollweg, J. A., 1984, private communication.